Long wave anti-plane motion in pre-stressed elastic laminates

Maha Mohammed Helmi

School of Computing and Mathematics

Keele University

Submitted in partial fulfilment of the requirement

for the degree of Doctor of Philosophy

June 1, 2020

Declaration

I certify that this thesis submitted for the degree of Doctor of Philosophy is the result of my own research, except where otherwise acknowledged, and that this thesis has not been submitted for a higher degree to any other university or institution.

Signed: _____ Date: _____
(Maha Mohammed Helmi)

Abstract

The propagation of long waves along pre-stressed compressible elastic laminates is considered, focusing on anti-plane shear type waves. Within this thesis we investigate the mechanical response of this type of motion for a class of compressible pre-stressed elastic materials in which the strain energy function depends only on the invariants of the strain tensor. The particular emphasis is on small-amplitude motions superimposed on the equilibrium caused by finite deformations. A number of strain-energy functions, including neo-Hookean, Mooney-Rivlin and Varga material models are examined in numerical analysis. The associated dispersion relations are derived by means of the propagator matrix technique, allowing explicit dispersion relations for the considered multi-layer structures, with perfect bonding assumed on the interfaces. The obtained dispersion relations are investigated numerically for three types of possible boundary conditions, including, free faces, fixed faces, and fixed-free faces.

This thesis aims at performing a comprehensive long wave asymptotic analysis for the low- and high-frequency regimes in multi-layered structures. The anti-plane assumption allows simple explicit asymptotic results for phase velocity and frequency in terms of elementary functions of the wave number.

The derived long wave low- and high-frequency approximations are shown to be in excellent agreement with the exact solution obtained numerically. First, a single pre-stressed layer is examined, subject to all three types of boundary conditions. Then, the consideration is extended for two- and three-layered structures. The associated dispersion relations are analysed, with the corresponding asymptotic approximations constructed. Finally, a specific type of a symmetric 3-layer laminate is considered for all three types of boundary conditions. In view of the symmetry of the laminate, symmetric and anti-symmetric motions are separated for free and fixed face boundary conditions. At the same time, in the fixed-free case, it is not possible to use symmetry about the mid-plane, hence, the results are more algebraically cumbersome.

Acknowledgement

First and foremost, I would like to express my deep and sincere gratitude to all of my supervisors Prof Graham Rogerson, Dr Ludmila Prikazchikova and Dr Danila Prikazchikov for their invaluable guidance during my PhD studies. None of this would have been achieved without their constant encouragement and support. During many hours of discussions, they gave me motivations and fruitful ideas which deeply inspired me. Also, they qualify me through giving the opportunity to attend various conferences and symposiums. It was a great privilege to conduct this research project under their supervision.

I owe special gratitude to my children for their support and patience through the toughest moments of my research. I am extremely grateful specially to my son Khalid and my daughter Nura for their caring, understanding, sacrifices and patience during my study in Keele university. I would like to extend my thanks to my beloved husband Mohammed for his love, keen and support. I gratefully acknowledge the support of all my brothers and sisters who have always been there for me through my entire life. Last, but certainly not least, I greatly appreciate the support of my friends from Keele University.

Contents

List of Figures

Chapter 1

Introduction

In recent years, a variety of major developments in the area of engineering structures and modern technology exist in which elastic composite materials are employed. These developments, using composite material technology, often involve multi-layered structures. Such technology is in high demand for aerospace industries. Multi-layered structures are becoming increasingly necessary by their widespread use in mechanical design. It is now common to find wing and tail sections, propellers and rotor blades made from advanced layered materials, along with much of the internal structure and fittings. The airframes of some smaller aircraft are made entirely from composites, as are the wing, tail and body panels of large commercial aircraft. Composite materials, including laminated and fibre-reinforced systems, play significant roles in many scientific and engineering realms, primarily due to their enhanced

physical and mechanical response characteristics, such as specific strength, fracture toughness and wear resistance. Epoxy based and rubber-like matrix materials have found extensive use in the aerospace industry, see Daniel et al. (1994) and Kelly (1999). In addition to the aerospace industry, there are also numerous applications in bio-mechanics, geo-mechanics and other branches of modern engineering, see e.g. Torr (1966), Noor(1973), Sheridan et al. (1992), Hauert (2003), Argatov and Mishuris (2018) and references therein. Some of the important practical applications of layered structures with high contrast in material and geometric properties can also be found in laminated glass, see Ivanov (2006), Viverge et al. (2016), photovoltaic panels Aßmus et al. (2017) and energy-scavenging devices, see Qin et al. (2008).

In view of the importance of layered structures, a substantial volume of research has been published over the last half-century elucidating the mechanical and dynamic properties of layers and focusing on the properties of their material constituents. The early studies were mostly within the framework of linear isotropic elasticity. Then, the idea of developing these theoretical studies to describe the mechanical response of elastic material subjected to large primary deformation (i.e. materials able to undergo significant deformation prior to failure), were of interest for a number of researchers. This interest is motivated by advanced material technology, see e.g. Mooney (1940), Treloar (1944), Treloar (1975) and Rivlin and Saunders (1951), and Ogden (1997).

Their experiments revealed a full understanding of the physical behaviour of such materials though an incompressibility assumption. For the compressible counterpart, we may cite the first work carried out by Blatz and Ko (1962).

Studies then have been extended to investigate a variety of problems in pre-stressed isotropic material, envisaged to be either some inherent material property, perhaps brought about in design, or be the result of external forces. Indeed, analysis of the mechanical behaviour when adding pre-stress to isotropic material, changing the mechanical properties of the elastic materials, gives rise to significant features which do not exist in the unstrained case, see e.g. Rogerson and Sandiford (1997) and Rogerson and Sandiford (2002), and Horgan (2015). The influence of pre-stress, which can make the analysis of wave propagation extremely complicated, has been studied by a high number of researchers. Among them we may cite first the work done by Hayes and Rivlin (1961) who examined surface wave propagation in both compressible and incompressible pre-stressed isotropic half spaces. Then, Flavin (1963) used two specific strain energy functions associated with neo-Hookean and Mooney-Rivlin materials to derive explicit expressions for the surface wave speed. In addition, biaxial deformations and uniaxially stressed configurations have been discussed in a series of papers by Willson (1973), (1974).

On the subject of surface wave, we may also cite the contribution by Chad-

wick and Jarvis (1979), who examined infinitesimal surface waves in a pre-stressed compressible elastic half space. More contributions include the work by Dowaikh and Ogden (1990), who derived the surface wave speed equation for an incompressible elastic half space subject to an initial primary deformation, and also examined the pre-stressed configuration which give rise to a unique surface wave, also having important applications for spectra of edge vibrations in Kaplunov et al. (2004). Another work by Dowaikh and Ogden (1991) focused on the propagation of surface waves in a pre-stressed compressible isotropic half space subject to normal surface stress. Surface wave propagation in an incompressible, transversely isotropic, pre-stressed elastic half-space in respect of a general in-plane fibre direction was investigated both numerically and analytically by Prikazchikov and Rogerson (2004). Recently, substantial progress for modelling surface waves has been achieved using the reciprocity theorem, see e.g. Phan et al. (2013), and also Phan et al. (2019). Another significant direction is related of the so-called "hyperbolic-elliptic" asymptotic models, see Kaplunov and Prikazchikov (2017) and references therein, and also recent extensions of the methodology to moving loads, anisotropy and pre-stress, see Erbaş et al. (2017), Nobili and Prikazchikov (2018), Khajiyeva et al. (2018), and Fu et al. (2020). Further developments include composite asymptotic models for an elastic layer Erbaş et al. (2018) and Erbaş et al. (2019). Similar asymptotic formulations have been derived

for dispersive localised waves, including Love waves and bending edge waves, see Ahmad et al. (2011), Kaplunov et al. (2016).

A common approach to layered problems is to determine the dispersion relation. The implicit relationship between wave speed and wave number, termed the dispersion relation, is one of the main features of wave propagation in layered elastic solids. This can be obtained by satisfying the equations of motion and boundary conditions. Such relations are usually complex transcendental equations, providing an infinite number of eigenmodes. The branches having a finite phase wave speed in the low wave number limit are typically referred to as fundamental modes, with all other branches, having infinite long wave speed limits, are termed harmonics. In fact, dispersion occurs when plane waves at the different wavelength have different velocities. It should be noted that the first studies regarding surface wave propagation in elastic half space by Rayleigh (1885) observed no dispersion, whereas the first developments in analysis of wave propagation in a layer of finite thickness by Rayleigh (1888) and Lamb (1889), involved dispersion. In these studies, they derived the dispersion relation, which is nowadays usually called the Rayleigh-Lamb dispersion relation.

In general, a complete understanding of the dispersion relation can be obtained through a combination of numerical and asymptotic analysis, with the approximations obtained relating phase speed (and frequency) and wave

number explicitly. These approximations have been established to determine qualitative features of the dispersion relation, see e.g. an early attempt by Achenbach (1969) who analysed the vibration of an elastic layer using the direct asymptotic integration. Often, asymptotic solutions are helpful for interpreting the finite element results Kaplunov et al. (2005). Originally, asymptotic methods were mostly arising within statics or low-frequency dynamics, see e.g. Friedrichs and Dressler (1961), Biot (1965), Goldenweiser (1961), Reiss and Locke (1961), Aksentian and Vorovich (1963), Goldenveizer et al. (1993), and Green et al. (1997) and references therein. More recent results include applications of direct asymptotic integration to contact problems Erbaş et al. (2011) and Borodich et al. (2019), nonlocal elasticity Chebakov et al. (2017), bending edge waves on a stiffened plate governed by a biharmonic operator Alzaidi et al. (2019), derivation of higher-order asymptotic theories for elastic beams Nolde et al. (2018), as well as treatment of non-classical boundary conditions Erbaş et al. (2018) and Kaplunov et al. (2019).

A full classification of asymptotic approximations of the Rayleigh-Lamb dispersion relation for an elastic layer and its developments for thin elastic shells can be found in Kaplunov et al. (1998), separating long-wave low-frequency, long-wave high-frequency, short-wave low-frequency and short-wave high-frequency asymptotic limits. It is emphasized that the low-frequency

approximations are focused on polynomial variation across thickness of the elastic layer, whereas high-frequency approximations are associated with the sinusoidal variation along the thickness. We also note that in the short-wave limit, a typical wavelength is of the order of the thickness of the layer, whereas in the long-wave approximation the wavelength is considered to be much greater than the thickness. High-frequency long-wave modes, emerging in the vicinity of the thickness resonant frequencies, were investigated in various formulations of linear elasticity, including interactions with fluid, various types of boundary conditions, the effect of incompressibility, see e.g. Kaplunov and Markushevich (1993) Kaplunov (1995), Kaplunov et al. (2000a), Kaplunov et al. (2000b), Kaplunov and Nolde (2002), Kaplunov et al. (2005). Asymptotic techniques are much less developed for initial value problems in elasticity, with a few exceptions including Kaplunov et al. (2006) and Nolde (2007).

The asymptotic theories associated with the appropriate limiting behaviour of the dispersion relation have also been constructed for pre-stressed solids. On this subject, we may cite the discussion of asymptotic analysis of the dispersion relation carried out by Kaplunov et al. (2006), Rogerson and Fu (1995) for a pre-stressed plate formed of a restricted class of incompressible material while the work by Rogerson (1997) was for general incompressible materials. Asymptotic theories for a pre-stressed incompress-

ible elastic layer have been developed in Kaplunov et al. (2000b), Kaplunov et al. (2002), Kaplunov et al. (2002), Pichugin and Rogerson (2001), Pichugin and Rogerson (2002), and Pichugin and Rogerson (2002), see also Pichugin (2001). In the case of a compressible pre-stressed elastic layer the asymptotic behaviour tends to be more sophisticated due to a presence of a longitudinal wave. The approximations of the associated dispersion relation were considered in Ogden and Roxburgh (1993), Nolde et al. (2004), and Prikazchikova et al. (2006), with the follow-up asymptotic theories derived in Rogerson et al. (2007), Rogerson and Prikazchikova (2009) and Lashhab et al. (2015).

Significant efforts have been devoted to the analysis of dispersion of elastic waves in layered structures, starting from early contributions of Mindlin (1959), Ustinov (1976) and Lee and Chang (1979).

The results have been extended to various problems, see e.g. textbooks by Wang et al. (2000), Qatu (2004), and Reddy (2004), and review papers of Carrera and Brischetto (2009), Kreja (2011) and Sayyad and Ghugal (2017), addressing mechanics of layered elastic media, including sandwich structures. We also note important contributions of Bigoni et al. (2008), Berdichevsky (2010), Ryazantseva and Antonov (2012), Belyankova and Kalinchuk (2014), Kaplunov et al. (2018), Kaplunov et al. (2019) , studying various aspects of the mechanics of layered media, including effects of thin coating layers on filtering and band gaps, approximate structural models for sandwich plates

and Green functions of a layered elastic half-space.

Another recent important research area is related to mechanics of layered and composite structures with high contrast in parameters of the layers, see e.g. Aşık and Tezcan (2005), Schulze et al. (2012), Kaplunov et al. (2016), Kudaibergenov et al. (2016) and Kaplunov et al. (2019). A contribution Martin et al. (2012) proposes a related meta-material which could contribute to high-tech industrial applications. We also mention the possibility of a two-mode low-frequency plate theories, discussed in Kaplunov et al. (2017) within the framework of related long-wave low-frequency approximations of the exact dispersion relation. An important industrial application of these theories is related to the modelling of laminated glass, see Viverge et al. (2016) and also Kaplunov et al. (2017). In addition, we note another recent paper by Prikazchikova et al. (2018) developing the models for anti-plane problems of elasticity for two contrast scenarios.

A substantial number of contributions were devoted to analysis of wave propagation in pre-stressed layered media. We cite, for example Rogerson and Sandiford (2000), who examined the effects of pre-stress on small amplitude waves in multi-layered media and obtained a general asymptotic analysis for both the long and short waves in plane strain and also the papers by Rogerson and Sandiford (1997) and Lutianov and Rogerson (2010). We also mention Kayestha et al. (2010) investigating time-harmonic waves propagat-

ing in a pre-stressed compressible bi-material elastic laminate, and Lashhab et al. (2015), analysing dispersion of elastic waves in pre-stressed symmetric three-layered structures.

Various types of boundary conditions will be discussed in this thesis. Traction-free boundary conditions on the upper and lower surface of the laminate structures is one of our concern, which were used in the early studies for isotropic elastic layers see e.g. Mindlin (1960), Rayleigh (1888) and Lamb (1889). In the context of a plain strain problem for a single layer plate, the effects of pre-stress on stability and vibration of pre-stressed plate, have previously been investigated for traction-free boundary condition, see for examples the two papers by Ogden and Roxburgh (1993) and Roxburgh and Ogden (1994). For an incompressible pre-stressed elastic plate, the two papers by Kaplunov et al. (2002) and Kaplunov et al. (2002), added further insights into asymptotic analysis of the long- and short-wave regimes, respectively. Some aspects of wave propagation in an incompressible as well as nearly incompressible elastic layer subject to fixed face boundary conditions were studied in Nolde and Rogerson (2002) and Kaplunov and Nolde (2002). We also mention the study by Pichugin and Rogerson (2002) elucidating the important features of wave propagation in pre-stressed incompressible elastic layers with either free or fixed faces boundary conditions. A complete asymptotic analysis for long- and short-wave behaviours in a pre-stressed

compressible elastic layer was carried out by Nolde et al. (2004).

Another type of boundary conditions, which might be of engineering interest in modelling, say, coated structures, is the so-called fixed-free faces boundary conditions, i.e. one fixed and one free face. The main difference in this type of boundary is that in (4-play) there is no symmetry about the mid-plane of the inner core. Furthermore, the numerical analysis in this case shows the lack of fundamental mode i.e. high frequencies are the only modes investigated in the long wave regimes, see the recent contribution by Lashhab et al. (2015).

The propagator matrix technique is one of the popular methods to derive the dispersion relation in layered media. Such a relation for even relatively simple layered structures is often rather algebraically sophisticated and leads to high order determinants. In order to resolve these difficulties, we use a propagator matrix technique in this thesis. The method was first introduced in the context of seismological studies, see Thomson (1950), Haskell (1953), and Gilbert and Backus (1966). The term 'Propagator matrix' was introduced for the transfer operator for stress and displacement. Such a method was used to facilitate the derivation of the dispersion relations of the laminates, see e.g. Rao et al. (2004).

Our specific aim in this thesis is to investigate small amplitude long wave motion in the form of anti-plane shear waves. Studying this type of wave

propagating in multi-layered laminates is carried out in respect of the most general appropriate constitutive framework. As pointed out in Horgan (1995) anti-plane shear deformations are one of the simplest classes of deformations that solids can undergo, thus anti-plane shear, with just a single axial displacement field, may be viewed as complementary to the more complicated plane strain deformation, with its two in-plane displacements.

In the last few decades, considerable attention has been paid to the analysis of anti-plane deformations within the context of various constitutive theories (linear and non-linear) of solid mechanics, see for example, Horgan and Miller (1994), Jiang and Beatty (1995) and Polignone and Horgan (1992). These studies in nonlinear were largely motivated by the promise of relative analytic simplicity compared with plane problems since the governing equations are a single second-order linear or quasi-linear partial differential equation rather than higher-order or coupled systems of partial differential equations. Thus, the anti-plane shear problem plays a useful role as a pilot problem, within which various aspects of solution in solid mechanics may be examined in a particularly simple setting.

Recently, modern developments have been presented concerning the anti-plane shear model and its applications, for example, the influence of non-linearity on deformation fields near crack tips. For non-linear studies, these were largely motivated by the promise of relative analytic simplicity com-

pared with plane problems, see Knowles (1976) and Knowles (1977) for incompressible and compressible isotropic materials. In these work results for non-linear elasticity homogeneous isotropic materials were summarized. Also, the work by Jiang and Knowles (1991) for the classes of incompressible or compressible materials which sustain non trivial equilibrium states of anti-plane shear. They proved that the governing partial differential equation is a second-order quasi-linear equation and under certain constitutive restrictions, this equation is elliptic. More contributions, for the linear theory and the anti-plane shear deformations, may be seen in the article review by Horgan and Miller (1994) for references of earlier works and Horgan and Saccomandi (2001).

Further description of long wave motion in anti-plane shear is still not rich enough and more effort is needed to address the aspects of such problems. Moreover, in view of the fact that there was a lot of studies of three-dimensional and plane-strain problems resulting in a rather algebraically cumbersome dispersion relations, understanding of the underlying physics may have been overlooked. Therefore, the consideration of dispersion of elastic waves in a pre-stressed layered media within the anti-plane mode is of importance, since it allows simpler explicit results, which could be easier for analysis, which provides an additional motivation for our research.

The thesis consists of five chapters, concluding remarks and bibliogra-

phy. Chapter 2 presents the main problem preliminaries and the basic equations which used across this thesis. Also, the chapter contains the basic equations of infinitesimal time-harmonic wave propagation in a compressible pre-stressed elastic layer, and also long wave motion formulated through expressing the incremental boundary value problems based on the theory of incremental elastic deformations. For the layer, a Cartesian system of coordinates is selected, with one coordinate axes normal to the layer. A travelling harmonic wave is used to represent these problem's solutions. The solutions obtained from secular equations could then be employed for the purposes of representing the overall wave solutions as the linearly independent component's superposition. The substitution of these representations into the boundary conditions results in a system of linear homogeneous equations. To the one layer setup, the propagator matrix method is presented, relating the tractions and displacement on the faces. This method will be further implemented for multi-layered structures in the following chapters. This leads to the derivations of the associated dispersions in anti-plane shear within pre-stressed and linear isotropic elastic materials. For a single layer, three types of boundary conditions are taken into consideration: free faces, fixed faces, and fixed-free faces. Among these three, the first one could be seen as the classical Neumann-type boundary condition. For the purposes of identifying their main characteristics and determining the difference between different

asymptotic regimes of wave propagation, numerical analysis of the dispersion associations done. Numerical analysis providing phase speed (and frequency) as functions of wave number and material parameters is presented for each case of boundary conditions in this chapter. First, the obtained results for various material parameters are presented with regards to overall pre-stressed materials. Later the results are presented for linear isotropic materials. The graphs presented in this chapter indicate that low frequency dose not exist for all types of boundary conditions in the long wave region.

In Chapter 3, long wave motion in anti-plane shear for a 2-layered laminated structure is considered. Matrix form is used for expressing the solutions for tractions and displacements. To obtain the dispersion relations, three types of boundary conditions are applied. This is followed by a numerical investigation of these associations for the three specific strain energy functions: those related to neo-Hookean, Mooney-Rivlin and Varga materials. With regards to pre-stressed elastic materials, the linear isotropic elastic materials are also investigated as an special case. Numerical analysis for each case of boundary conditions in this chapter is provided. Results for certain material parameters are firstly presented for pre-stressed materials by using three strain energy functions associated with neo-Hookean, Mooney-Rivlin and Varga materials. This is followed by a presentation of the results obtained for linear isotropic elastic materials. Good insights into the behaviour

of harmonics can be obtained from the graphs. These graphs show that in the long wave limit, the fundamental mode exists for one type of boundary conditions (free faces) with no mode retaining finite wave speed limit for other boundary condition types.

Then asymptotic analysis of the long wave for low- and high-frequency approximations is provided. We derive asymptotic approximations for long wave high frequency motion (i.e. motion within the vicinity of thickness shear and stretch resonance frequencies) through through an expansion of the secular equation's roots and employment of the scaled frequency's expansion. These are then inserted into the dispersion relations, a process that leads to obtaining the expansion, which include the first and second orders of scaled frequency. It is noted that in the long wave high frequency limits, the limits for the all harmonics are non-zero. In this case, the frequencies are not obtainable in explicit form, with the cut-off frequencies of harmonics satisfying the transcendental equations obtained. Various graphs are then employed for presenting the agreement between the asymptotic and numerical results. Such graphs are plotted for both pre-stressed and linear isotropic elastic materials.

In Chapter 4, we provide a discussion of long wave motion in 3-layered structure subject to the three types of boundary conditions. Derivation of the resulting dispersion relation for both pre-stressed and linear elastic materials

cases is carried out using the propagator matrix. For pre-stressed materials, numerical results are obtained through the employment of the presented three strain energy functions. Such results start with the one associated to the neo-Hookean in the free-faces case. The results that follow are those for the Mooney-Rivlin materials for the fixed-free boundary value problem. The establishment of the third boundary value problem, fixed faces, is done using Varga materials. First, the low- and high-frequency asymptotic approximations are carried out for the pre-stressed case. This shows good agreement between the asymptotic expansions and numerical results for both high and low frequency in the long wave system. Then, these approximations are made for linear isotropic materials.

Chapter 5 is concerned with the propagation of long waves in an anti-plane shear in a symmetric 3 layers (4-ply) with the three types of boundary conditions considered. The laminate is composed of an inner core of thickness $2h$ and perfectly bonded to two outer layers each of thickness h. Therefore, it can be noted that the thickness of this structure is finite while in other directions, it is infinite lateral. As a result of the asymmetry about the mid-plane, the structure is generally termed asymmetric 4-ply laminate. In most cases, these types of structures are made from bonding together 2-ply laminated plates. Nonetheless, the underlying symmetry of the problem allows this system to be separated into two systems of 3 equations, which

match what is called symmetric and anti-symmetric solutions.

In general, the dispersion relations associated with a symmetric 3-layer (4-ply) laminate would be obtained from the condition that a system of six homogeneous equations in six unknowns has non-trivial solutions. In view of symmetry, this problem may be reduced to two systems of three equations in three unknowns, one analogous to the symmetric wave problem, one with the anti-symmetric problem. The dispersion relations associated with symmetric and anti-symmetric waves are derived via propagator matrices. This leads to a form of the symmetric dispersion relations which is specifically appropriate to the numerical investigations in Chapter 3. However, this chapter conducts an analysis of the anti-symmetric dispersion relations. Numerical and asymptotic analysis of the anti-symmetric dispersion relation is then performed first for a specific strain energy function, namely this associated with Mooney-Rivlin materials and investigate for the three types of boundary conditions. Then, an analysis is carried out for linear isotropic elastic materials. For every numerical case presented, it has been concluded that the limiting behaviour of the long-wavelength is the same, based on the realisation that in the long wave regime, there is no existence of fundamental mode. In the long wave low frequency regime for free and fixed boundary conditions we found that the fundamental mode of anti-symmetric motion is infinite, while the corresponding symmetric limit is finite.

This chapter is also concerned with the long wave motion in anti-plane shear of a pre-stressed 4-ply laminate with fixed-free boundary conditions. The main difference in this case is that there is no symmetry about the mid-plane of the inner core. Hence, we cannot divide this problem into two sub-cases. The associated dispersion relation is, in this case, derived from a system of six homogeneous equations in six unknowns, and is again derived by using the propagator matrix. The dispersion relations are then investigated numerically in case of Mooney-Rivlin material parameters with same material parameters used in Chapter 3 and followed by linear isotropic materials. The numerical investigation reveals an interesting characteristic of the dispersion curves in fixed free faces case, namely the global low frequency. Long wave high frequency approximations are established and shown to provide excellent approximations to the numerical solution at the end of this chapter.

Chapter 2

Preliminaries and governing equations for single layer

2.1 Material configuration

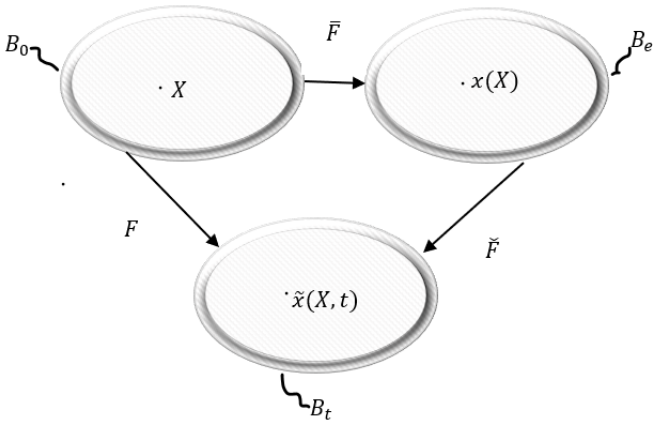

Figure 2.1: Configuration of a pre-stressed body.

The main feature in investigating long wave propagation is that of dispersion, meaning that wave phase speeds depend not just on material properties and direction of propagation, but also on wave number. For pre-stressed elastic solids, body waves, which propagate in an unbounded medium, are typically non-dispersive, as are surface and interfacial waves propagating along the free surface of an elastic half-space, see Chadwick and Jarvis (1979), Dowaikh and Ogden (1990), (1991). In the case of layered media, waves are generally dispersive. Thus, in this chapter we present the governing equations of pre-stressed solids and examine dispersion of elastic waves in a single pre-stressed, compressible layer with various boundary conditions, including free faces, fixed faces and fixed-free faces. The specific problem to be investigated is that of anti-plane shear waves. In respect of anti-plane shear, the only non-zero displacement component, u_3 say, is independent of x_3.

Before we concentrate on the long wave analysis, we will review the underlying aspects of continuum mechanics which we need in our research. We consider a body B composed of homogeneous elastic material which possesses a natural isotropic unstressed state B_0. A fundamental assumption of the underlying continuum theory is that the body B is formed as a set of material points, the points denoted by position vector $\mathbf{X}$ in the unstressed configuration B_0. A purely homogeneous static deformation is imposed upon B_0, resulting in a finitely stressed equilibrium state, termed as a reference

configuration B_e. A small time-dependent motion is then superimposed upon B_e, in which the material point $\mathbf{X}$ occupies the point with position vector $\mathbf{x}$ according to

$$\mathbf{x} = \boldsymbol{\chi}(\mathbf{X}), \quad \mathbf{X} \in B_0, \tag{2.1}$$

where $\boldsymbol{\chi}$ is a one-to-one mapping, defined as $\boldsymbol{\chi} : B_0 \to B_e$, see Rogerson and Prikazchikova (2009).

We have the final configuration, termed the current configuration and denoted by B_t. The position vectors of a representative particle are denoted by $X_A, x_i(x_A)$ and $\widetilde{x}_i(x_A, t)$ in B_0, B_e and B_t, respectively, see Figure 2.1. The position vector $\widetilde{x}_i(X_A, t)$ may therefore be expressed as

$$\widetilde{x}_i(X_A, t) = x_i(X_A) + u_i(X_A, t), \tag{2.2}$$

where $\boldsymbol{u}(X, t)$ is defined as a small time-dependent motion associated with the secondary deformation $B_e \to B_t$. This motion is termed small in the sense that all second and higher order terms in the displacement gradient may be neglected in Taylor series expansions of the governing equations.

The deformation gradients $\mathbf{F}$ and $\bar{\mathbf{F}}$, associated with the overall deformation $B_0 \to B_t$ and the primary static deformation $B_0 \to B_e$, respectively, are

given in component form by

$$F_{iA} = \frac{\partial \widetilde{x}_i}{\partial X_A}, \;\; \bar{F}_{iA} = \frac{\partial x_i}{\partial X_A}. \tag{2.3}$$

On making use of equation (2.2), and the definitions given in equation (2.3), it may be shown that the two deformation gradients are related by

$$F_{iA} = (\delta_{ij} + u_{i,j})\bar{F}_{jA}, \tag{2.4}$$

where a comma indicates differentiation with respect to the implied spatial coordinate component in B_e and delta is the Kronecker delta. The summation convention over repeated suffices is applied here and in all further chapters unless stated otherwise.

2.1.1 Equations of motion

For unconstrained materials, W is the strain-energy function and this function may be regarded as depending on $\mathbf{F}$ only through the principal stretches $\lambda_1, \lambda_2, \lambda_3$ and being a symmetric function of them. The associated nominal and Cauchy stress tensors, denoted by $\boldsymbol{\pi}$ and $\boldsymbol{\sigma}$, can be expressed in the

component form by

$$\pi_{iA} = \frac{\partial W}{\partial F_{iA}}, \qquad \sigma_{ij} = J^{-1} F_{iA} \frac{\partial W}{\partial F_{jA}}, \;\; J = det\bar{\mathbf{F}}. \tag{2.5}$$

According to the polar decomposition theorem, see Chadwick (2012) and Spencer (2004), we are able to express an arbitrary invertible tensor $\mathbf{F}$ in the form $\mathbf{F} = \mathbf{R}\,\mathbf{U} = \mathbf{V}\mathbf{R}$; where $\boldsymbol{R}$ is a proper orthogonal tensor, so $\boldsymbol{R}\,\boldsymbol{R}^T = \boldsymbol{R}^T\boldsymbol{R} = \boldsymbol{I}$, where the superscript T denotes the transpose of a tensor and $\boldsymbol{I}$ is the identity tensor. $\mathbf{U}$ and $\mathbf{V}$ are positive definite symmetric tensors and each of these tensors can be written in the spectral representations. For example, we have

$$\mathbf{U} = \sum \lambda_r (\mathbf{p_r} \bigotimes \mathbf{p_r}), \tag{2.6}$$

where λ_r are the eigenvalues of $\mathbf{U}$, or the principal stretches, and $\mathbf{p_r}$ the eigenvector of $\mathbf{U}$. Furthermore, $\mathbf{U}$ and $\mathbf{V}$ are named as the right and left stretch tensors, respectively. We introduce now two tensors $\mathbf{B}$ and $\mathbf{C}$, as

$$\mathbf{C} = \bar{\mathbf{F}}^T\bar{\mathbf{F}} = \mathbf{U^2}, \qquad \mathbf{B} = \bar{\mathbf{F}}\bar{\mathbf{F}}^T = \mathbf{V}^2, \tag{2.7}$$

where $\mathbf{B}$ and $\mathbf{C}$ are left and right Cauchy-Green strain tensors.

Alternatively, we may be regarded W as an isotropic function of three independent invariants, I_1, I_2 and I_3. Within axes coincident with the prin-

cipal axes of deformation, these may be defined and related to λ_1, λ_2 and λ_3 through

$$\begin{aligned} I_1 &= \mathrm{tr}\mathbf{B} = \lambda_1^2 + \lambda_2^2 + \lambda_3^2, \\ I_2 &= \frac{1}{2}\left\{(\mathrm{tr}\mathbf{B})^2 - \mathrm{tr}\mathbf{B}^2\right\} = \lambda_2^2\lambda_3^2 + \lambda_3^2\lambda_1^2 + \lambda_1^2\lambda_2^2, \\ I_3 &= \det\mathbf{B} = \lambda_1^2\lambda_2^2\lambda_3^2, \\ J &= \lambda_1\lambda_2\lambda_3, \end{aligned} \tag{2.8}$$

where tr denotes the trace of the tensor. Let ρ_0 and ρ_e denote the mass densities in the natural and reference configurations, respectively. Then the conservation of mass equation may presented as

$$\rho_0 = \rho_e J. \tag{2.9}$$

By considering an incremental time-independent motion superimposed upon B_e, resulting in the current configuration B_t, the linearised equations for small-amplitude motion superimposed upon the pre-stressed equilibrium state B_e may be derived.

In the absence of body forces, the equations of motion may be written as

$$\pi_{iA,j}\bar{F}_{jA} = \rho\ddot{u}_i, \tag{2.10}$$

where ρ is the mass density in the current configuration, u_i is the incremental displacement and a superimposed dot here and after indicates differentiation with respect to time, see for example Ogden (1997). Expanding π_{iA} as a Taylor series around the static state B_e ($\mathbf{F} = \bar{\mathbf{F}}$), yields

$$\pi_{iA} = \bar{\pi}_{iA} + (F_{lk} - \bar{F}_{lk}) \left.\frac{\partial \pi_{iA}}{\partial F_{lk}}\right|_{B_e} + ... \tag{2.11}$$

with an over-bar denoting evaluation in B_e. Within the linearisation, we retain only the leading order and thus ignore higher order terms in (2.11), see Ogden (1997). The formal requirement for small amplitude motion around B_e is

$$|F_{lk} - \bar{F}_{lk}| = |u_{l,j}\bar{F}_{jk}| \ll 1. \tag{2.12}$$

On making use of relation (2.12), equation (2.11) may be express within this small amplitude approximation as

$$\pi_{iA} = \bar{\pi}_{iA} + u_{l,c}\bar{F}_{ck} \left.\frac{\partial \pi_{iA}}{\partial F_{lk}}\right|_{\bar{F}=F}, \tag{2.13}$$

within which

$$\frac{\partial \pi_{iA}}{\partial F_{lk}} = \frac{\partial^2 W}{\partial F_{iA} \partial F_{lk}}. \tag{2.14}$$

Using the above relation, and substituting expansion (2.13) into (2.11), we obtain the linearised equation of motion

$$C_{kicl}u_{l,kc} = \rho\ddot{u}_i, \tag{2.15}$$

where C_{kicl} denote the components of the fourth order elasticity tensor, which are defined by

$$C_{kicl} = J^{-1}\bar{F}_{kA}\bar{F}_{cP}\left.\frac{\partial^2 W}{\partial F_{iA}\partial F_{lP}}\right|_{B_e}. \tag{2.16}$$

The elasticity tensor components, expressed in terms of the principal invariants defined in (2.8), take the form

$$\begin{aligned} JC_{kicl} = & \\ & 2W_1\delta_{li}B_{kc} + 2W_2(2B_{cl}B_{ki} - B_{kl}B_{ic} + \delta_{il}H_{kc} - B_{kc}B_{il} + 2W_3I_2(2\delta_{ki}\delta_{cl} \\ & - \delta_{kl}\delta_{ci}) + (4W_{11}B_{ki}B_{cl}) + 4W_{12}(B_{ki}H_{cl} + B_{cl}H_{ki}) + 4W_{13}I_2(B_{ki}\delta_{cl}+ \\ & B_{cl}\delta_{ki}) + 4W_{22}H_{ki}H_{cl} + 4W_{23}I_2(\delta_{lc}H_{ki} + \delta_{ki}H_{cl}) + 4I_2^2W_{33}(\delta_{ki}\delta_{cl}), \end{aligned} \tag{2.17}$$

with

$$H_{kl} = I_1B_{kl} - B_{kp}B_{lp}, \;\; k,l \in \{1,2,3\},$$

where B_{kl} are the components of $\mathbf{B} = \mathrm{diag}(\lambda_1^2, \lambda_2^2, \lambda_3^2)$, $W_i = \partial W/\partial\lambda_i$ and

$W_{ij} = \partial W/\partial\lambda_i\lambda_j$. The only non-zero components of the elasticity tensor have the form C_{iijj}, C_{ijji} or C_{ijij}, $i, j \in \{1, 2, 3\}$, see Ogden (1997). Corresponding to classical linear isotropic elasticity theory equations (2.17) reduce to

$$C_{iiii} = \lambda + 2\mu, \quad C_{iijj} = \lambda, \quad C_{ijij} = C_{ijji} = \mu, \quad i \neq j, \tag{2.18}$$

where λ and μ are the so-called Lame constants. The non-zero components of the elasticity tensor may also be represented in terms of the principal stretches of the underlying deformation, taking the form

$$JC_{iijj} = \lambda_i\lambda_j W_{ij},$$

$$JC_{ijij} = \begin{cases} \dfrac{(\lambda_i W_i - \lambda_j W_j)\lambda_i^2}{\lambda_i^2 - \lambda_j^2}. & i \neq j, \lambda_j \neq \lambda_i \\ \dfrac{1}{2}\left(JC_{iiii} - JC_{iijj} + \lambda_i W_i\right) & i \neq j, \lambda_j = \lambda_i \end{cases}$$

$$JC_{ijji} = JC_{jiij} = JC_{ijij} - \lambda_i W_i, \quad i \neq j, \tag{2.19}$$

for $i, j = 1, 2, 3$, all other components being zero.

To conclude this section, we provide the linearised equations of motion for a pre-stressed compressible isotropic elastic body, derived by making use

of (2.15) with (2.5), as

$$C_{1111}u_{1,11} + (C_{1122} + C_{2112})u_{2,12} + (C_{1133} + C_{3113})u_{3,13} + C_{2121}u_{1,22} + C_{3131}u_{1,33} = \rho\ddot{u}_1, \quad (2.20)$$

$$(C_{2211} + C_{1221})u_{1,12} + C_{2222}u_{2,22} + (C_{2233} + C_{3223})u_{3,23} + C_{1212}u_{2,11} + C_{3232}u_{2,33} = \rho\ddot{u}_2, \quad (2.21)$$

$$(C_{3311} + C_{1331})u_{1,13} + (C_{3322} + C_{2332})u_{2,23} + C_{3333}u_{3,33} + C_{1313}u_{3,11} + C_{2323}u_{3,22} = \rho\ddot{u}_3. \quad (2.22)$$

2.1.2 Incremental surface traction

In this section, we proceed to derive the increment traction vector. Therefore, we will first consider dS an element of area with the outward normal to a material surface given by $\mathbf{N}$ in the natural unstressed state B_0. Consider next two corresponding elements of material surface $d\bar{s}$ and ds in B_e and B_t, respectively. If we denote the two associated outward unit normals in the reference and current configurations B_e and B_t by $\bar{\mathbf{n}}$ and $\mathbf{n}$, respectively,

then through Nanson's formula, and for the deformation $B_0 \to B_e$, we have

$$\bar{\mathbf{n}} d\bar{s} = J(\bar{\mathbf{F}}^{-1})^T \mathbf{N} dS, \tag{2.23}$$

and for the deformation $B_0 \to B_t$ we have

$$\mathbf{n} ds = J(\mathbf{F}^{-1})^T \mathbf{N} dS, \tag{2.24}$$

see Ogden (1997). Using these two equations we deduce that

$$\mathbf{n} ds = (\bar{\mathbf{F}}\mathbf{F}^{-1})^T \bar{\mathbf{n}} d\bar{s}. \tag{2.25}$$

Now we consider the increment of contact force $\Delta\mathbf{f}$, associated with the secondary deformation $B_e \to B_t$ in the form

$$\Delta\mathbf{f} = \boldsymbol{\sigma}^T \mathbf{n} ds - \bar{\boldsymbol{\sigma}}^T \bar{\mathbf{n}} d\bar{s}, \tag{2.26}$$

where $\bar{\boldsymbol{\sigma}}^T \bar{\mathbf{n}} d\bar{s}$ is the contact force on the surface in B_e and $\boldsymbol{\sigma}^T \mathbf{n} ds$ is the contact force acting on this element in B_t.

On substituting equation (2.25) into equation (2.26), we obtain

$$\Delta\mathbf{f} = \boldsymbol{\tau}_{\bar{\mathbf{n}}} d\bar{s}, \tag{2.27}$$

where $\boldsymbol{\tau}_{\bar{\mathbf{n}}}$ is an incremental surface traction associated with the deformation $B_e \to B_t$. A measure of incremental surface traction is found by making use of equations (2.5) in the form

$$\boldsymbol{\tau}_{\bar{\mathbf{n}}} = J^{-1}(\pi_{iA} - \bar{\pi}_{iA})\bar{\mathbf{F}}^T\bar{\mathbf{n}}, \tag{2.28}$$

where $\bar{\pi}_{iA} = \pi_{iA}(\bar{\mathbf{F}})$. To conclude and represent a linearised measure of incremental surface traction in component form, we use the expansion (2.11), thus

$$\tau_{\bar{n}_i} = C_{kijl}u_{l,j}\bar{n}_k. \tag{2.29}$$

2.1.3 Formulation of anti-plane dynamic problems

A specific type of incremental motion will be considered in this thesis, so-called anti-plane shear. In the case of anti-plane shear, we specifically assume that the displacement is independent of x_3 and that u_3, the only non-zero displacement, is a function of x_1, x_2 and t. Thus $(u_1, u_2, u_3) = (0, 0, u_3)$ and $u_3 = u(x_1, x_2, t)$. In this chapter, we will consider anti-plane shear waves propagating in a pre-stressed compressible single-layer elastic plate of thickness h, orientated such that $0 \leq x_2 \leq h$, and infinite in the other two spatial directions. The origin, O, lies at the lower surface and Ox_2 is

orthogonal to the layer, see Figure 2.2.

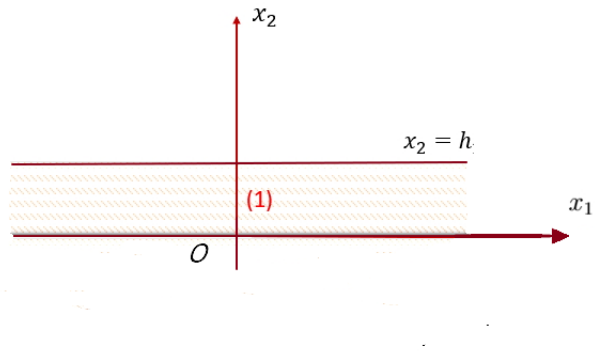

Figure 2.2: Single layer structure.

2.2 Some specific material models

Characterising the elastic properties of any body, B, may be done within the strain energy function $W(\mathbf{F})$. This then helps provide the so-called constitutive equations. All of the derivations in this thesis will be performed for the most general hyperelastic material models whose the stress-strain relationships derive from W, however, we will need to specialise to specific forms of W in the numerical calculations and comparing these with asymptotic solutions. Some specific strain energy functions are considered below.

2.2.1 Neo-Hookean material

The neo-Hookean strain energy function, with only one material constant, considers as one of the simplest forms for the strain energy function for elastic

materials. Within the framework of Gaussian molecular statistical theory, this function was derived and a compressible form of it may be represented as

$$W = \frac{\mu}{2}(I_1 - 3 - 2\mathrm{lnJ}) + \frac{\kappa'}{2}\left(\mathrm{J} - 1\right)^2, \tag{2.30}$$

within which $\kappa' = \kappa - \frac{2}{3}\mu$, κ is the bulk modulus of the material, μ and ($\kappa' = \lambda$) are Lame moduli in the ground state and I_1 is the invariant defined in (2.8), see Roxburgh and Ogden (1994) and Treloar (1944). Furthermore, the two elasticity tensor components in this case can be represented as

$$C_{1313} = \frac{\mu\lambda_1}{\lambda_2\lambda_3}, \quad C_{2323} = \frac{\mu\lambda_2}{\lambda_1\lambda_3}. \tag{2.31}$$

2.2.2 Mooney-Rivlin material

A general form of the strain energy function for which the shear is proportional to the shearing stress was given by Mooney (1940)

$$W = \frac{\mu_1}{2}(I_1 - 3) + \frac{\mu_2}{2}(I_2 - 3), \tag{2.32}$$

in which μ_1 and μ_2 are empirically determined material constants. The Mooney-Rivlin strain energy function expressed by (2.32) which is a linear

combination of the two invariants of left and right Cauchy-Green deformation tensor, sometimes provides serious simplifications within analysis, see, Boulanger and Hayes (1992) who revealed that the propagation of finite amplitude elastic waves in a pre-stressed Mooney-Rivlin material is in fact governed by a linear equation. The experiments of Rivlin and Saunders (1951) indicated that the range of applicability of (2.32) is similar to that of the neo-Hookean function (2.30). In order to model a several rubber-like materials, the Mooney-Rivlin strain energy function has been used successfully, see Boulanger and Hayes (1992). Furthermore, the Mooney-Rivlin strain energy function used with local values of the strains and added a limitation on the possible material parameters values, see e.g. Fu and Rogerson (1994) and Rogerson and Sandiford (1996). Meanwhile, it did not describe the full range of material response. For this reason the Varga strain energy function was also used.

The associated components of the elasticity tensor for a Mooney-Rivlin

material may be represented by using (2.19), yielding

$$\begin{aligned} JC_{iiii} &= (\mu_1 + \mu_2(\lambda_j^2 + \lambda_k^2))\lambda_i^2, \\ JC_{iijj} &= 2\mu_2\lambda_i^2\lambda_j^2, \\ JC_{ijji} &= -\mu_2\lambda_i^2\lambda_j^2, \\ JC_{ijij} &= (\mu_1 + \mu_2\lambda_k^2)\lambda_i^2, \\ i \neq j \neq k, &\quad i,j,k \in \{1,2,3\}. \end{aligned} \tag{2.33}$$

When the case of anti-plane strain considered, corresponding to a compressible pre-stressed elastic materials, from (2.33), we only need two components which may be introduced explicitly as

$$C_{1313} = \frac{\lambda_1\left(\mu_1 + \mu_2\lambda_2^2\right)}{\lambda_2\lambda_3}, \quad C_{2323} = \frac{\lambda_2\left(\mu_1 + \mu_2\lambda_1^2\right)}{\lambda_1\lambda_3}. \tag{2.34}$$

2.2.3 Varga material

In respect of incompressible and nearly incompressible, the Varga strain energy functions is, perhaps, the most simple form which describes the full range of material response, see Rogerson (1997) and Rogerson and Sandiford (2002). The strain energy function which was first introduced as a compressible generalisation of the incompressible model by Varga (1966), has

the form

$$W = \mu(\lambda_1 + \lambda_2 + \lambda_3 - 3 - \ln J), \tag{2.35}$$

where μ is a shear modulus. Notwithstanding its simplistic representation in terms of the stretches, the dynamic response of a Varga material is richer than that of a neo-Hookean or Mooney-Rivlin material. The reason for this is that full range of material response can be obtained by using a Varga strain energy function whilst using a neo-Hookean or Mooney-Rivlin material are restricted to possible values of material parameters, see for example Rogerson and Fu (1995) and Rogerson and Sandiford (1997). The components of the elasticity tensor corresponding to the Varga material may be given by

$$C_{iiii} = 0, \;\; C_{iijj} = 0, \;\; C_{ijij} = \frac{\mu\lambda_i^2}{J(\lambda_i + \lambda_j)}, \;\; C_{ijji} = \frac{\mu\lambda_i\lambda_j}{J(\lambda_i + \lambda_j)}, \\ i \neq j, \quad i, j \in \{1, 2, 3\}, \tag{2.36}$$

with no summation over repeated suffices. A feature of Varga material for all deformations given $\mu > 0$ is that this material is strongly elliptic. Ogden (1972) found that Varga material with $\mu = 8.0 kg/cm^2$, in particular comprise the strong ellipticity of this material. This is provided in order to suite the data of Treloar (1944). We will use this material in our numerical com-

putations. Although the range of applicability of the Varga model is similar to that of a neo-Hookean or a Mooney-Rivlin material (only relatively small deformations are allowed), it is principally different from both of them since the strain energy function (2.35) does not possess a (simple) representation in terms of the invariants of the deformation (2.8). This indicates that in general, the strain energy function is not a simple function of the invariants. In the case of anti-plane shear, the only two components of the elasticity tensor needed are expressible in terms of the principal stretches as

$$C_{1313} = \frac{\mu\lambda_1}{(\lambda_1+\lambda_3)\lambda_2\lambda_3}, \quad C_{2323} = \frac{\mu\lambda_2}{(\lambda_2+\lambda_3)\lambda_1\lambda_3}. \tag{2.37}$$

2.3 Propagator matrix for a finite layer and anti-plane shear

A convenient method for treating multi-layered media is the propagator matrix which is used to facilitate this study in later chapters. The governing equations for a pre-stressed, compressible elastic layer are now derived in terms of the propagator matrix. Such matrices have found application within the study of wave motion in layered media and were first introduced in seismological studies by Gilbert and Backus (1966). With use of the

components of the elasticity tensor $\mathbf{C}$ shown in equations (2.19), the single equation of motion in respect of anti-plane shear, with $(u_1, u_2, u_3) = (0, 0, u_3)$ and $u_3 = u(x_1, x_2, t)$, for a pre-stressed, compressible elastic material, may be express as

$$C_{1313}u_{3,11} + C_{2323}u_{3,22} = \rho\ddot{u}_3. \tag{2.38}$$

Now we will seek solutions of the equation of motion as a travelling wave solution

$$u_3(x_1, x_2, t) = Ue^{kqx_2}e^{ik(x_1-\upsilon t)}, \tag{2.39}$$

where k is the wave number, U is an arbitrary constant, υ is the phase speed and q is to be determined. After substituting the above solution into (2.38), we obtain a homogeneous equation, this equation possesses a non-trivial solution if and only if

$$C_{2323}q^2 - C_{1313} + \rho\upsilon^2 = 0, \tag{2.40}$$

providing

$$q^2 = \frac{C_{1313} - \rho\upsilon^2}{C_{2323}}. \tag{2.41}$$

The solution for u_3 may be represented as a linear combination of the two independent solutions associated with the roots of (2.41). This solution may then be recast in the form

$$u_3 = Ae^{kqx_2} + Be^{-kqx_2}. \tag{2.42}$$

We now note that the incremental surface traction is given by

$$\widehat{\tau} = \frac{\tau_3}{k} = C_{2323}\left(Aqe^{kqx_2} - Bqe^{-kqx_2}\right). \tag{2.43}$$

A displacement-traction vector may now be written in the matrix form as

$$\begin{pmatrix} u_3 \\ \\ \widehat{\tau} \end{pmatrix} = \begin{pmatrix} e^{kqx_2} & e^{-kqx_2} \\ \\ q\,C_{2323}e^{kqx_2} & -q\,C_{2323}e^{-kqx_2} \end{pmatrix} \begin{pmatrix} A \\ \\ B \end{pmatrix}. \tag{2.44}$$

In later multi-layered problems, composed of perfectly bonded layers, this vector is assumed continuous across each interface.

We now consider a layer, with the upper surface located at $x_2 = x_u$,

with $u_3 = u_3^u$ and $\widehat{\tau} = \widehat{\tau}^u$ at this location. Thus, the relation (2.44) may be introduced for the upper surface in the form

$$\begin{pmatrix} u_3^u \\ \\ \widehat{\tau}^u \end{pmatrix} = \begin{pmatrix} e^{kqx_u} & e^{-kqx_u} \\ \\ q\, C_{2323} e^{kqx_u} & -q\, C_{2323} e^{-kqx_u} \end{pmatrix} \begin{pmatrix} A \\ \\ B \end{pmatrix}. \tag{2.45}$$

At the lower interface, the analogue of the above yields

$$\begin{pmatrix} u_3^l \\ \\ \widehat{\tau}^l \end{pmatrix} = \begin{pmatrix} e^{kqx_l} & e^{-kqx_l} \\ \\ q\, C_{2323} e^{kqx_l} & -q\, C_{2323} e^{-kqx_l} \end{pmatrix} \begin{pmatrix} A \\ \\ B \end{pmatrix}. \tag{2.46}$$

From (2.45) we have

$$\begin{pmatrix} A \\ \\ B \end{pmatrix} = \left(\frac{1}{2q\, C_{2323}}\right) \begin{pmatrix} -qC_{2323} e^{-kqx_u} & -e^{-kqx_u} \\ \\ -qC_{2323} e^{kqx_u} & e^{kqx_u} \end{pmatrix} \begin{pmatrix} u_3^u \\ \\ \widehat{\tau}^u \end{pmatrix}. \tag{2.47}$$

By now inserting equation (2.47) into (2.46), we obtain

$$\begin{pmatrix} u_3^l \\ \\ \widehat{\tau}^l \end{pmatrix} = \begin{pmatrix} \dfrac{e^{kqx_l}}{2q\, C_{2323}} & \dfrac{e^{-kqx_l}}{2q\, C_{2323}} \\ \\ \frac{1}{2} e^{kqx_l} & -\frac{1}{2} e^{-kqx_l} \end{pmatrix} \begin{pmatrix} -qC_{2323} e^{-kqx_u} & -e^{-kqx_u} \\ \\ -qC_{2323} e^{kqx_u} & e^{kqx_u} \end{pmatrix} \begin{pmatrix} u_3^u \\ \\ \widehat{\tau}^u \end{pmatrix}. \tag{2.48}$$

It is easy to deduce that the above relationship may be written in the fol-

lowing form

$$\mathbf{Y}(x_l) = \mathbf{Q}\ \mathbf{Y}(x_u), \tag{2.49}$$

in which $\mathbf{Y}(x_l)$ and $\mathbf{Y}(x_u)$ are the appropriate column vector of the displacements and tractions for lower and upper surface defined by $(u_3^l, \widehat{\tau}^l)^T$ and $(u_3^u, \widehat{\tau}^u)^T$, respectively. The $\mathbf{Q}$ matrix may be directly expressed as

$$\mathbf{Q} = \begin{pmatrix} \cosh(kq(x_l - x_u)) & \dfrac{1}{q\, C_{2323}} \sinh(kq(x_l - x_u)) \\ q\, C_{2323} \sinh(kq(x_l - x_u)) & \cosh(kq(x_l - x_u)) \end{pmatrix}. \tag{2.50}$$

On the other hand, equation (2.49) can be formulated as

$$\mathbf{Y}(x_u) = \mathbf{P}\ \mathbf{Y}(x_l), \tag{2.51}$$

with, $\mathbf{P} = \mathbf{Q}^{-1}$.

The propagator matrix formula for a single layer plate will be given as

$$\begin{pmatrix} u_3^u \\ \widehat{\tau}^u \end{pmatrix} = \begin{pmatrix} p_{11} & p_{12} \\ p_{21} & p_{22} \end{pmatrix} \begin{pmatrix} u_3^l \\ \widehat{\tau}^l \end{pmatrix}. \tag{2.52}$$

By considering a single layer plate of thickness h, thus $x_u - x_l = h$, we can introduce the elements p_{11}, p_{12}, p_{21} and p_{22} as

$$
\begin{aligned}
p_{11} &= p_{22} = \cosh(kqh) \\
p_{12} &= \frac{1}{q\, C_{2323}} \sinh(kqh), \\
p_{21} &= q\, C_{2323} \sinh(kqh).
\end{aligned}
\tag{2.53}
$$

2.4 Analysis of the dispersion relation for single layer

We shall now derive and investigate the dispersion relation associated with anti-plane shear waves propagating in a single layer plate. Such a relation provides a relationship between wave speed (or frequency) and wave number. These are obtained by satisfying boundary conditions at the upper and lower surfaces of the layer. This will be carried out in respect of three different sets of boundary conditions. The first is the so-called free case, in which traction vanishes on each free surface, the second type of boundary condition, which we term fixed-free, is one in which the traction vanishes on one surface with the displacement vanishing on the other. The third, so-called fixed, assumes the vanishing of displacement.

2.4.1 Pre-stressed elastic materials

To present the analysis of long wave motion for pre-stressed materials in a fairly transparent manner, we first consider the numerical analysis of the dispersion relation associated with three different boundary value problems to demonstrate the range of materials response, as follows.

Free-faces case

The first investigated boundary value problem of the pre-stressed elastic layer is the free-faces problem, i.e. the incremental surface tractions vanish at upper and lower surfaces, providing

$$\widehat{\tau}_3^u = \widehat{\tau}_3^l = 0 \quad \text{at} \;\; x_2 = 0 \;\; \text{and} \;\; x_2 = h. \tag{2.54}$$

Employing the above boundary conditions into the solution (2.51), yields

$$0 = p_{21} u_3^l. \tag{2.55}$$

Hence, $p_{21} = 0$, which gives the dispersion relation for a single layer plate in the form

$$\sinh(kqh) = 0. \tag{2.56}$$

The dispersion relation (2.56) gives relationship between the wave number kh and the scaled phase speed $\rho\upsilon = \bar{\upsilon}$ (or scaled frequency $\bar{\Omega} = \bar{\upsilon}(kh)$) for a given state of the pre-stress.

In this case $\bar{\upsilon} \to \infty$ in the long wave region, accordingly the associated dispersion relation (2.56) will be represented as $\sin k\widehat{q}h = 0$, with $q = i\widehat{q}$ which dictates that $k\widehat{q}h = n\pi$. For a single layer, both scaled wave speed and frequency can be expressed explicitly in analytical form, from which we will present the squared phase wave speed and scaled frequency as functions of kh in the following form

$$\bar{\upsilon}^2 = C_{1313} + C_{2323}\left(\frac{n\pi}{kh}\right)^2, \tag{2.57}$$

and

$$\bar{\Omega}^2 = C_{2323}\,(n\pi)^2 + C_{1313}(kh)^2. \tag{2.58}$$

In this section, some values of the two parameters C_{1313} and C_{2323} relating to material models considered are used to generate the figures presented. Plots of scaled phase speed and scaled frequency against scaled wave number are presented for some branches of the dispersion relations (2.56), in Figures 2.3 and 2.4, respectively.

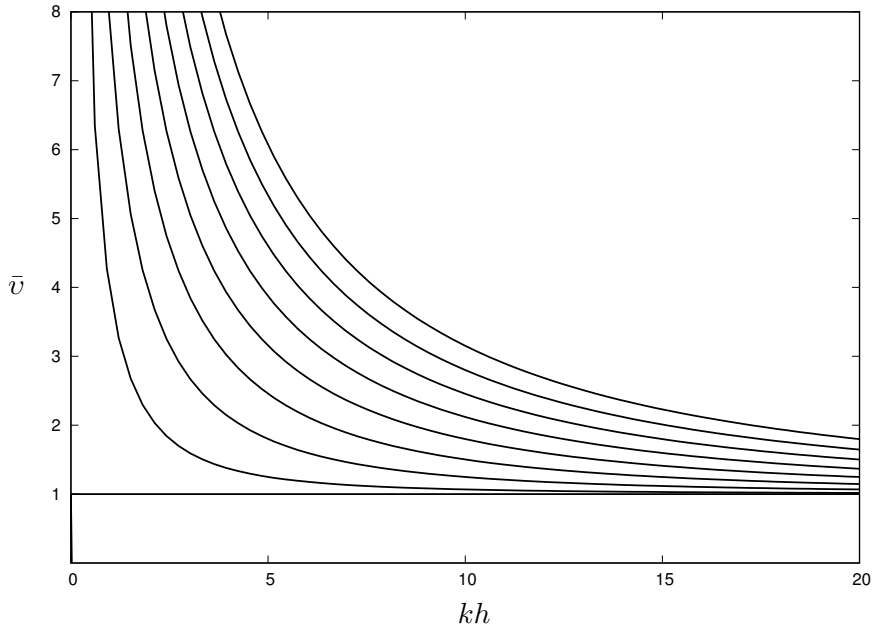

Figure 2.3: Scaled wave speed against scaled wave number for the free-faces dispersion relation (2.56); $C_{1313} = 1, C_{2323} = 1.414$.

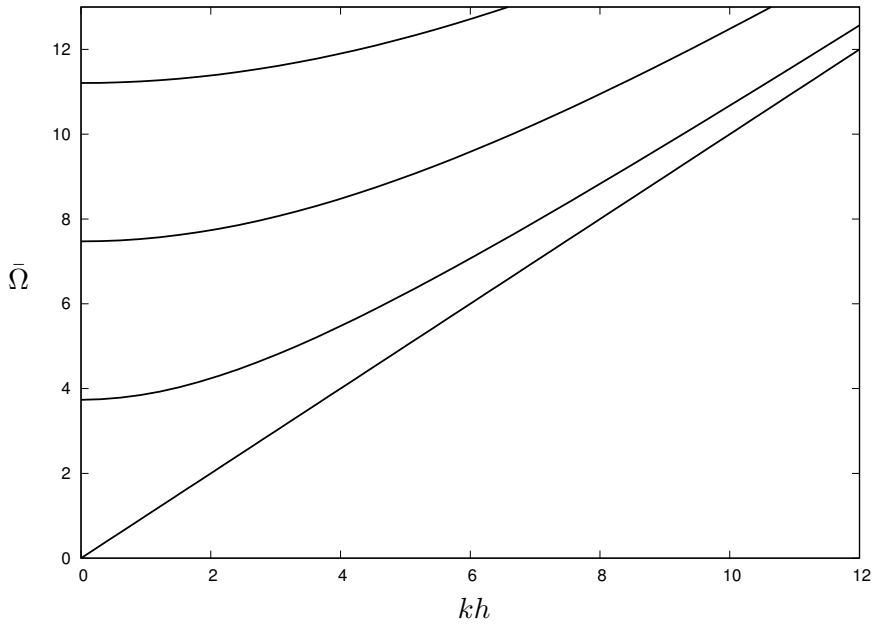

Figure 2.4: Scaled frequency against scaled wave number for the free-faces dispersion relation (2.56); $C_{1313} = 1, C_{2323} = 1.414$.

It is noted that, for small wave number, no mode except for the fundamental one retains finite wave speed, and all harmonics have an associated large wave speed. Also, we note here, that each corresponding frequency harmonics have non-zero limits. Moreover, the phase speed is scaled by the square root of the material parameter C_{1313}.

Fixed-free case

Now we will investigate a single layer with a traction free upper boundary and no displacement on its lower boundary, a problem which we will refer to as the fixed-free faces problem. The appropriate expression of boundary conditions are provided by

$$\widehat{\tau}^l = 0 \quad \text{at} \;\; x_2 = 0 \;\; \text{and} \;\; u_3^u = 0 \;\; \text{at} \; x_2 = h. \tag{2.59}$$

After applying the above boundary conditions, into (2.49), we arrive at

$$0 = p_{11} u_3^l, \tag{2.60}$$

therefore, $p_{11} = 0$, which implies the dispersion relation in the form

$$\cosh\left(kqh\right) = 0. \tag{2.61}$$

Figure 2.5 shows scaled wave speed against scaled wave number for the first thirteen curves of the dispersion relation (2.61). Clearly, there is no finite phase speed limits and $\bar{v} \to \infty$ in the long wave region. Thus, the scaled phase speed and frequency for this case may be introduced as follows

$$\bar{v}^2 = C_{1313} + \frac{C_{2323}}{(kh)^2}\left(\frac{(2n+1)\pi}{2}\right)^2, \tag{2.62}$$

and

$$\bar{\Omega}^2 = C_{2323}\left(\frac{(2n+1)\pi}{2}\right)^2 + C_{1313}(kh)^2. \tag{2.63}$$

The associated scaled frequencies are presented in Figure 2.6. In all these respect figures, it is remarked that the non-zero frequency limits, termed the cut-off frequencies, are not too small, for all dispersion curves. An important feature is that, no fundamental mode observed as $kh \to 0$, and the lowest cut-off frequency given by, $\bar{\Omega} \approx 3.7$ in free-faces case and $\bar{\Omega} \approx 1.82$ in fixed free faces.

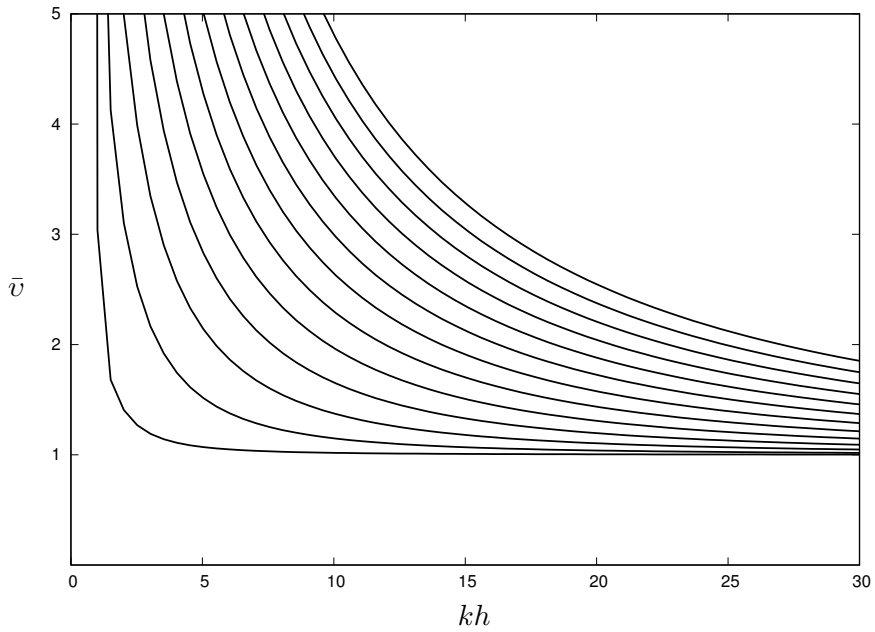

Figure 2.5: Scaled wave speed against scaled wave number for the fixed-free faces dispersion relation (2.61); $C_{1313} = 1, C_{2323} = 1.414$.

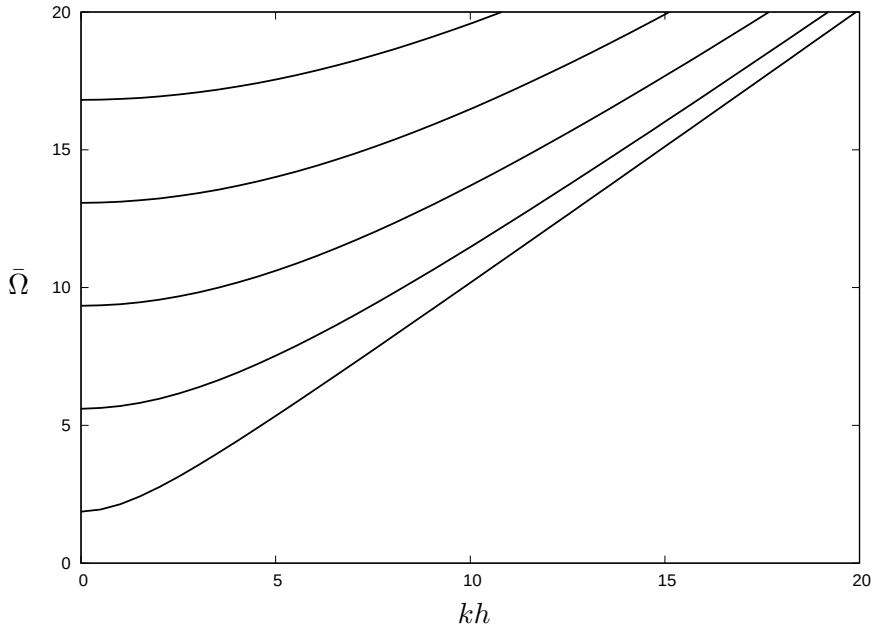

Figure 2.6: Scaled frequency against scaled wave number for the fixed-free faces dispersion relation (2.61); $C_{1313} = 1, C_{2323} = 1.414$.

Fixed-faces case

Consider now a layer with fixed faces, the so-called fixed problem. The associated boundary conditions of zero displacement on the upper and lower faces of the single layer are specified by

$$u_3^u = u_3^l = 0, \text{at } \; x_2 = 0 \; \text{ and } \; x_2 = h. \tag{2.64}$$

After inserting the above conditions into (2.49), we arrive at

$$p_{12}\widehat{\tau}^l = 0, \tag{2.65}$$

leading to $p_{12} = 0$, this gives the same dispersion relation as the free faces boundary value problem (2.56) in the form

$$\sinh(kqh) = 0. \tag{2.66}$$

From the numerical analysis made for a pre-stressed layer it may be observed that no mode has a finite wave speed limit at $kh = 0$ except for the fundamental mode in case of free faces, and all harmonics possess speeds of $O((kh)^{-1})$.

2.4.2 Linear isotropic materials

Here we establish the special case of pre-stressed materials which is linear isotropic for the anti-plane shear problem. In this case, $C_{1313} = C_{2323} = \mu$ and accordingly the only parameter describing material response is the shear modulus μ. It is worth to mention that (2.41) may be expressed in terms of μ as

$$q^2 = 1 - \frac{\rho \upsilon^2}{\mu}. \tag{2.67}$$

Free-faces case

In this case, we assume a free face problem with the lower and upper layer located at $x_2 = 0$ and $x_2 = h$, respectively. The boundary conditions therefore are similar as (2.54) in the pre-stressed case. Upon using (2.52) and (2.54), the associated dispersion relation is shown to be

$$\sinh(kqh) = 0. \tag{2.68}$$

To gain some insight into the character of the dispersion relations, we present the cases through some graphs within $\mu = 0.5$ for all figures presented. At this stage, this value is taken just to illustrate general material response, rather than model any specific material. In Figure 2.7 a plot of scaled phase

speed $\bar{v}$, where $\bar{v}^2 = \rho v^2$, against scaled wave number kh is presented for the first sixteen branches for a dispersion relation associated with a layer with free faces. We remark that, in the long wave limit (low wave number) there is no fundamental mode and the wave speeds all tend to infinity. In Figure 2.8, a plot of scaled frequency $\bar{\Omega} = \bar{v}(kh)$ against scaled wave number is presented. In this figure we first note that the long wave limit of each harmonic is non-zero. Usually we refer to these limits as cut-off frequencies. Another feature of this graph is that, the lowest cut-off frequency is located at $\bar{\Omega} \approx 2.12$.

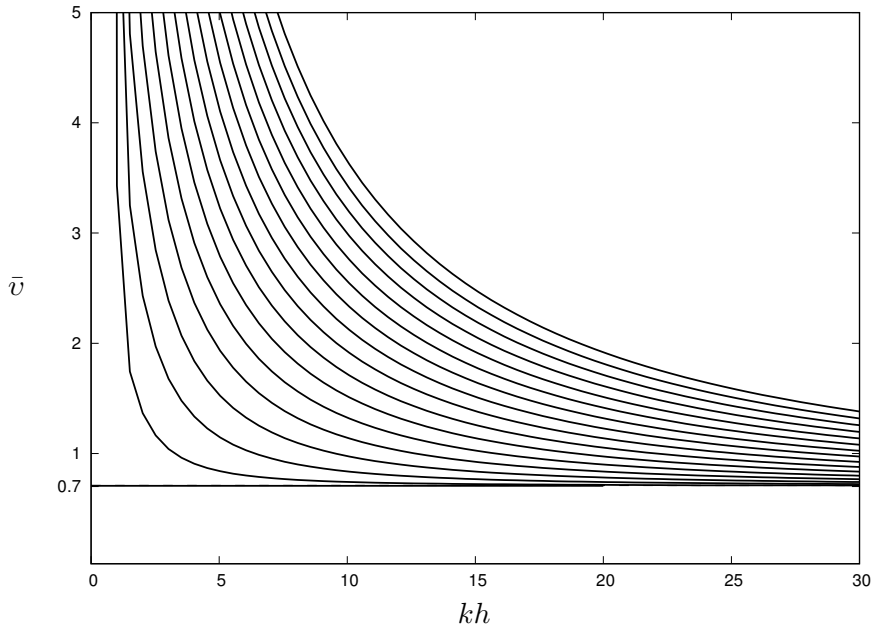

Figure 2.7: Scaled wave speed against scaled wave number for the free-faces dispersion relation (2.68); $\mu = 0.5$.

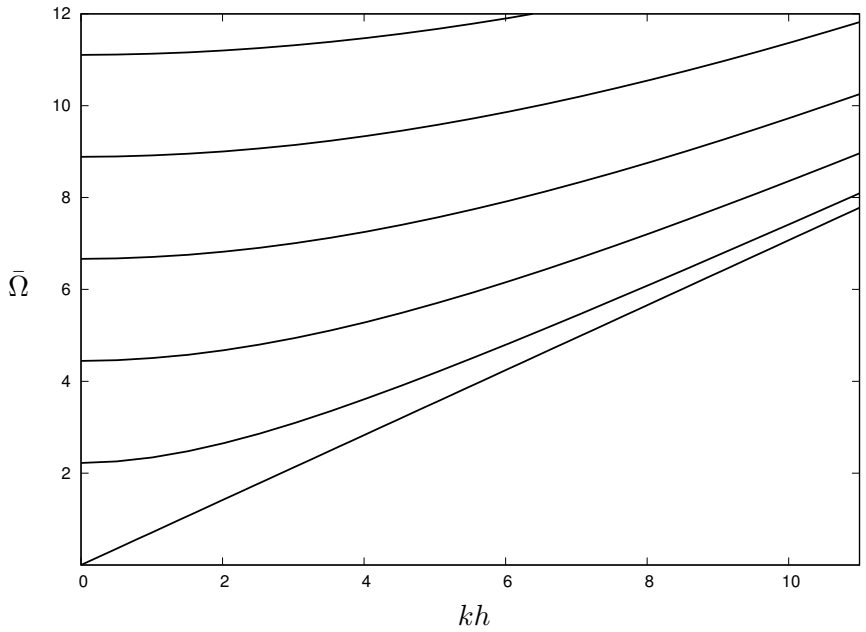

Figure 2.8: Scaled frequency against scaled wave number for the free-faces dispersion relation (2.68); $\mu = 0.5$

Fixed-free faces case

We now consider a layer subject to a traction free upper boundary and no displacement on its lower boundary, which may be expressed as follows

$$\widehat{\tau}^u = 0 \quad \text{at} \quad x_2 = h, \quad u_3^l = 0 \quad \text{at} \quad x_2 = 0. \tag{2.69}$$

After employing these boundary conditions in (2.51), we arrive at the dispersion relation for fixed-free faces problem, giving by

$$\cosh(kqh) = 0. \tag{2.70}$$

Motivated by issues previously discussed for free-faces boundary condition, together with the dispersion relation in this case, we will reintroduce (2.70) as $\cos k\hat{q}h = 0$, which dictates $k\hat{q}h = \dfrac{(2n+1)\pi}{2}$, n is integer. Then the squared phase wave speed and scaled frequency may be presented as functions of kh in the following form

$$\bar{v}^2 = \mu + \frac{\mu}{(kh)^2}\left(\frac{(2n+1)\pi}{2}\right)^2, \tag{2.71}$$

$$\bar{\Omega}^2 = \mu\left(\frac{(2n+1)\pi}{2}\right)^2 + \mu(kh)^2. \tag{2.72}$$

Figures 2.9 and 2.10 show scaled phase speed and frequency against the scaled wave number for the dispersion relation (2.70), respectively. Numerical analysis in figures 2.9 and 2.10 reveals that for a layer with fixed-free faces, there is no low frequency motion in the low wave number (long wave) region ($kh \to 0$). We also note that, each harmonic has a non-zero finite value and for all branches, it is the case that as ($kh \to 0$), ($\bar{v} \to \infty$).

Fixed-faces case

This case of boundary as with the pre-stressed case, so we have the same dispersion relation (2.68).

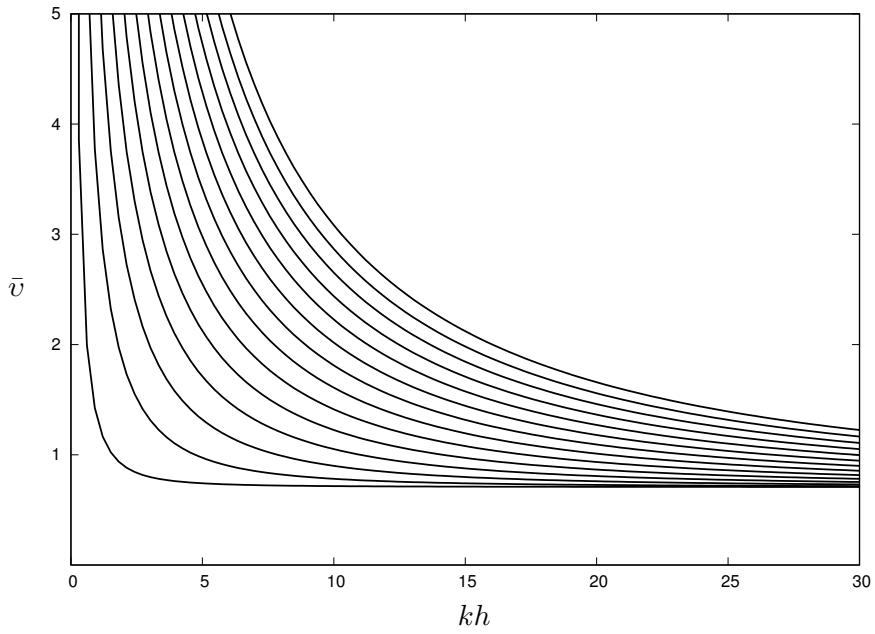

Figure 2.9: Scaled wave speed against scaled wave number for the fixed-free faces dispersion relation (2.70); $\mu = 0.5$.

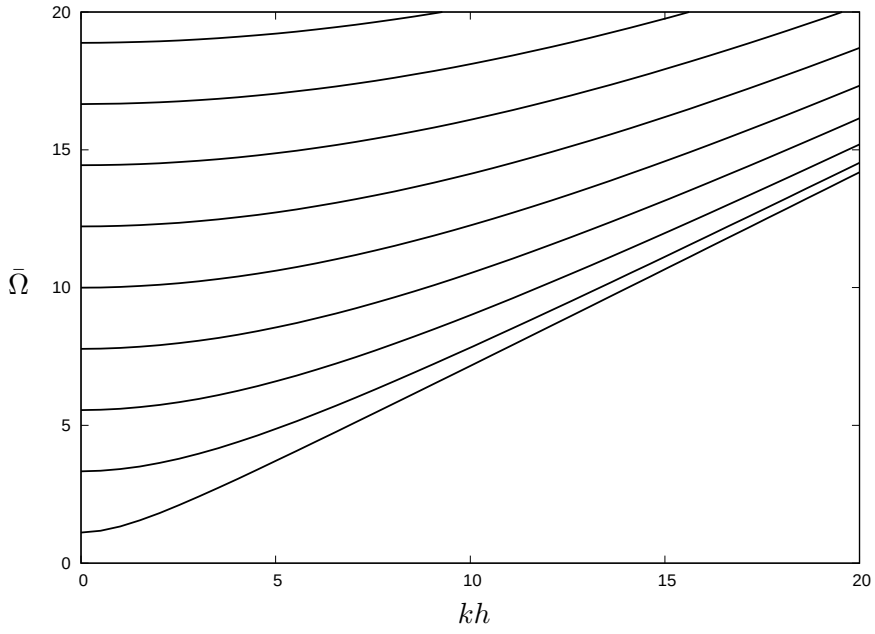

Figure 2.10: Scaled frequency against scaled wave number for the fixed-free faces dispersion relation (2.70); $\mu = 0.5$.

Chapter 3

Long wave motion in a 2-layered laminate structure

The propagation of travelling waves in a compressible pre-stressed, 2-layered laminate will be considered in this chapter. Having, in Chapter 2 obtained the equations governing the propagation of small amplitude waves in pre-stressed compressible elastic media for a single layer, we will now derive the governing equations for similar waves propagating along a common principal direction in a pre-stressed, compressible 2-layered laminate structure.

3.1 Governing equations

The laminate under consideration in this chapter is formed by layer 1 and layer 2 of the same thickness h (which is often the case in industrial applications), with again Ox_2 orthogonal to the laminate. The structure is finite in the Ox_2 direction and infinite in both other directions. The layer 1 of thickness h is defined from $0 \leq x_2 \leq h$ and layer 2 is defined from $h \leq x_2 \leq 2h$, see Figure 3.1. Furthermore, it is also assumed that the interface between layer 1 and layer 2 is perfectly bonded, ensuring continuity of both traction and displacement at the interface. We adopt a state of anti-plane shear for this two layer problem. Thus the displacement is independent of Ox_3 and of the form $(u_1, u_2, u_3) = (0, 0, u_3)$ and the linearised equations of motion, (2.38) in Chapter 2, may now establish for each layer of the 2-layered structure as follows

$$C^{(n)}_{1313} u^{(n)}_{3,11} + C^{(n)}_{2323} u^{(n)}_{3,22} = \rho \ddot{u}^{(n)}_3. \tag{3.1}$$

In a similar way to previously mentioned in Chapter 2, the solution of the equations of motion is sought as a travelling wave in the form

$$u^{(n)}_3(x_1, x_2, t) = U e^{kq_n x_2} e^{ik(x_1 - \upsilon t)}, \quad n = 1, 2, \tag{3.2}$$

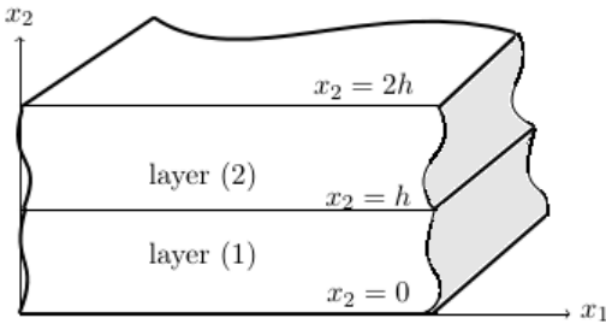

Figure 3.1: Two layers structure.

where k is the wave number, U is an arbitrary constant, ρ is the common density for both layers, υ is the phase wave speed. Also in (3.2) the subscript (n) denotes the layer number, $n = 1, 2$ and q_n is to be determined. After substituting the above solution into (3.1), and following the analysis of Chapter 2, we obtain a linearised equation, which possesses a non-trivial solution provided

$$C^{(n)}_{2323} q_n^2 - C^{(n)}_{1313} + \rho \upsilon^2 = 0, \tag{3.3}$$

and the displacement can be written as

$$u_3^{(n)} = A_n e^{k q_n x_2} + B_n e^{-k q_n x_2}. \tag{3.4}$$

In addition, the non-zero incremental traction may be written in component

form by

$$\widehat{\tau}^{(n)} = \frac{\tau_3^{(n)}}{k} = C_{2323}^{(n)} \left(A_n q_n e^{kq_n x_2} - B_n q_n e^{-kq_n x_2} \right), \tag{3.5}$$

in which,

$$q_1^2 = \frac{C_{1313}^{(1)} - \bar{\upsilon}^2}{C_{2323}^{(1)}},\ q_2^2 = \frac{C_{1313}^{(2)} - \bar{\upsilon}^2}{C_{2323}^{(2)}}, \tag{3.6}$$

where $\bar{\upsilon}^2 = \rho \upsilon^2$.

Propagator matrix for a two-layered laminate structure

The solutions of displacements and tractions are represented by the propagator matrix form shown in (2.51) in Chapter 2, as

$$\mathbf{Y}(x_u) = \mathbf{P}\, \mathbf{Y}(x_l), \tag{3.7}$$

where, u and l denote to the upper and lower surfaces of the appropriate layer, respectively. The appropriate material parameters for layer 1 are denoted by $C_{2323}^{(1)}$ and $C_{1313}^{(1)}$. Accordingly, appropriate matrix form of (3.4) and (3.5) are given, similar to equations (2.45) and (2.46) in Chapter2, by

$$\begin{pmatrix} u_3^{(1)} \\ \\ \widehat{\tau}^{(1)} \end{pmatrix} = \begin{pmatrix} e^{kq_1 h} & e^{-kq_1 h} \\ \\ q_1 C_{2323}^{(1)} e^{kq_1 h} & -q_1 C_{2323}^{(1)} e^{-kq_1 h} \end{pmatrix} \begin{pmatrix} A_1 \\ \\ B_1 \end{pmatrix}, \tag{3.8}$$

and for layer 2, by

$$\begin{pmatrix} u_3^{(2)} \\ \\ \widehat{\tau}^{(2)} \end{pmatrix} = \begin{pmatrix} e^{kq_2h} & e^{-kq_2h} \\ \\ q_2C_{2323}^{(2)}e^{kq_2h} & -q_2C_{2323}^{(2)}e^{-kq_2h} \end{pmatrix} \begin{pmatrix} A_2 \\ \\ B_2 \end{pmatrix}. \tag{3.9}$$

By using (3.7) we may write the relationship between the upper boundary $x_2 = h$ and the lower boundary $x_2 = 0$ in the following matrix form

$$\begin{pmatrix} u_3^{(1)} \mid_{x_2=h} \\ \\ \widehat{\tau}^{(1)} \mid_{x_2=h} \end{pmatrix} = \begin{pmatrix} \cosh(kq_1h) & \dfrac{\sinh(kq_1h)}{C_{2323}^{(1)}q_1} \\ \\ C_{2323}^{(1)}q_1 \sinh(kq_1h) & \cosh(kq_1h) \end{pmatrix} \begin{pmatrix} u_3^{(1)} \mid_{x_2=0} \\ \\ \widehat{\tau}^{(1)} \mid_{x_2=0} \end{pmatrix}, \tag{3.10}$$

which also can be expressed in the form

$$\mathbf{Y}(h) = \mathbf{P}^{(1)}\, \mathbf{Y}(0). \tag{3.11}$$

Following the analysis for layer 1, we can write the similar relation (3.10) for layer 2 as

$$\begin{pmatrix} u_3^{(2)} \mid_{x_2=2h} \\ \\ \widehat{\tau}^{(2)} \mid_{x_2=2h} \end{pmatrix} = \begin{pmatrix} \cosh(kq_2h) & \dfrac{\sinh(kq_2h)}{C_{2323}^{(2)}q_2} \\ \\ C_{2323}^{(2)}q_2 \sinh(kq_2h) & \cosh(kq_2h) \end{pmatrix} \begin{pmatrix} u_3^{(2)} \mid_{x_2=h} \\ \\ \widehat{\tau}^{(2)} \mid_{x_2=h} \end{pmatrix}, \tag{3.12}$$

which is can be readily presented as

$$\mathbf{Y}(2h) = \mathbf{P}^{(2)}\,\mathbf{Y}(h). \tag{3.13}$$

Inserting equation (3.11) into (3.13), yielding

$$\mathbf{Y}(2h) = \mathbf{P}^{(2)}\,\mathbf{P}^{(1)}\,\mathbf{Y}(0), \tag{3.14}$$

where,

$$\mathbf{P}^{(1)} = \begin{pmatrix} \cosh(kq_1h) & \dfrac{1}{C^{(1)}_{2323}q_1}\sinh(kq_1h) \\ C^{(1)}_{2323}q_1\sinh(kq_1h) & \cosh(kq_1h) \end{pmatrix}, \tag{3.15}$$

$$\mathbf{P}^{(2)} = \begin{pmatrix} \cosh(kq_2h) & \dfrac{1}{C^{(2)}_{2323}q_2}\sinh(kq_2h) \\ C^{(2)}_{2323}q_2\sinh(kq_2h) & \cosh(kq_2h) \end{pmatrix}. \tag{3.16}$$

The previous solution (3.14) may be introduced in the following form

$$\mathbf{Y}(2h) = \mathbf{P}\,\mathbf{Y}(0), \tag{3.17}$$

which also can be introduced as

$$\begin{pmatrix} u_3^{(2)}\,|_{x_2=2h} \\ \widehat{\tau}^{(2)}\,|_{x_2=2h} \end{pmatrix} = \begin{pmatrix} p_{11} & p_{12} \\ p_{21} & p_{22} \end{pmatrix} \begin{pmatrix} u_3^{(1)}\,|_{x_2=0} \\ \widehat{\tau}^{(1)}\,|_{x_2=0} \end{pmatrix}, \tag{3.18}$$

in which,

$$\mathbf{P} = \mathbf{P}^{(2)}\,\mathbf{P}^{(1)} = \begin{pmatrix} p_{11} & p_{12} \\ p_{21} & p_{22} \end{pmatrix}. \tag{3.19}$$

The components of the propagator matrix $\mathbf{P}$ are given explicitly in the following forms as

$$\begin{aligned}
p_{11} &= \cosh(kq_2h)\cosh(kq_1h) + \frac{C_{2323}^{(1)}q_1}{C_{2323}^{(2)}q_2}\sinh(kq_2h)\sinh(kq_1h), \\
p_{12} &= \frac{1}{C_{2323}^{(2)}q_2}\sinh(kq_2h)\cosh(kq_1h) + \frac{1}{C_{2323}^{(1)}q_1}\cosh(kq_2h)\sinh(kq_1h), \\
p_{21} &= C_{2323}^{(1)}q_1\cosh(kq_2h)\sinh(kq_1h) + C_{2323}^{(2)}q_2\sinh(kq_2h)\cosh(kq_1h), \\
p_{22} &= \cosh(kq_2h)\cosh(kq_1h) + \frac{C_{2323}^{(2)}q_2}{C_{2323}^{(1)}q_1}\sinh(kq_2h)\sinh(kq_1h).
\end{aligned}$$

3.2 Derivation of the dispersion relation of two layers

We will derive the dispersion relation for three problems by applying each boundary condition of each case on the solution (3.17) in this section. In

what follows the three boundary conditions problems considered in Chapter 2, will be studied in turn.

Free-faces case

By applying the boundary conditions of zero traction at the upper and lower surface of the two-layered structure, which has the form

$$\widehat{\tau}^{(1)} = 0 \ \text{ on } \ x_2 = 0, \qquad \widehat{\tau}^{(2)} = 0 \ \text{ on } \ x_2 = 2h, \tag{3.20}$$

and the condition of continuity across the perfectly bonded interface along $x_2 = h$, given by

$$\widehat{\tau}^{(1)} = \widehat{\tau}^{(2)}, \qquad u_3^{(1)} = u_3^{(2)}, \tag{3.21}$$

into (3.17), the dispersion relation for the free-faces case is obtained and my be written in the form

$$C_{2323}^{(1)} q_1 \sinh(kq_1h)\cosh(kq_2h) + C_{2323}^{(2)} q_2 \sinh(kq_2h)\cosh(kq_1h) = 0. \tag{3.22}$$

Fixed-free-faces case

The boundary conditions in this case are

$$u_3^{(2)} = 0 \ \text{ at } \ x_2 = 2h, \ \text{ and } \ \widehat{\tau}^{(1)} = 0 \ \text{ at } \ x_2 = 0. \tag{3.23}$$

Following the usual procedure, we arrive at the dispersion relation for fixed-free boundary value problem in the form

$$C^{(2)}_{2323}q_2\cosh(kq_2h)\cosh(kq_1h)+C^{(1)}_{2323}q_1\sinh(kq_2h)\sinh(kq_1h)=0. \quad (3.24)$$

Fixed-faces case

To obtain the dispersion relation for the third type of boundary conditions, namely the fixed-faces conditions, we will impose these conditions

$$u_3^{(1)}=0 \quad \text{at} \quad x_2=0, \quad \text{and} \quad u_3^{(2)}=0 \quad \text{at} \quad x_2=2h, \quad (3.25)$$

with the continuity conditions (3.21) into (3.17), allows us to arrive at the dispersion relation associated with this case in the form

$$C^{(1)}_{2323}q_1\sinh(kq_2h)\cosh(kq_1h)+C^{(2)}_{2323}q_2\cosh(kq_2h)\sinh(kq_1h)=0. \quad (3.26)$$

In the case of linear isotropy, it may be deduced from Chapter 2 that the two material parameters will be

$$C^{(n)}_{2323}=C^{(n)}_{1313}=\mu_n, \quad n=1,2. \quad (3.27)$$

Using now the traction-free boundary conditions (3.20) with continuity

conditions assumed in (3.17), the dispersion relation for the free-faces case is given by

$$\mu_1 q_1 \sinh(kq_1 h)\cosh(kq_2 h) + \mu_2 q_2 \sinh(kq_2 h)\cosh(kq_1 h) = 0. \tag{3.28}$$

For the fixed-free faces we obtain the dispersion relation in the form

$$\mu_1 q_1 \cosh(kq_1 h)\cosh(kq_2 h) + \mu_2 q_2 \sinh(kq_2 h)\sinh(kq_1 h) = 0, \tag{3.29}$$

whereas in case of fixed faces we result in

$$\mu_1 q_1 \sinh(kq_2 h)\cosh(kq_1 h) + \mu_2 q_2 \cosh(kq_2 h)\sinh(kq_1 h) = 0. \tag{3.30}$$

3.3 Numerical results

Throughout this section numerical results will be presented for various material parameters which elucidate the character of the dispersion relation. The resulting dispersion relations are first investigated numerically for pre-stressed materials by using three strain energy functions associated with the neo-Hookean, Mooney-Rivlin and Varga materials. This numerical investigations are then used to guide establishment of asymptotic of the wave speed as a function of wave number and pre-stress in the low wave number

regime. The particular parameters are chosen to demonstrate the range of material response which might be anticipated, rather than model any specific material. To demonstrate different types of behaviour of a compressible pre-stressed elastic materials in anti-plane shear for 2 layers, we will investigate in turn some particular strain-energy function associated with neo-Hookean, Mooney-Rivlin and Varga materials.

3.3.1 Neo-Hookean material

We will now establish some graphs, with the corresponding constitutive part of the strain-energy function presented in (2.30) in Chapter 2. A neo-Hookean material modelled by a strain-energy function depends on the first invariant of the strain tensor. Accordingly, we can introduce the two material parameters associated with the strain-energy function by

$$C_{1313}^{(n)} = \frac{\mu^{(n)}\lambda_1^{(n)}}{\lambda_2^{(n)}\lambda_3^{(n)}}, \quad C_{2323}^{(n)} = \frac{\mu^{(n)}\lambda_2^{(n)}}{\lambda_1^{(n)}\lambda_3^{(n)}}, \quad n = 1, 2. \tag{3.31}$$

Table 3.1: Neo-Hookean material used in numerical results

Materials	$\mu^{(n)}$	$\lambda_1^{(n)}$	$\lambda_2^{(n)}$	$\lambda_3^{(n)}$	$C_{1313}^{(n)}$	$C_{2323}^{(n)}$
Layer 1	0.6	1	1.5	0.5	0.8	1.80
Layer 2	2.2	2.5	1.5	2	1.83	0.660

In Figure 3.2, a plot of scaled phase speed $\bar{v}$ against scaled wave number K is presented for the first thirteen branches in respect of the dispersion relations for the neo-Hookean material subject to free faces boundary conditions. A significant difference from the previous work on a single layer is that there is one mode remains finite in the long wave limit, i.e. this mode has a distinct finite phase speed limit as $K \to 0$, therefore, the limiting wave speed being dependent on material parameters. We also note that in the low wave number (long wave region), all other harmonics have infinite phase speed limits and from which it can be observed that $\bar{v} \to \infty$ as $K \to 0$.

In Figure 3.3, corresponding plots of scaled frequency against scaled wave number are presented. We remark that the limit of the fundamental mode is zero and the harmonics limits are non-zero in the long wave region. Figure 3.4 and Figure 3.6 present a plot of scaled phase speed against scaled wave number for the dispersion relation (3.24) and (3.26), respectively. These figures show that $\bar{v} \to \infty$ as $K \to 0$. Also, these dispersion relations do not support the fundamental mode with zero cut-off frequency.

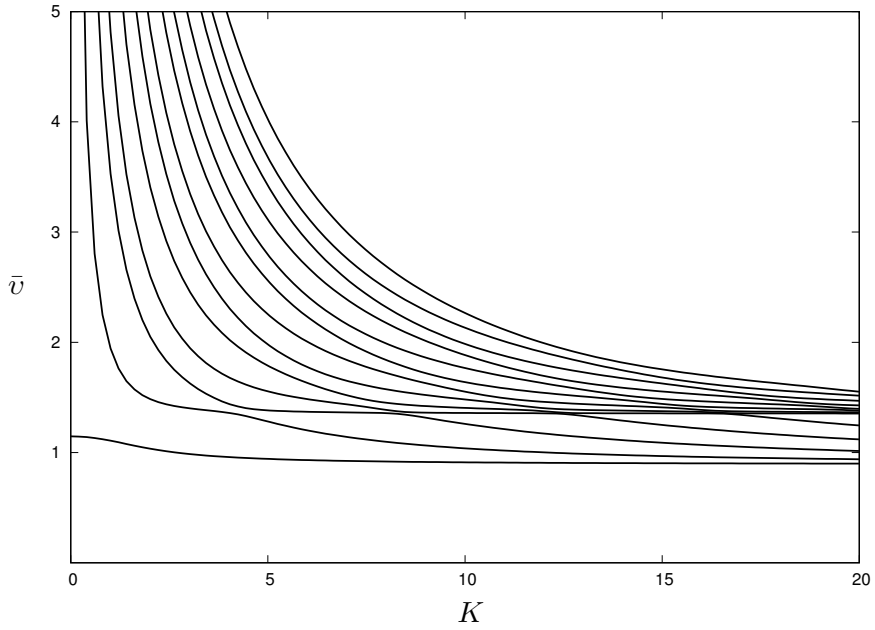

Figure 3.2: Scaled wave speed against scaled wave number for neo-Hookean materials 1 and 2 from Table 3.1 in layer 1 and layer 2, respectively, for the free-faces dispersion relation (3.22).

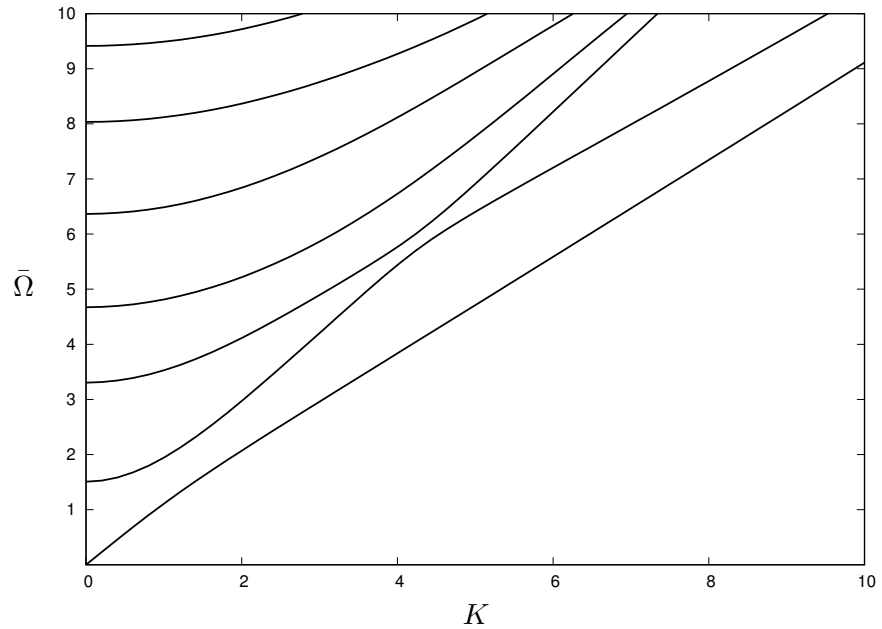

Figure 3.3: Scaled frequency against scaled wave number for a neo-Hookean materials 1 and 2 from Table 3.1 in layer 1 and layer 2, respectively, for the free-faces dispersion relation (3.22)

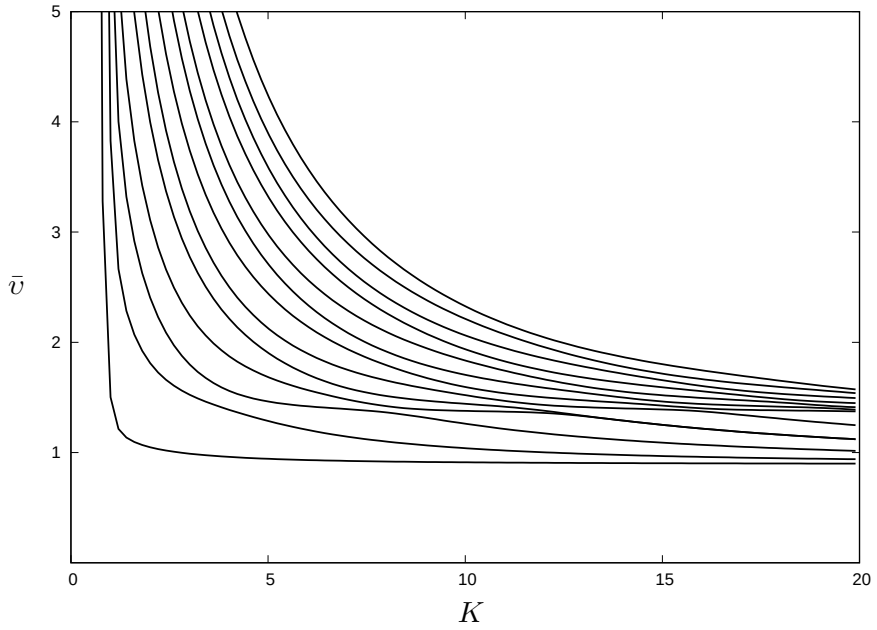

Figure 3.4: Scaled wave speed against scaled wave number for a neo-Hookean materials 1 and 2 from Table 3.1 in layer 1 and layer 2, respectively, for the fixed-free faces dispersion relation (3.24).

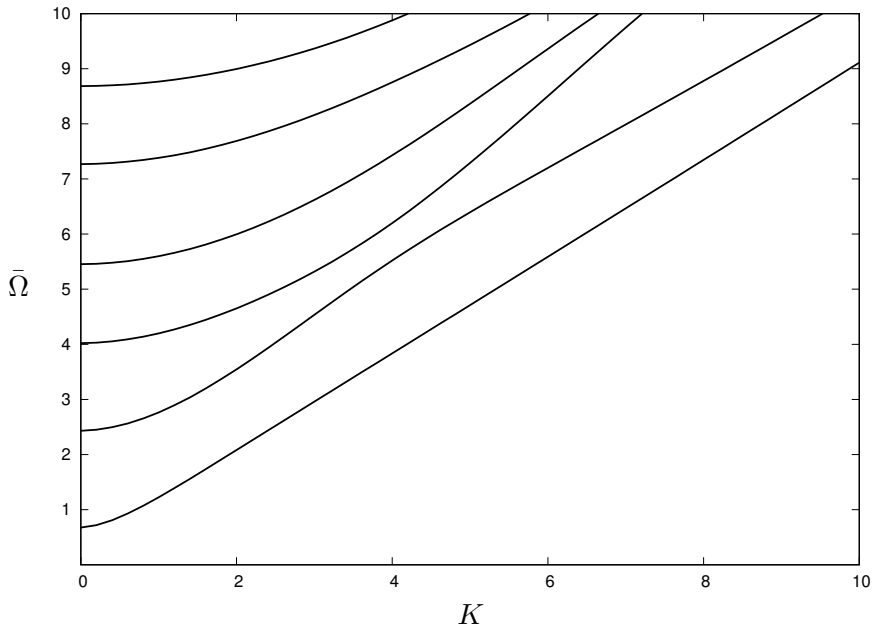

Figure 3.5: Scaled frequency against scaled wave number for a neo-Hookean materials 1 and 2 from Table 3.1 in layer 1 and layer 2, respectively, for the fixed-free faces dispersion relation (3.24).

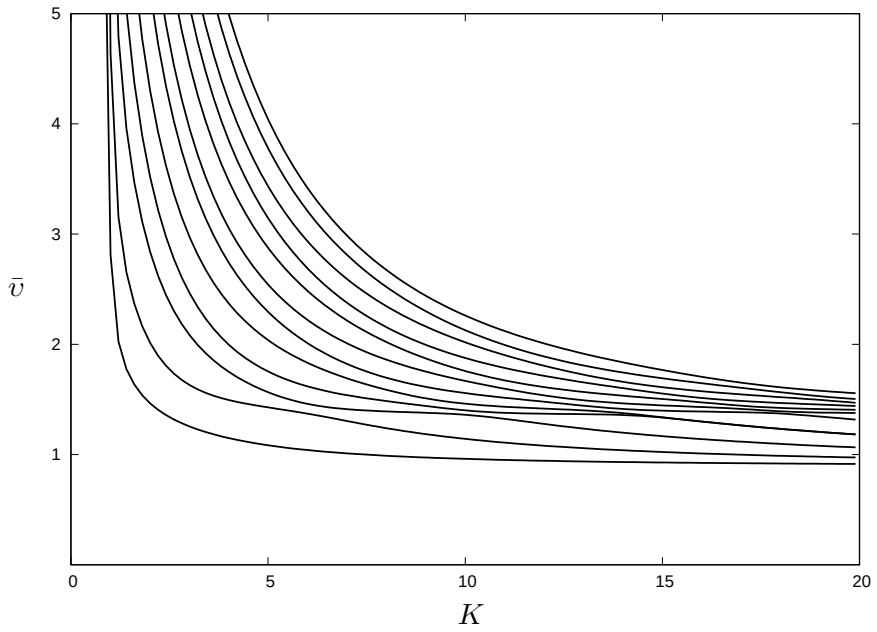

Figure 3.6: Scaled wave speed against scaled wave number for a neo-Hookean materials 1 and 2 from Table 3.1 in layer 1 and layer 2, respectively, for the fixed-faces dispersion relation (3.26).

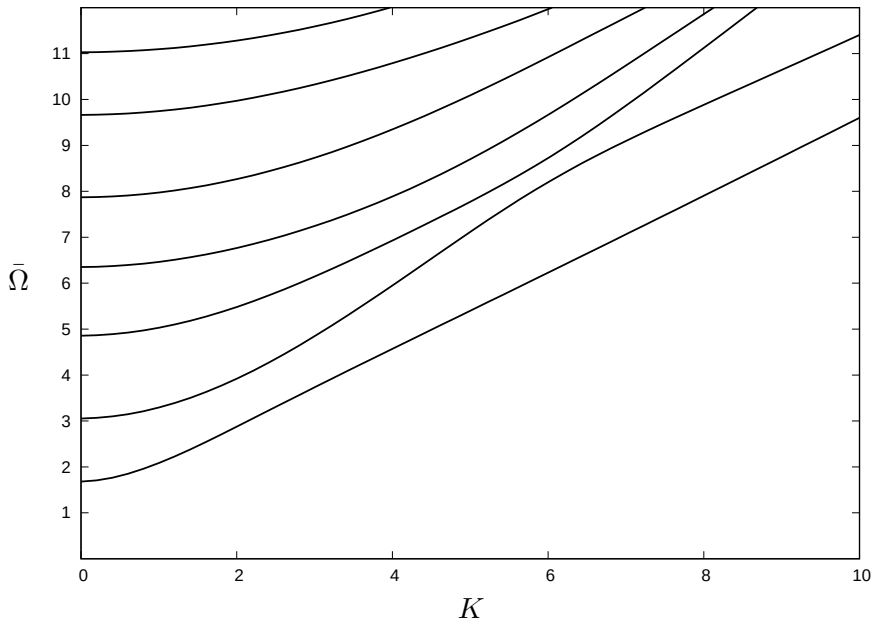

Figure 3.7: Scaled frequency against scaled wave number for a neo-Hookean materials 1 and 2 from Table 3.1 in layer 1 and layer 2, respectively, for the fixed-faces dispersion relation (3.26)

Figure 3.5 and Figure 3.7 show scaled frequency against scaled wave number in the case of the compressible neo-Hookean material in Table 3.1, for the dispersion relations (3.24) and (3.26), respectively. We remark that the long wave limit of each harmonic is non-zero. In doing so, the fundamental mode dose not exist in these types of boundary conditions.

3.3.2 Mooney-Rivlin material

Dispersion curves, subjected to the three types of boundary conditions, will be presented using material parameters for the two layers generated from the Mooney-Rivlin strain energy function provided in (2.32), with the two parameters taking the form

$$C_{1313}^{(n)} = \frac{\lambda_1^{(n)}\left(\mu_1^{(n)} + \mu_2^{(n)}(\lambda_2^{(n)})^2\right)}{\lambda_2^{(n)}\lambda_3^{(n)}}, \quad C_{2323}^{(n)} = \frac{\lambda_2^{(n)}\left(\mu_1^{(n)} + \mu_2^{(n)}(\lambda_1^{(n)})^2\right)}{\lambda_1^{(n)}\lambda_3^{(n)}}, \quad n = 1, 2. \tag{3.32}$$

Table 3.2: Mooney-Rivlin materials (MRM) used in numerical results

Materials	$\mu_1^{(n)}$	$\mu_2^{(n)}$	$\lambda_1^{(n)}$	$\lambda_2^{(n)}$	$\lambda_3^{(n)}$	$C_{1313}^{(n)}$	$C_{2323}^{(n)}$
Layer 1	1.2	0.3	1	1.1	1	1.42	1.65
Layer 2	1	1.1	2	2	10	0.64	0.54

We will now present some graphs, demonstrating the behaviour of Mooney-Rivlin materials listed in Table 3.2.

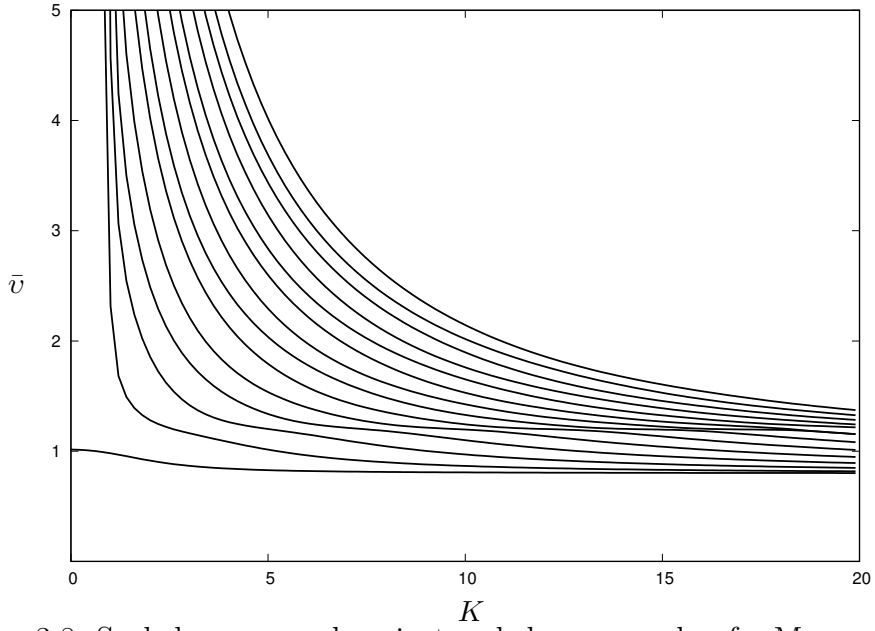

Figure 3.8: Scaled wave speed against scaled wave number for Mooney-Rivlin materials from Table 3.2 in layer 1 and layer 2, respectively, for the free-faces dispersion relation (3.22).

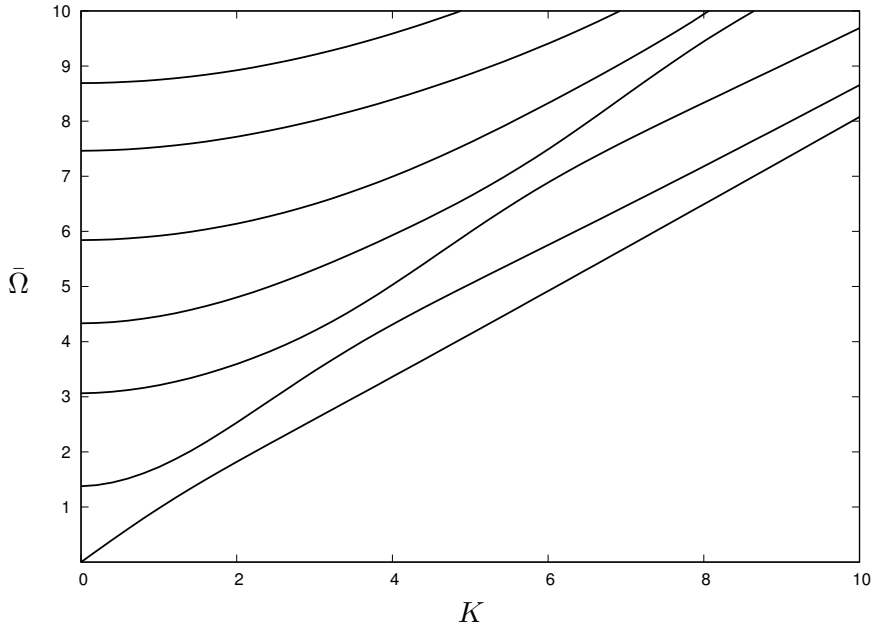

Figure 3.9: Scaled frequency against scaled wave number for Mooney-Rivlin materials from Table 3.2 in layer 1 and layer 2, respectively, for the free-faces dispersion relation (3.22).

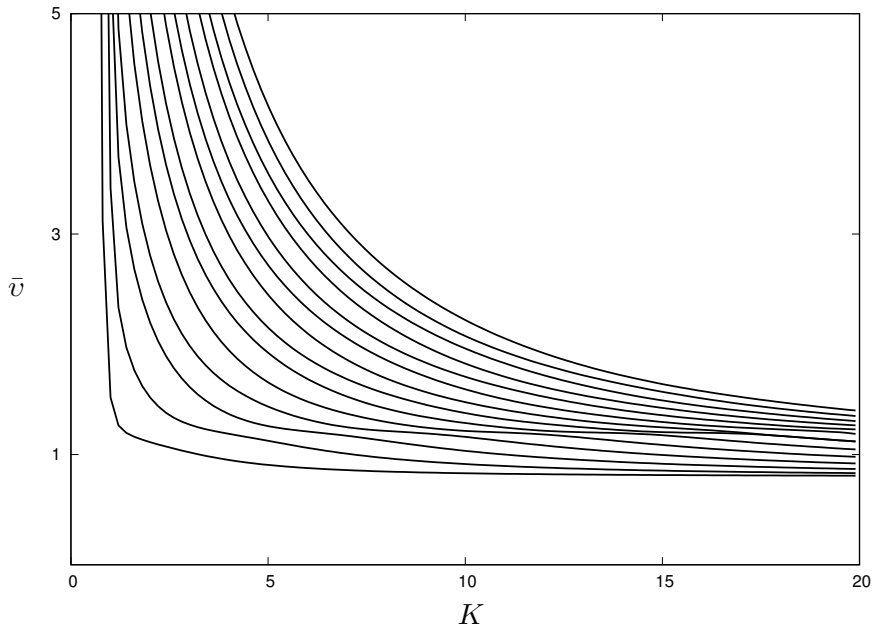

Figure 3.10: Scaled wave speed against scaled wave number for Mooney-Rivlin materials 1 and 2 from Table 3.2 in layer 1 and layer 2, respectively, for the fixed-free faces dispersion relation (3.24).

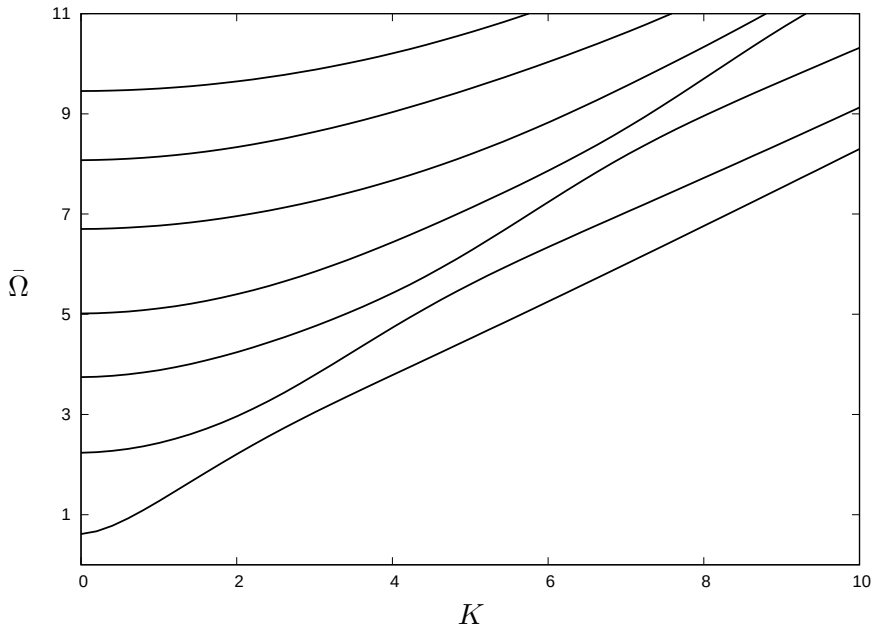

Figure 3.11: Scaled frequency against scaled wave number for Mooney-Rivlin materials 1 and 2 from Table 3.2 in layer 1 and layer 2, respectively, for the fixed-free faces dispersion relation (3.24).

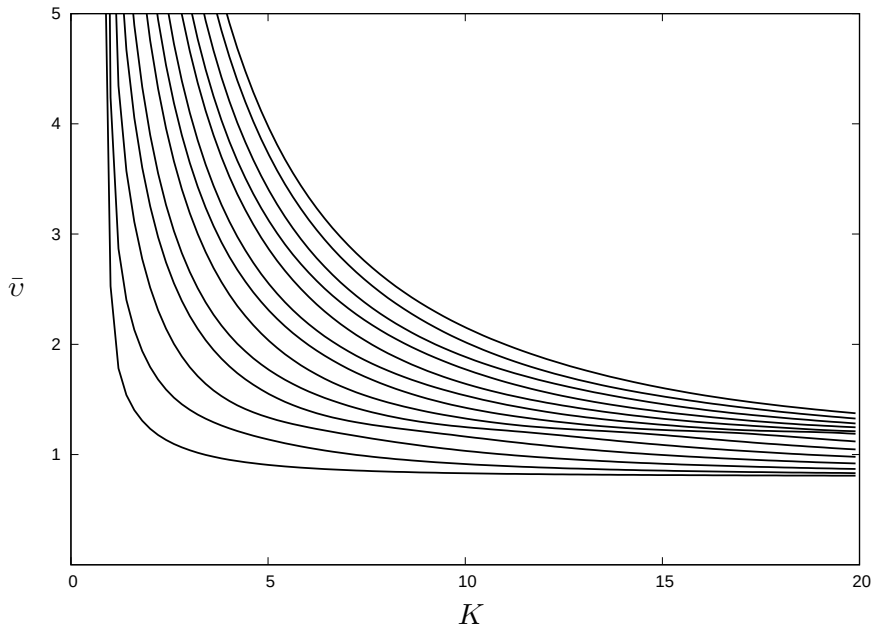

Figure 3.12: Scaled wave speed against scaled wave number for Mooney-Rivlin materials 1 and 2 from Table 3.2 in layer 1 and layer 2, respectively, for the fixed-faces dispersion relation (3.26).

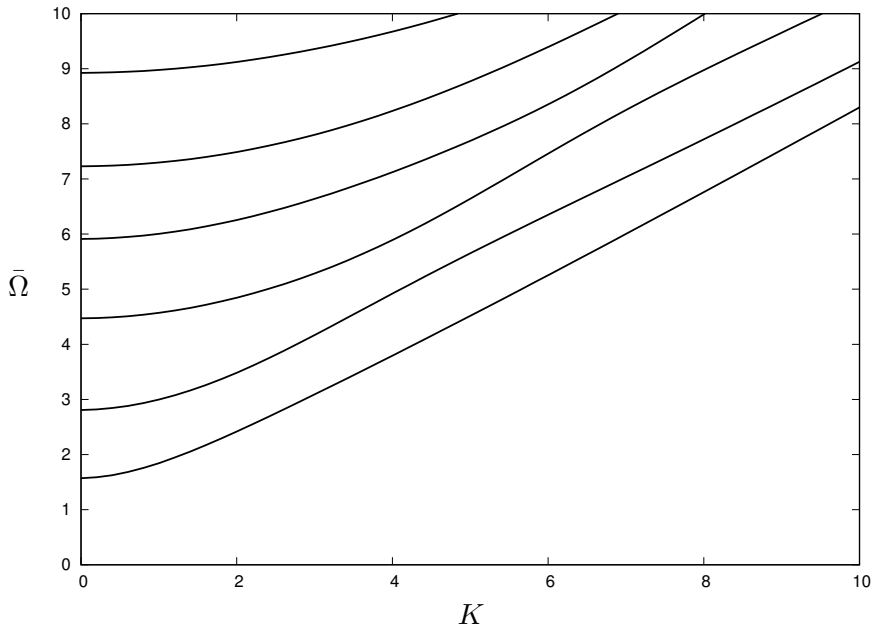

Figure 3.13: Scaled frequency against scaled wave number for Mooney-Rivlin materials 1 and 2 from Table 3.2 in layer 1 and layer 2, respectively, for the fixed-faces dispersion relation (3.26).

For the plots presented in Figure 3.8, we again note that in free-faces case the only branch with a finite long wave limit is the fundamental mode and all associated harmonics having infinite phase speed in the long wave region. Also, the first harmonic in Figure 3.9 is the only branch has zero limit with all other harmonics termed cut-off frequencies have non-zero limits.

Numerical solutions of dispersion relations (3.24) and (3.26) are given in Figure 3.10 and Figure 3.12, respectively. As well as, these figures show corresponding plot of scaled wave speed $\bar{v}$ against scaled wave number K. As might be expected, the fundamental mode is not observed as $K \to 0$. Also, $\bar{v} \to \infty$ in the long wave regime. As can be seen in Figures 3.11 and 3.13, all high-frequency branches for both the fixed-free and fixed-face boundary conditions have non-zero limits in the regime within which $K \to 0$, confirming the absence of the fundamental mode for both cases.

3.3.3 Varga material

In using the Varga strain-energy function presented in (2.35), we investigate the dispersion relation for two values of the material parameters of the following form

$$C_{1313}^{(n)} = \frac{\mu^{(n)}\lambda_1^{(n)}}{(\lambda_1^{(n)} + \lambda_3^{(n)})\lambda_2^{(n)}\lambda_3^{(n)}}, \quad C_{2323}^{(n)} = \frac{\mu^{(n)}\lambda_2^{(n)}}{(\lambda_2^{(n)} + \lambda_3^{(n)})\lambda_1^{(n)}\lambda_3^{(n)}}. \tag{3.33}$$

To model this specific material, we introduce the following table with some values of the parameters considered.

Table 3.3: Varga materials used in numerical results

Materials	$\mu^{(n)}$	$\lambda_1^{(n)}$	$\lambda_2^{(n)}$	$\lambda_3^{(n)}$	$C_{1313}^{(n)}$	$C_{2323}^{(n)}$
Layer 1	4.5	1.5	1	2	0.964	0.5
Layer 2	2	2	1.8	0.5	1.950	1.72

We will conclude the pre-stressed subsection with some numerical results in case of Varga materials subject to the three types of boundary conditions considered in this chapter. Three sets of two graphs will be presented here using material parameters summarised in Table 3.3 and generated from the Varga strain energy function. All the next figures display the scaled wave speed $\bar{\upsilon}$ and the scaled frequency $\bar{\Omega}$ against the scaled wave number K.

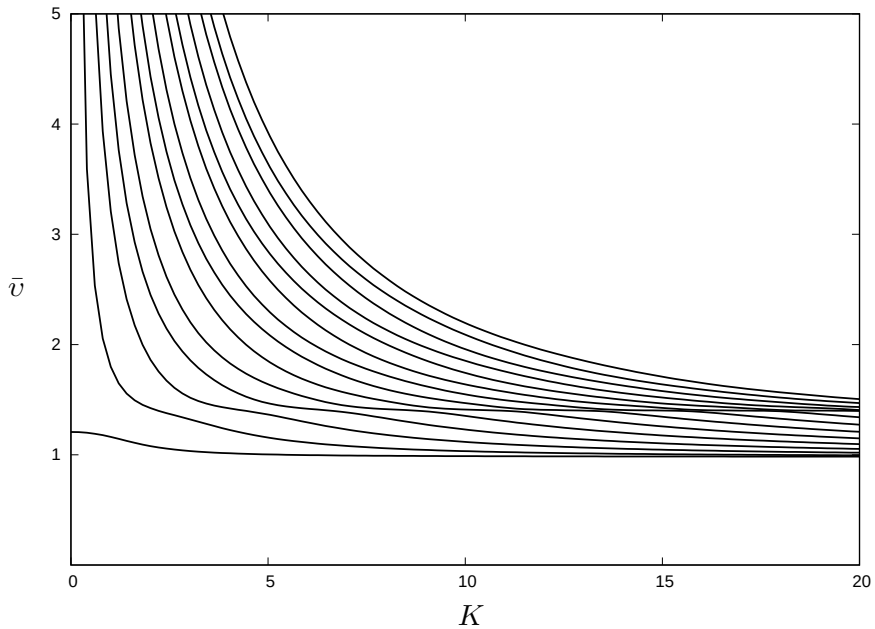

Figure 3.14: Scaled wave speed against scaled wave number for Varga materials 1 and 2 from Table 3.3 in layer 1 and layer 2, respectively, for the free-faces dispersion relation (3.22).

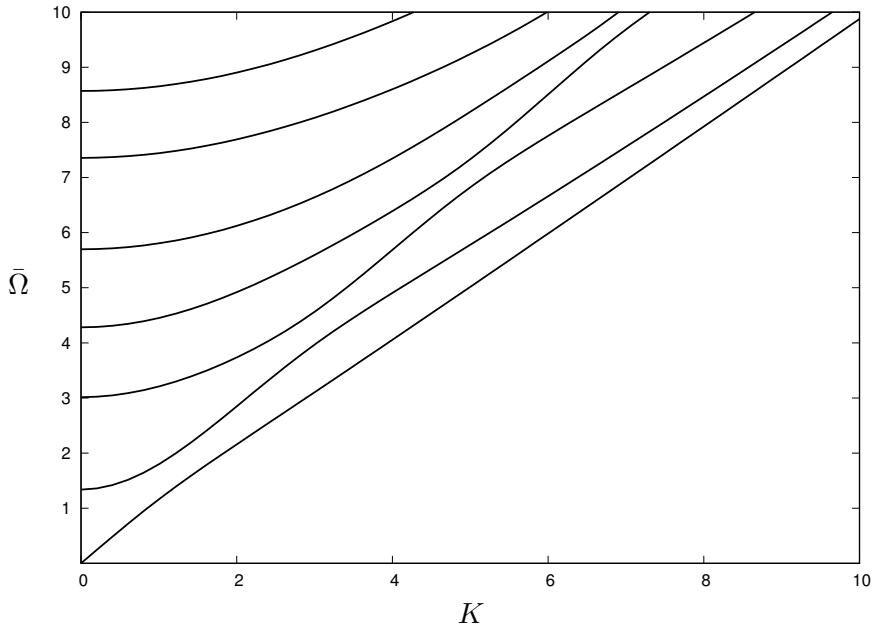

Figure 3.15: Scaled frequency against scaled wave number for Varga materials 1 and 2 from Table 3.3 in layer 1 and layer 2, respectively, for the free-faces dispersion relation (3.22).

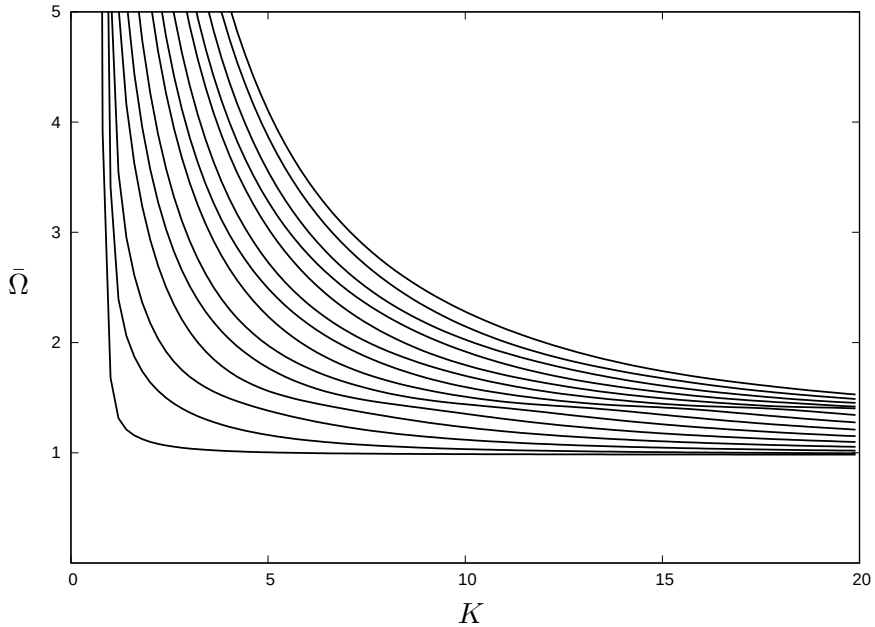

Figure 3.16: Scaled wave speed against scaled wave number for Varga materials 1 and 2 from Table 3.3 in layer 1 and layer 2, respectively, for the fixed-free faces dispersion relation (3.24).

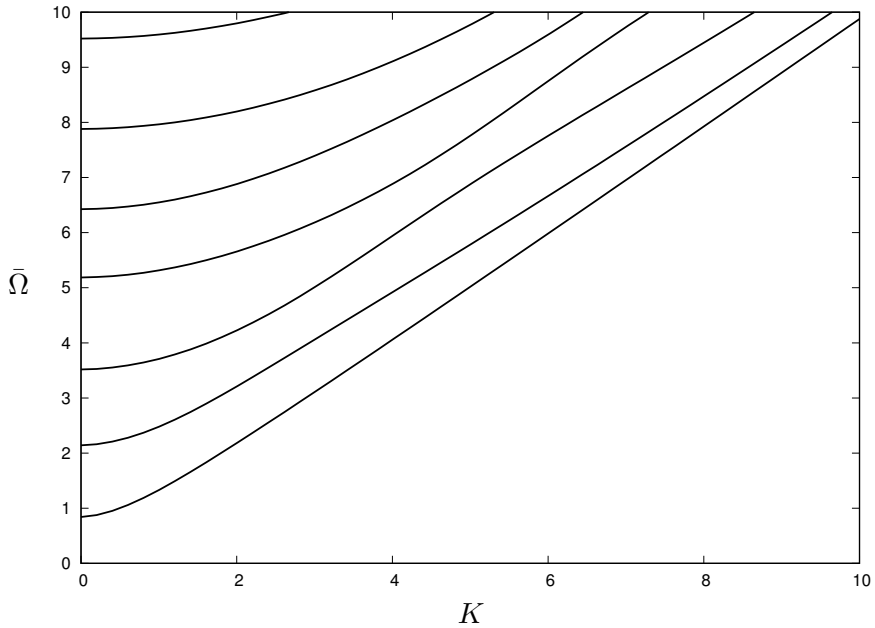

Figure 3.17: Scaled frequency against scaled wave number for Varga materials 1 and 2 from Table 3.3 in layer 1 and layer 2, respectively, for the fixed-free face dispersion relation (3.24).

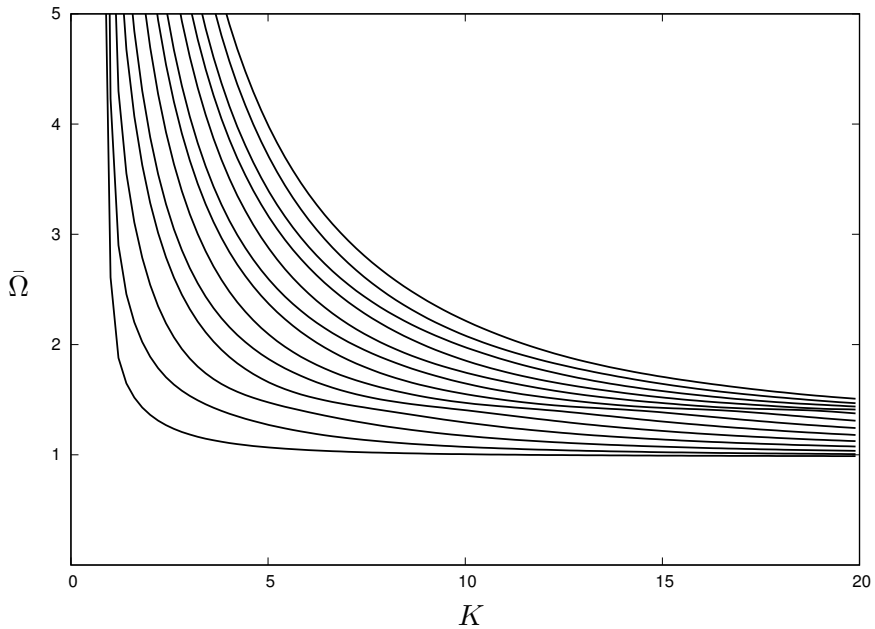

Figure 3.18: Scaled wave speed against scaled wave number for Varga materials 1 and 2 from Table 3.3 in layer 1 and layer 2, respectively, for the fixed-faces dispersion relation (3.26).

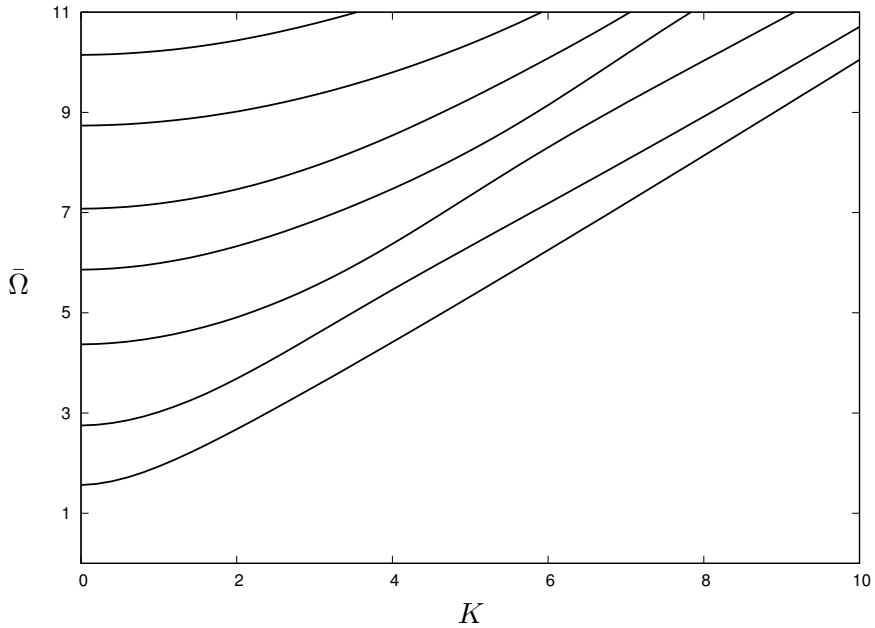

Figure 3.19: Scaled frequency against scaled wave number for Varga materials 1 and 2 from Table 3.3 in layer 1 and layer 2, respectively, for the fixed-faces dispersion relation (3.26).

In Figure 3.14 and Figure 3.15, it is worth noting that in the long wave region ($K \to 0$), only the fundamental mode remains finite wave speed, with all harmonics having an associated large wave speed. Also, for this case, slight oscillations can be seen in the dispersion curves. In the two other cases of boundaries and with the same parameters provided in Table 3.3, plots of the dispersion relations associated with both fixed and fixed-free cases, are presented in Figure 3.16 and Figure 3.18, respectively. In these figures scaled wave speed $\bar{v}$ against scaled wave number K for the first thirteen harmonics is presented. From these figures it is noted that no mode has distinct finite phase speed with infinite phase speed limits for all modes as $K \to 0$. Also, for the scaled frequency $\bar{\Omega}$ against scaled wave number K, Figure 3.17 and Figure 3.19 show that as $K \to 0$, no long wave low frequency for both fixed and fixed-free cases. From the seven harmonics in these figures, we note that no mode has zero limit with each associated harmonic has a non- zero limit.

3.4 Long wave approximations

In this section we will proceed to the derivation of some long wave approximations of the dispersion relations. The numerical behaviour of the dispersion relation we have just discussed will guide us. This discussion will be considered for both low frequency and high frequency. First we remark that

$K = kh$ is a small geometric parameter and may be thought physically as the ratio of plate thickness to the wavelength l, with k the wave number. The thickness of the 2-layered laminate structure is $2h$, so that each layer is of h thickness. It is worth to mention that in the long wave limit there are no fundamental modes for both the fixed and fixed-free cases. We begin our derivation of long wave motion with an investigation of the dispersion relation of two layers with pre-stressed materials and then for linear isotropic materials.

3.4.1 Long-wave low-frequency limit for free faces

It is well known that long wave low frequency motion is characterised by allowing $K \to 0$ and $\bar{v}$ is not large as wave number is small. Thus, all the hyperbolic functions obtained in the dispersion relation associated with the free-faces case will be expanded by Taylor series as

$$\cosh(q_n K) = 1 + \frac{q_n^2 K^2}{2} + O(K^4). \tag{3.34}$$

and

$$\sinh(q_n K) = q_n K + \frac{q_n^3 K^3}{6} + O(K^5),\ n = 1, 2. \tag{3.35}$$

Thus, we first will express relation (3.22) as

$$C^{(1)}_{2323} q_1 \tanh(K q_1) + C^{(2)}_{2323} q_2 \tanh(K q_2) = 0. \tag{3.36}$$

Then we will present the squared scaled phase wave speed as a function of powers of K in the form

$$\bar{v}^2 = \upsilon_0 + \upsilon_2 K^2 + O(K^4) + ... \tag{3.37}$$

To obtain the asymptotic expansion of the dispersion relation (3.36), we will make use of (3.34) and (3.35), to arrive at the following approximation

$$\beta_1 K^2 + \beta_2 + \beta_3 K^2 \bar{v}^2 + \beta_4 \bar{v}^2 + ... \approx 0, \tag{3.38}$$

where $\bar{\Omega} = \bar{v} K$ and the coefficients β_i are given by

$$\begin{aligned}
\beta_1 &= \frac{C^{(1)}_{2323}}{3C^{(1)}_{1313}} \left(C^{(1)}_{2323} + 3C^{(1)}_{2323} \right) + \frac{C^{(2)}_{2323}}{3C^{(2)}_{1313}} \left(1 + 3C^{(1)}_{2323} \right), \\
\beta_2 &= C^{(1)}_{1313} + C^{(2)}_{1313}, \\
\beta_3 &= -\frac{1}{2} \left[C^{(1)}_{2323} \left(\frac{1}{C^{(1)}_{1313}} + \frac{1}{C^{(2)}_{1313}} \right) + \frac{C^{(2)}_{2323}}{3} \left(\frac{1}{C^{(1)}_{1313}} + \frac{1}{C^{(2)}_{1313}} \right) \right], \\
\beta_4 &= -2.
\end{aligned} \tag{3.39}$$

The leading order term of the dispersion relation (3.36) as $K \to 0$ is readily established by using the solutions (3.6) together with the expansion (3.37), yielding

$$\upsilon_0 = \frac{C^{(1)}_{1313} + C^{(2)}_{1313}}{2}. \tag{3.40}$$

The next order of (3.37), gives

$$\upsilon_2 = -\frac{1}{24\, C^{(1)}_{1313} C^{(2)}_{1313}} \left(C^{(1)}_{1313} + C^{(2)}_{1313}\right) \left(C^{(1)}_{2323} - C^{(2)}_{2323}\right)^2. \tag{3.41}$$

The relations (3.40) and (3.41) may be now inserted into (3.37), establishing the wave speed expansion associated with this case as

$$\bar{v}^2 = \upsilon_0 - \frac{1}{24}\left(\left(\frac{1}{C^{(2)}_{1313}} + \frac{1}{C^{(1)}_{1313}}\right)\left(C^{(1)}_{2323} - C^{(2)}_{2323}\right)^2\right) K^2 + O(K^4). \tag{3.42}$$

At low frequencies, the corresponding scaled frequency expansion takes the form $\bar{\Omega}^2 = \Omega_2 K^2 + \ldots$. We will now provide two figures showing a comparison between the asymptotic approximations and the numerical solutions in the low wave number regime for free faces case. In Figure 3.20 the asymptotic expansions given in equation (3.42) are superimposed on numerical solution obtained for the material parameters used in Figure 3.2. In this figure the fundamental mode of the dispersion relation are presented which indicates excellent agreement between the asymptotic approximation and the numer-

ical curves. Also, in Figure 3.21 better agreement with the numerical result for the fundamental mode of the dispersion relation (3.22) in Figure 3.3, is obtained for the scaled frequency against scaled wave number.

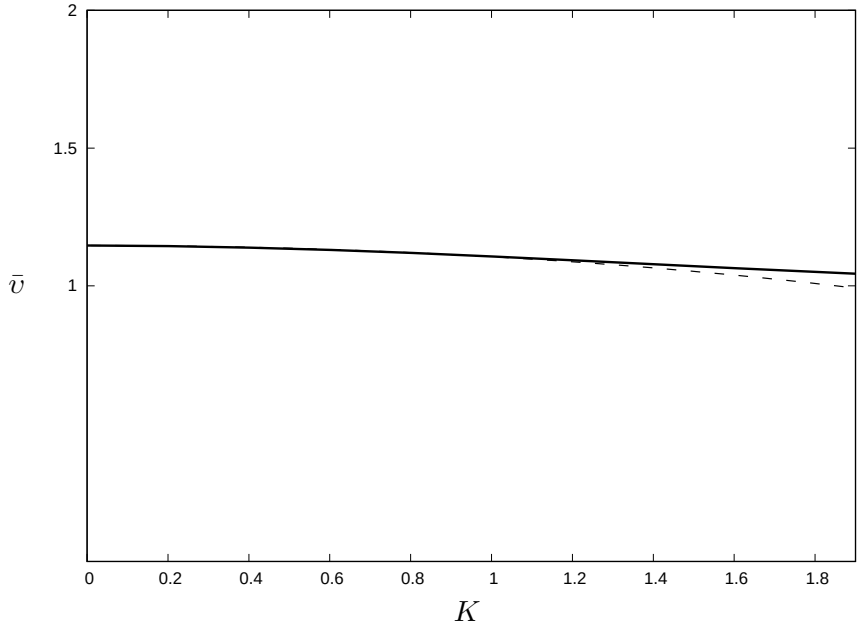

Figure 3.20: Fundamental mode from numerical solution of the free-faces dispersion relation (3.22) and asymptotic expansion (3.42) for scaled wave speed against scaled wave number in neo-Hookean material in Table 3.3.

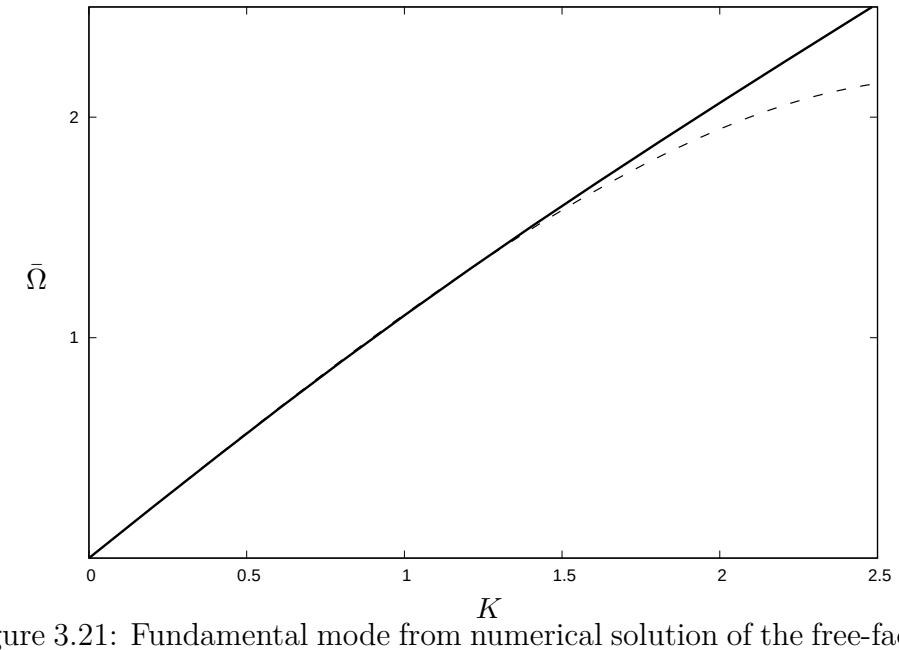

Figure 3.21: Fundamental mode from numerical solution of the free-faces dispersion relation (3.22) and asymptotic expansion (3.42) for scaled frequency against scaled wave number in neo-Hookean material in Table 3.3.

3.4.2 Long wave high frequency limits

In this section, we consider the long wave high frequency regime of the dispersion curves, i.e. the so-called harmonics within the low wave number regime. In this type of motion $\bar{v}^2 \gg 1$. We remark that, q_1^2 and q_2^2 are negative as $K \to 0$, i.e. $q_1 = i\widehat{q}_1$ and $q_2 = i\widehat{q}_2$. Using the previous knowledge, we arrive at

$$\widehat{q}_1^2 = \frac{\bar{v}^2 - C_{1313}^{(1)}}{C_{2323}^{(1)}}, \;\; \widehat{q}_1^2 = \frac{\bar{v}^2 - C_{1313}^{(2)}}{C_{2323}^{(2)}}, \tag{3.43}$$

with $\widehat{q}_1$, $\widehat{q}_2 \to \infty$ within the long wave high frequency regime. In this case of high frequency we will note

$$K\widehat{q}_1 = \left(\frac{K^2\bar{v}^2 - C_{1313}^{(1)}K^2}{C_{2323}^{(1)}} \right)^{\frac{1}{2}} = \left(\frac{\bar{\Omega}^2 - C_{1313}^{(1)}K^2}{C_{2323}^{(1)}} \right)^{\frac{1}{2}}, \tag{3.44}$$

$$K\widehat{q}_2 = \left(\frac{K^2\bar{v}^2 - C_{1313}^{(2)}K^2}{C_{2323}^{(2)}} \right)^{\frac{1}{2}} = \left(\frac{\bar{\Omega}^2 - C_{1313}^{(2)}K^2}{C_{2323}^{(2)}} \right)^{\frac{1}{2}}. \tag{3.45}$$

(3.44) and (3.45) can be expanding as follows

$$K\widehat{q}_1 = \frac{\bar{\Omega}}{\sqrt{C_{2323}^{(1)}}} \left(1 - \frac{C_{1313}^{(1)}K^2}{2\bar{\Omega}^2} + ... \right), \tag{3.46}$$

$$K\widehat{q}_2 = \frac{\bar{\Omega}}{\sqrt{C^{(2)}_{2323}}}\left(1 - \frac{C^{(2)}_{1313}K^2}{2\bar{\Omega}^2} + ...\right). \tag{3.47}$$

Within the long wave high frequency region we assume $\bar{v}^2 \sim O(K^{-2})$. In addition, we assume $\bar{\Omega}^2$ has the following expansion

$$\bar{\Omega}^2 = \Omega_0 + \Omega_2 K^2 + O(K^4). \tag{3.48}$$

Free-faces case

On making use of relations previously mentioned, $q_1 = i\widehat{q}_1$ and $q_2 = i\widehat{q}_2$, the dispersion (3.22) may be expressed in the form

$$C^{(1)}_{2323}\widehat{q}_1 \tan(K\widehat{q}_1) + C^{(2)}_{2323}\widehat{q}_2 \tan(K\widehat{q}_2) = 0, \tag{3.49}$$

which then can be represented as

$$\sqrt{C^{(1)}_{2323}}\left(1 - \frac{C^{(1)}_{1313}K^2}{2\bar{\Omega}^2}\right)\tan\left(\frac{\bar{\Omega}}{\sqrt{C^{(1)}_{2323}}}\left(1 - \frac{C^{(1)}_{1313}K^2}{2\bar{\Omega}^2}\right)\right) + \sqrt{C^{(2)}_{2323}}\left(1 - \frac{C^{(2)}_{1313}K^2}{2\bar{\Omega}^2}\right)\tan\left(\frac{\bar{\Omega}}{\sqrt{C^{(2)}_{2323}}}\left(1 - \frac{C^{(2)}_{1313}K^2}{2\bar{\Omega}^2}\right)\right) = 0. \tag{3.50}$$

We now consider Taylor series approximation for the trigonometric functions in the above equations, thus on inserting the expansion (3.48) into (3.50), we

get

$$\Omega_0 \left(\sqrt{C_{2323}^{(1)}} F_1(\Omega_0) + \sqrt{C_{2323}^{(2)}} F_2(\Omega_0) \right) + \left(\Psi_3(\Omega_0) + \Psi_4(\Omega_0)\Omega_2 \right) K^2 + O(K^4) \approx 0, \tag{3.51}$$

where

$$F_1(\Omega_0) = \tan\left(\sqrt{\frac{\Omega_0}{C_{2323}^{(1)}}} \right), \quad F_2(\Omega_0) = \tan\left(\sqrt{\frac{\Omega_0}{C_{2323}^{(2)}}} \right),$$

$$\Psi_3(\Omega_0) = \sqrt{C_{2323}^{(1)}} F_1(\Omega_0) + \sqrt{C_{2323}^{(2)}} F_2(\Omega_0) + \sqrt{\Omega_0} \left(F_1^2(\Omega_0) + 1 \right) + \sqrt{\Omega_0} \left(F_2^2(\Omega_0) + 1 \right),$$

$$\Psi_4(\Omega_0) = -\frac{1}{2} \left(C_{1313}^{(1)} \left(1 + F_1^2(\Omega_0) \right) \sqrt{\Omega_0} + C_{1313}^{(2)} \left(1 + F_2^2(\Omega_0) \right) \sqrt{\Omega_0} + \sqrt{C_{2323}^{(1)}} F_1(\Omega_0) C_{1313}^{(1)} + \sqrt{C_{2323}^{(2)}} F_2(\Omega_0)\, C_{1313}^{(2)} \right).$$

Therefore, it can be easily seen that the leading order is given by

$$\sqrt{C_{2323}^{(1)}} \tan \sqrt{\frac{\Omega_0}{C_{2323}^{(1)}}} + \sqrt{C_{2323}^{(2)}} \tan \sqrt{\frac{\Omega_0}{C_{2323}^{(2)}}} = 0, \tag{3.52}$$

where Ω_0 is a solution of equation (3.52), defines the cut-off frequencies. Also, it can be shown numerically to provide an implicit conditions for the cut-off

frequencies.

The next order terms of the expansion (3.51) provides Ω_2 in the following formula

$$\Omega_2 = \Psi_3(\Omega_0)/\Psi_4(\Omega_0). \tag{3.53}$$

The scaled frequency may therefore be written in the form

$$\bar{\Omega}^2 = \Omega_0 + \frac{\Psi_3(\Omega_0)}{\Psi_4(\Omega_0)} K^2 + O(K^4). \tag{3.54}$$

A neo-Hookean material is chosen to be an example of pre-stress materials for the free-faces case. For this material we provide Figure 3.22 showing good agreement for numerical and asymptotic solutions.

It is interesting to investigate behaviour of a coefficient Ω_2 defined by (3.53), depending on the ratio of shear moduli $\mu = \mu_2/\mu_1$. The coefficient is expected to remain of order unity within the appropriate range of ratio $\mu \sim 1$. In Figure 3.23 below the value $\mu_1 = 0.6$ is fixed, while μ_2 is changing from 0.12 up to 3.0, with stretches λ_i taken as in Figure 3.22. A regular behaviour of Ω_2 is observed, seemingly excluding possibilities of degenerate behaviour reported previously in Kaplunov and Markushevich (1993), Kaplunov et al. (1998).

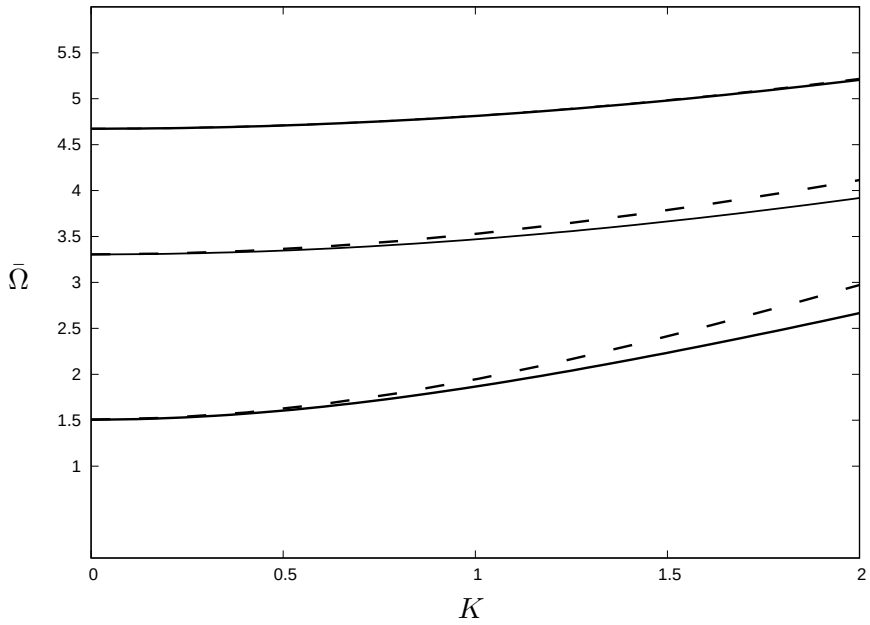

Figure 3.22: Numerical solutions corresponding to the free-faces dispersion relation (3.22) (solid line) and asymptotic expansion (3.54) (dashed line) for scaled frequency against scaled wave number in a neo-Hookean material.

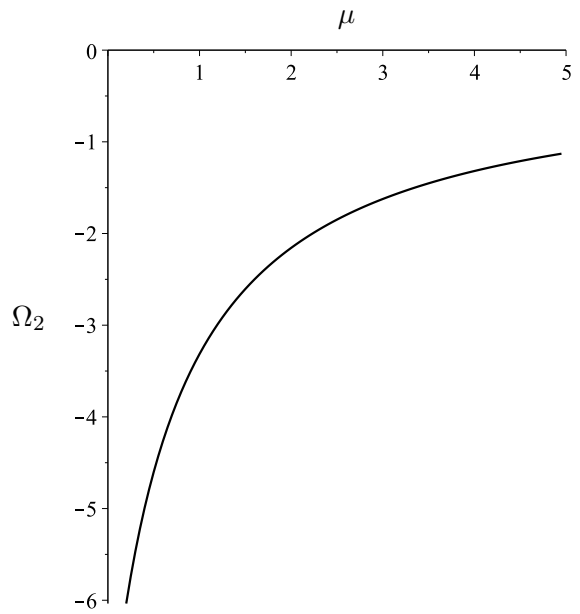

Figure 3.23: Dependence of coefficient Ω_2 (3.53) on the ratio of shear moduli μ for a neo-Hookean material.

Fixed-free faces case

In fixed-free case, the dispersion relation may be presented in the form

$$C^{(2)}_{2323}\widehat{q}_2 - C^{(1)}_{2323}\widehat{q}_1 \tan(K\widehat{q}_1)\tan(K\widehat{q}_2) = 0. \tag{3.55}$$

Performing a similar analysis to that precisely used for free-faces case, we arrive at the leading order term in the form

$$\sqrt{C^{(2)}_{2323}} - \sqrt{C^{(1)}_{2323}}\tan\left(\sqrt{\frac{\Omega_0}{C^{(1)}_{2323}}}\right)\tan\left(\sqrt{\frac{\Omega_0}{C^{(2)}_{2323}}}\right) = 0. \tag{3.56}$$

The next order term provides Ω_2 in the following formula

$$\Omega_2 = \bar{\Psi}_3(\Omega_0)/\bar{\Psi}_4(\Omega_0), \tag{3.57}$$

where

$$\begin{aligned}\bar{\Psi}_3(\Omega_0) = \sqrt{\Omega_0}\left(C^{(1)}_{1313}F_1(\Omega_0)F_2(\Omega_0)\sqrt{C^{(1)}_{2323}C^{(2)}_{2323}} - C^{(2)}_{1313}C^{(2)}_{2323}\right) + \\ \Omega_0\left(\sqrt{C^{(2)}_{2323}}F_1^2(\Omega_0)F_2(\Omega_0)C^{(1)}_{1313} + \sqrt{C^{(1)}_{2323}}F_1(\Omega_0)F_2^2(\Omega_0)C^{(2)}_{1313}\right) \\ + \left(C^{(2)}_{1313}\sqrt{C^{(1)}_{2323}}F_1(\Omega_0) + C^{(1)}_{1313}\sqrt{C^{(2)}_{2323}}F_2(\Omega_0)\right)\Omega_0,\end{aligned}$$

$$\bar{\Psi}_4(\Omega_0) = \sqrt{\Omega_0}\left(2F_1(\Omega_0)F_2(\Omega_0)\sqrt{C^{(1)}_{2323}C^{(2)}_{2323}} - 2C^{(1)}_{2323}\right) + \left(F_1(\Omega_0)\sqrt{C^{(1)}_{2323}}\right.$$
$$\left. + F_1^2(\Omega_0)F_2(\Omega_0)\sqrt{C^{(2)}_{2323}} + \sqrt{C^{(2)}_{2323}}F_2(\Omega_0) + \sqrt{C^{(1)}_{2323}}F_1(\Omega_0)F_2^2(\Omega_0)C^{(2)}_{1313}\right)\Omega_0.$$

The scaled frequency may therefore be written in the form

$$\bar{\Omega}^2 = \Omega_0 + \frac{\bar{\Psi}_3(\Omega_0)}{\bar{\Psi}_4(\Omega_0)}K^2 + O(K^4), \tag{3.58}$$

where Ω_0 is a solution of (3.56).

We consider now a Mooney-Rivlin material as an example of pre-stress materials in the fixed-free faces case. For this material we provide a comparison between numerical solutions and asymptotic expansions (3.58) for scaled frequency against scaled wave number with the same material parameters from Table 3.2 in Mooney-Rivlin material with fixed-free faces dispersion relation (3.55). Figure 3.24 shows good agreement for numerical results and asymptotic expansions for the high wave limits.

Fixed-faces case

The dispersion relation (3.26) can be expressed in the form

$$C^{(2)}_{2323}\widehat{q}_2\tan(K\widehat{q}_1) + C^{(1)}_{2323}\widehat{q}_1\tan(K\widehat{q}_2) = 0. \tag{3.59}$$

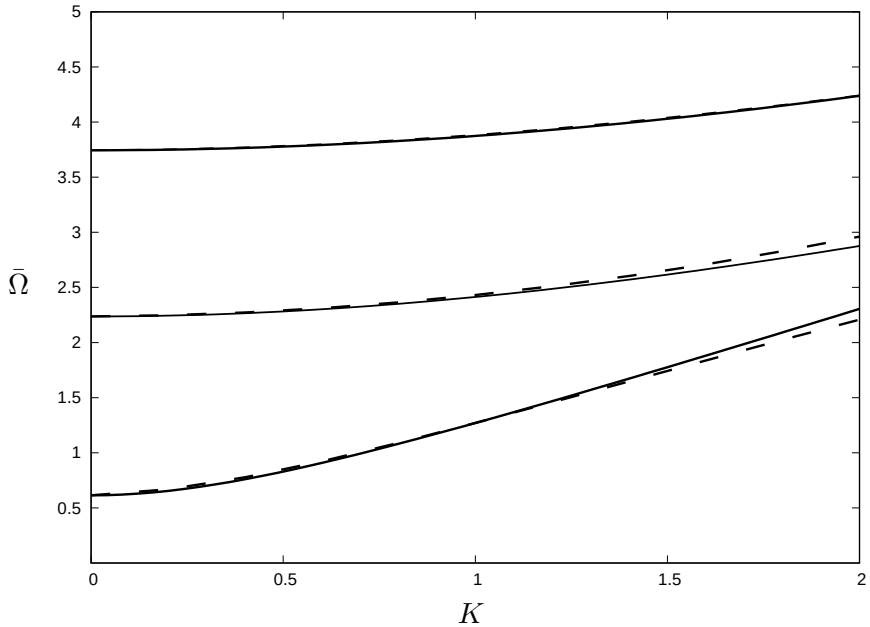

Figure 3.24: Numerical solutions corresponding to the fixed-free faces dispersion relation (3.24) (solid line) and asymptotic expansion (3.58) (dashed line) for scaled frequency against scaled wave number in case of Mooney-Rivlin material.

Following the previously outlined procedures to get the expansion of (3.59),

yielding

$$\frac{1}{\sqrt{C^{(1)}_{2323}}}\left(1-\frac{C^{(2)}_{1313}K^2}{2\bar{\Omega}^2}\right)\tan\left(\frac{\bar{\Omega}}{C^{(1)}_{2323}}\left(1-\frac{C^{(1)}_{1313}K^2}{2\bar{\Omega}^2}\right)\right)+$$
$$\frac{1}{\sqrt{C^{(2)}_{2323}}}\left(1-\frac{C^{(1)}_{1313}K^2}{2\bar{\Omega}^2}\right)\tan\left(\frac{\bar{\Omega}}{C^{(2)}_{2323}}\left(1-\frac{C^{(2)}_{1313}K^2}{2\bar{\Omega}^2}\right)\right)=0. \quad (3.60)$$

After inserting (3.48) into the above expansion, as previously, the leading order may introduce the following form

$$\sqrt{C^{(2)}_{2323}}\tan\sqrt{\frac{\Omega_0}{C^{(1)}_{2323}}}+\sqrt{C^{(1)}_{2323}}\tan\sqrt{\frac{\Omega_0}{C^{(2)}_{2323}}}=0. \tag{3.61}$$

The next order term of the expansion (3.60) provides Ω_2 in the following formula

$$\Omega_2=\widetilde{\Psi}_3(\Omega_0)/\widetilde{\Psi}_4(\Omega_0), \tag{3.62}$$

where

$$\widetilde{\Psi}_3(\Omega_0)=-\sqrt{C^{(2)}_{2323}}\sqrt{C^{(1)}_{2323}}\left(\sqrt{C^{(2)}_{1313}}F_2(\Omega_0)+\sqrt{C^{(1)}_{1313}}F_1(\Omega_0)\right)+\sqrt{\Omega_0}$$
$$\left(C^{(2)}_{2323}F_1^2(\Omega_0)\sqrt{C^{(1)}_{1313}}+C^{(1)}_{2323}F_2^2(\Omega_0)\sqrt{C^{(2)}_{1313}}+C^{(1)}_{2323}\sqrt{C^{(2)}_{1313}}+C^{(2)}_{2323}\sqrt{C^{(1)}_{1313}}\right),$$

$$\widetilde{\Psi}_4(\Omega_0)=\left[C^{(1)}_{2323}C^{(2)}_{2323}F_2^2(\Omega_0)F_1(\Omega_0)+C^{(1)}_{2323}C^{(2)}_{2323}\right]\sqrt{\Omega_0}$$
$$-\left(C^{(2)}_{2323}\sqrt{C^{(1)}_{2323}}F_1(\Omega_0)+C^{(1)}_{2323}\sqrt{C^{(2)}_{2323}}\,F_2(\Omega_0)\right).$$

The asymptotic approximation in this case is expressed $\bar{\Omega}^2$ in the following formula

$$\bar{\Omega}^2=\Omega_0+\frac{\widetilde{\Psi}_3(\Omega_0)}{\widetilde{\Psi}_4(\Omega_0)}K^2+O(K^4), \tag{3.63}$$

where Ω_0 is a solution of (3.61).

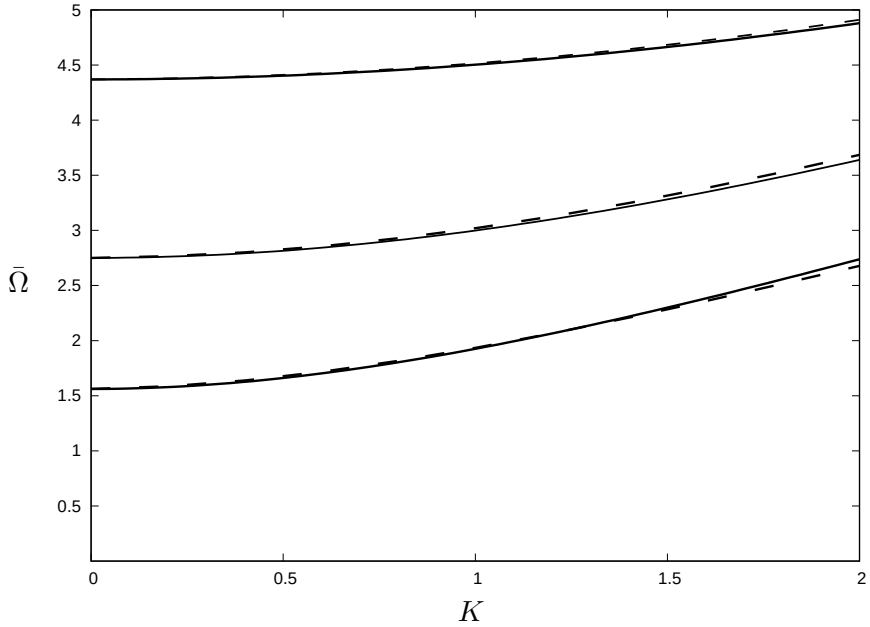

Figure 3.25: A comparison of numerical solution corresponding to (3.26) (solid line) and asymptotic expansion (dashed line) (3.63) for scaled frequency against scaled wave number in case of Varga material with fixed faces.

A comparison of numerical solution and asymptotic expansion for scaled frequency against scaled wave number using Varga material is presented for the high wave limit in Figure 3.25. The same material parameters from Table 3.3 are used.

Chapter 4

Long wave motion in a 3-layered laminate structure

In this chapter the problem of long wave propagation in a 3-layered laminate, the layers of which are assumed to be composed of compressible pre-stressed materials, will be considered.

4.1 Governing equations

The 3-layered structure is built by adding one layer of thickness h, namely layer 3, to the 2-layered structure in Chapter 3. This added layer occupies the region $2h \leq x_2 \leq 3h$, see Figure 4.1. Furthermore, this problem is again considered within anti-plane setup, with non-zero displacement components

u_3 being independent of x_3 variable. As previously, the interfaces between the inner core and the two outer layers are perfectly bonded.

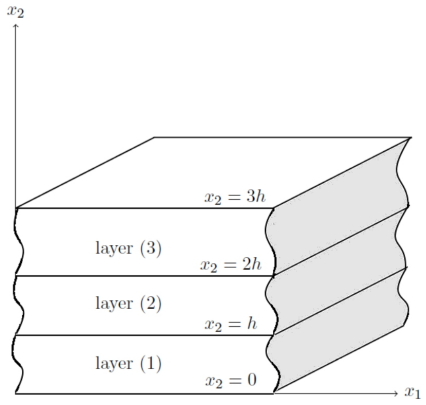

Figure 4.1: Three layers structure.

Therefore, the equation of motion in this case can be expressed as

$$C^{(n)}_{1313}u^{(n)}_{3,11} + C^{(n)}_{2323}u^{(n)}_{3,22} = \rho\ddot{u}^{(n)}_3, \tag{4.1}$$

with the same travelling wave solution (3.2), $n = 1, 2, 3$. The material parameters of the layers are denoted by $C^{(n)}_{1313}$, $C^{(n)}_{2323}$ and the related displacement is formed as

$$u^{(n)}_3 = A_n e^{kq_n x_2} + B_n e^{-kq_n x_2}, \tag{4.2}$$

and the non-zero incremental traction takes the component form

$$\widehat{\tau}^{(n)} = \tau^{(n)}_3/k = C^{(n)}_{2323}\left(A_n q_n e^{kq_n x_2} - B_n q_n e^{-kq_n x_2}\right), \tag{4.3}$$

Accordingly, (4.2) and (4.3) may be expressed in the matrix form as

$$\begin{pmatrix} u_3^{(n)} \\ \widehat{\tau}^{(n)} \end{pmatrix} = \begin{pmatrix} e^{kq_n x_2} & e^{-kq_n x_2} \\ q_n C_{2323}^{(n)} e^{kq_n x_2} & -q_n C_{2323}^{(n)} e^{-kq_n x_2} \end{pmatrix} \begin{pmatrix} A_n \\ B_n \end{pmatrix}, \tag{4.4}$$

where

$$q_n = \frac{C_{1313}^{(n)} - \rho v^2}{C_{2323}^{(n)}}, \quad n = 1, 2, 3. \tag{4.5}$$

However, the appropriate solution for $u_3^{(n)}$ and $\widehat{\tau}^{(n)}$ has previously been provided in the matrix form (2.51) and it can be again expressed for each layer as

$$\mathbf{Y}(x_u) = \mathbf{P}^{(n)} \mathbf{Y}(x_l). \tag{4.6}$$

The propagator matrix for layer 1 and layer 2 are obtained in the previous chapters (3.15), (3.16), namely by $\mathbf{P}^{(1)}$ and $\mathbf{P}^{(2)}$, respectively.

Now we will first express the solution (4.6) for layer 3 in the form

$$\mathbf{Y}(3h) = \mathbf{P}^{(3)} \mathbf{Y}(2h), \tag{4.7}$$

where $\mathbf{P}^{(3)}$ is the propagator matrix of the distance $3h - 2h = h$, given by

$$\mathbf{P}^{(3)} = \begin{pmatrix} \cosh(kq_3h) & \dfrac{1}{q_3C^{(3)}_{2323}}\sinh(kq_3h) \\ q_3C^{(3)}_{2323}\sinh(kq_3h) & \cosh(kq_3h) \end{pmatrix} \tag{4.8}$$

The relationship between the upper surface $x_2 = 3h$ and the interface $x_2 = 2h$ may be introduced as

$$\begin{pmatrix} u_3^{(3)}\,|_{x_2=3h} \\ \widehat{\tau}^{(3)}\,|_{x_2=3h} \end{pmatrix} = \begin{pmatrix} \cosh(kq_3h) & \dfrac{1}{q_3C^{(3)}_{2323}}\sinh(kq_3h) \\ q_3C^{(3)}_{2323}\sinh(kq_3h) & \cosh(kq_3h) \end{pmatrix} \begin{pmatrix} u_3^{(2)}\,|_{x_2=2h} \\ \widehat{\tau}^{(2)}\,|_{x_2=2h} \end{pmatrix}. \tag{4.9}$$

The continuity conditions along the interface $x_2 = 2h$ are given by

$$\widehat{\tau}^{(2)} = \widehat{\tau}^{(3)}, \quad u_2^{(1)} = u_3^{(3)}. \tag{4.10}$$

Making use of the propagator matrix (4.8) and substituting $\mathbf{P}$ from (3.19) in Chapter 3 in conjunction with the continuity condition (4.10), yielding the solution for the 3-layered laminate in the form

$$\mathbf{Y}(3h) = \mathbf{P}\,\mathbf{Y}(0), \tag{4.11}$$

where $\mathbf{P} = \mathbf{P}^{(3)}\mathbf{P}^{(2)}\mathbf{P}^{(1)}$ is the overall propagator matrix for the whole struc-

ture

$$\mathbf{P} = \begin{pmatrix} p_{11} & p_{12} \\ \\ p_{21} & p_{22} \end{pmatrix}, \tag{4.12}$$

within which

$$\begin{aligned}
p_{11} &= \Big(C^{(1)}_{2323} q_1 \cosh(kq_1h)\cosh(kq_2h) + C^{(2)}_{2323} q_2 \sinh(kq_1h)\sinh(kq_2h)\Big) \\
&\quad \times \frac{\cosh(kq_3h)}{C^{(2)}_{2323} q_2} + \Big(C^{(1)}_{2323} q_1 \sinh(kq_1h)\cosh(kq_2h) \\
&\quad + C^{(2)}_{2323} q_2 \sinh(kq_2h)\cosh(kq_1h)\Big)\frac{\sinh(kq_3h)}{C^{(3)}_{2323} q_3}, \\
p_{12} &= \Big(C^{(2)}_{2323} q_2 \sinh(kq_1h)\cosh(kq_2h) + C^{(1)}_{2323} q_1 \cosh(kq_1h)\sinh(kq_2h)\Big) \\
&\quad \times \frac{\cosh(kq_2h)}{C^{(1)}_{2323} q_1\, C^{(2)}_{2323} q_2} + C^{(2)}_{2323} q_2 \Big(C^{(1)}_{2323} q_1 \cosh(kq_1h)\cosh(kq_2h) \\
&\quad + C^{(2)}_{2323} q_2 \sinh(kq_1h)\sinh(kq_2h)\Big)\frac{\sinh(kq_3h)}{C^{(1)}_{2323} q_1\, C^{(3)}_{2323} q_3}, \\
p_{21} &= \Big(C^{(1)}_{2323} q_1 \sinh(kq_1h)\cosh(kq_2h) + C^{(2)}_{2323} q_2 \cosh(kq_1h)\sinh(kq_2h)\Big) \\
&\quad \times \cosh(kq_3h) + C^{(3)}_{2323} q_3 \Big(C^{(1)}_{2323} q_1 \sinh(kq_1h)\sinh(kq_2h) \\
&\quad + C^{(2)}_{2323} q_2 \cosh(kq_1h)\cosh(kq_2h)\Big)\frac{\sinh(kq_3h)}{C^{(2)}_{2323} q_2}, \\
p_{22} &= \Big(C^{(2)}_{2323} q_2 \cosh(kq_1h)\cosh(kq_2h) + C^{(1)}_{2323} q_1 \sinh(kq_1h)\sinh(kq_2h)\Big) \\
&\quad \times \frac{\cosh(kq_3h)}{C^{(2)}_{2323} q_2} + C^{(2)}_{2323} q_2 \Big(C^{(1)}_{2323} q_1 \sinh(kq_1h)\cosh(kq_2h) \\
&\quad + \sinh(kq_2h)\cosh(kq_1h)\Big)\frac{\sinh(kq_3h)}{C^{(3)}_{2323} q_3}.
\end{aligned} \tag{4.13}$$

4.2 Derivation of the dispersion relation

Free faces case

A similar derivation may be performed for this case by applying the so-called free faces boundary conditions on the upper and lower surface of the laminate

$$\widehat{\tau}^{(3)} = 0,\ x_2 = 3h \ \text{ and } \ \widehat{\tau}^{(1)} = 0, \quad x_2 = 0, \tag{4.14}$$

which then provide the following dispersion relation

$$\begin{aligned}
&\Big(C^{(1)}_{2323} q_1 \sinh(kq_1 h)\cosh(kq_2 h) + C^{(2)}_{2323} q_2 \cosh(kq_1 h)\sinh(kq_2 h)\Big) \\
&\quad \times \cosh(kq_3 h) C^{(2)}_{2323} q_2 + C^{(3)}_{2323} q_3 \Big(C^{(1)}_{2323} q_1 \sinh(kq_1 h)\sinh(kq_2 h) + \\
&\quad C^{(2)}_{2323} q_2 \cosh(kq_1 h)\cosh(kq_2 h)\Big)\sinh(kq_3 h) = 0.
\end{aligned} \tag{4.15}$$

Fixed-free faces case

If we apply the mixture boundary conditions wit zero displacement on the upper surface and zero traction on the lower surface of the 3-layered laminate, which may be specified by

$$u_3^{(3)} = 0,\ \ x_2 = 3h \ \text{ and } \ \widehat{\tau}^{(1)} = 0, \quad x_2 = 0, \tag{4.16}$$

into the relation (4.11), we will arrive at the dispersion relation for fixed-free faces problem in the form

$$\Big(C^{(2)}_{2323}q_2\cosh(kq_1h)\cosh(kq_2h)+C^{(1)}_{2323}q_1\sinh(kq_1h)\sinh(kq_2h)\Big)\times$$
$$\cosh(kq_3h)C^{(3)}_{2323}q_3+C^{(2)}_{2323}q_2\sinh(kq_3h)\Big(C^{(1)}_{2323}q_1\sinh(kq_1h)\cosh(kq_2h)+$$
$$C^{(2)}_{2323}q_2\sinh(kq_2h)\cosh(kq_1h)\Big)=0. \tag{4.17}$$

Fixed faces case

We will now apply zero displacement on the upper and lower surfaces of the laminate, given by

$$u^{(3)}_3=0,\quad x_2=3h\quad\text{and}\quad u^{(1)}_3=0,\quad x_2=0. \tag{4.18}$$

The dispersion relation for this case can be derived after inserting the above boundary conditions in (4.11), and given in the following form

$$\Big(C^{(2)}_{2323}q_2\sinh(kq_1h)\cosh(kq_2h)+C^{(1)}_{2323}q_1\cosh(kq_1h)\sinh(kq_2h)\Big)\times$$
$$\cosh(kq_3h)C^{(3)}_{2323}q_3+C^{(2)}_{2323}q_2\Big(C^{(1)}_{2323}q_1\cosh(kq_1h)\cosh(kq_2h)+$$
$$C^{(2)}_{2323}q_2\sinh(kq_1h)\sinh(kq_2h)\Big)\sinh(kq_3h)=0. \tag{4.19}$$

4.3 Numerical results

In this section we will present numerical results of the exact dispersion relation corresponding to anti-plane shear waves propagating in a pre-stressed and linear isotropic 3-layered elastic laminate. In what follows, the notations $\rho v^2 = \bar{v}^2$ and $kh = K$ will be used. The numerical analysis will be carried out for three specified types of boundary conditions.

Let us now introduce a Varga material model as an example of pre-stressed materials. Thus, numerical results for all boundary conditions cases will depend on Varga material parameters in the following table.

Table 4.1: Varga material used in numerical results

Materials	$\mu^{(n)}$	$\lambda_1^{(n)}$	$\lambda_2^{(n)}$	$\lambda_3^{(n)}$	$C_{1313}^{(n)}$	$C_{2323}^{(n)}$
Layer 1	4.5	1.5	1	2	0.964	0.5
Layer 2	2	2	1.8	0.5	1.950	1.72
Layer 3	2.3	2.2	1.7	1.1	0.8199	0.577

Free-faces case

We will investigate this case for the material parameters in Table 4.1. In Figure 4.2 dispersion curves for a 3-layered laminate structure with free faces are demonstrated, showing scaled phase speed against scaled wave number for the first seventeen branches in respect to Varga strain-energy function. This figure shows a possibility of wave speed formed in a variety of ways. We

also notice from this figure, there are monotonic convergence for each two harmonics. We first note that in the long wave region $K \to 0$ the fundamental mode exist for the dispersion relation (4.15). Also, as $K \to 0$, the long wave limit of each harmonic is infinite.

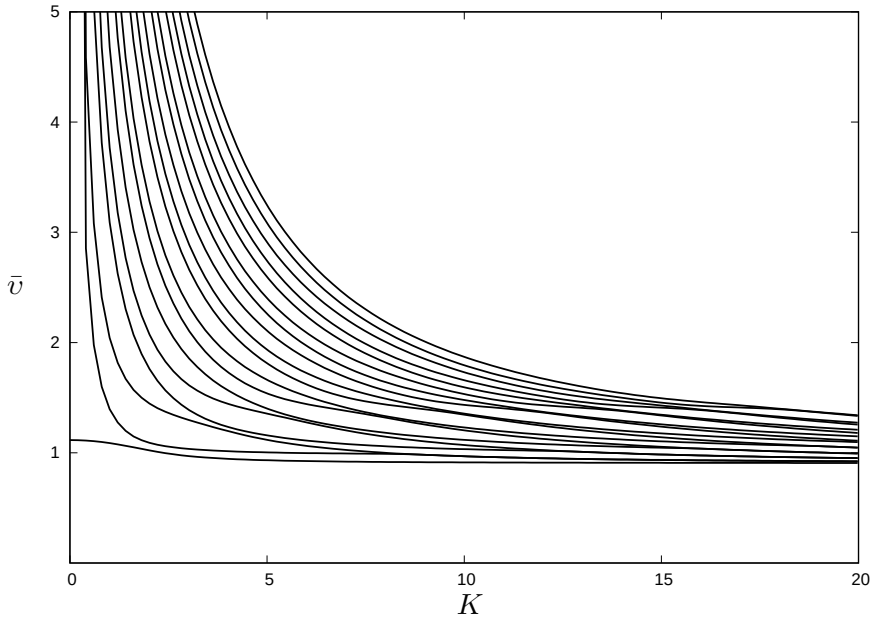

Figure 4.2: Scaled wave speed against scaled wave number for the free-faces dispersion relation (4.15) for Varga material parameters in Table 4.1.

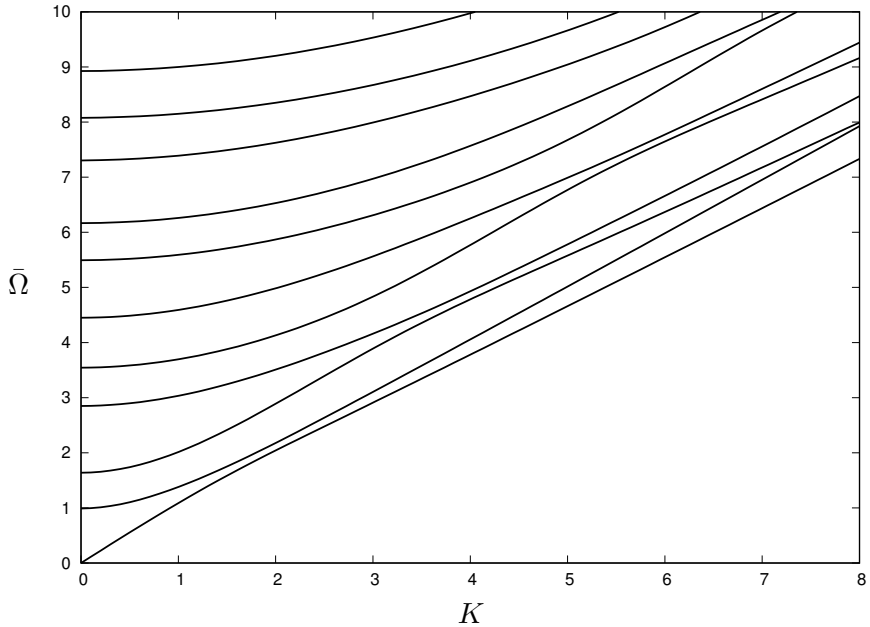

Figure 4.3: Scaled frequency against scaled wave number for the free-faces dispersion relation (4.15) for Varga material parameters in Table 4.1.

We present Figure 4.3, showing scaled frequency $\bar{\Omega}$ against scaled wave number K. From this figure, it can be seen that the only branch has finite long wave limit is the fundamental mode with other branches termed as cut-off frequencies, have non zero limits.

Fixed-free faces case

The absence of fundamental mode of the relation (3.24) in this case indicates that the numerical analysis will be only provided for long wave high frequency limit. In Figure 4.4, it can be shown that the scaled phase speed $\bar{v}$ propagate in pairs against scaled wave number K and all harmonics have infinite limits in the long wave region ($K \to 0$). In Figure 4.5, a plot of scaled frequency $\bar{\Omega}$

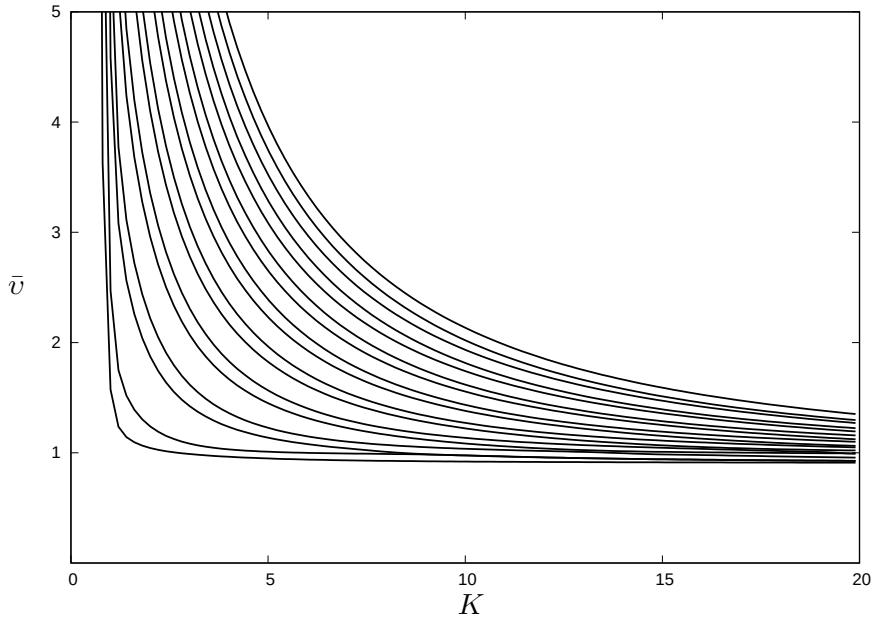

Figure 4.4: Scaled wave speed against scaled wave number for the fixed-free faces dispersion relation (4.17) for Varga material parameters in Table 4.1.

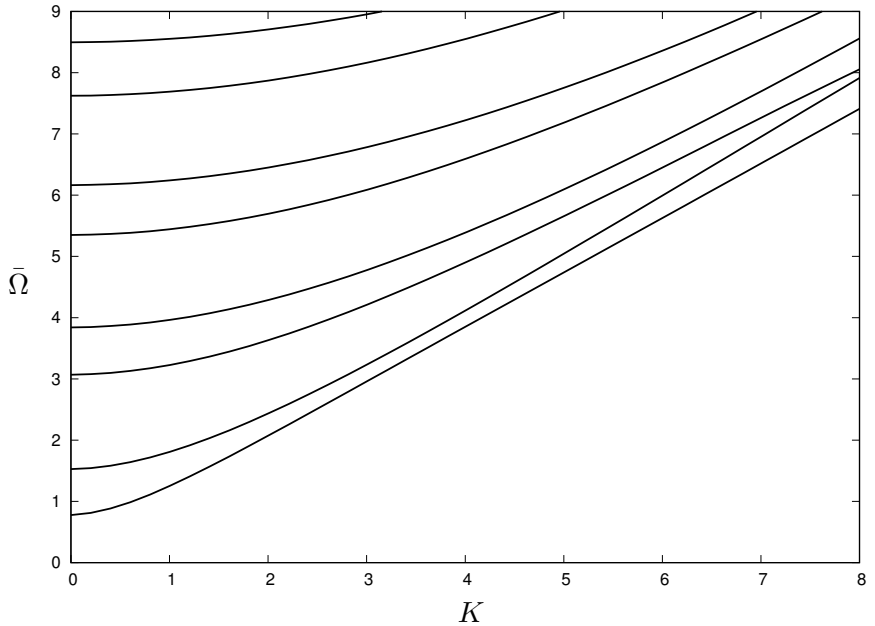

Figure 4.5: Scaled frequency against scaled wave number for the fixed-free faces dispersion relation (4.17) for Varga material parameters in Table 4.1.

against scaled wave number K is presented, showing all harmonics curves in this case with non zero limits.

Fixed-faces case

Figure 4.6 presents a plot of scaled wave speed against scaled wave number of the dispersion relation (4.19) with fixed faces. We first remark that, the fundamental mode does not exist. Also, the other harmonics, which have non-zero long-wave limits, are close to harmonics in Figure 4.2. In Figure 4.7, corresponding plots of scaled frequency $\bar{\Omega}$ against scaled wave number K are presented. From the numerical analysis shown for fixed faces, we can notice that the long wave limits are not zero.

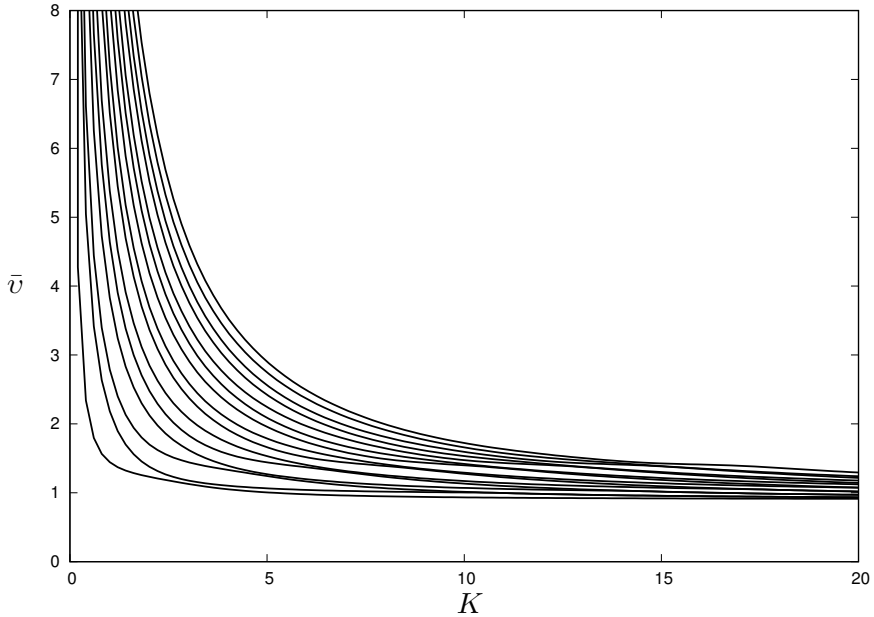

Figure 4.6: Scaled wave speed against scaled wave number for the fixed-faces dispersion relation (4.19) for Varga material parameters in Table 4.1.

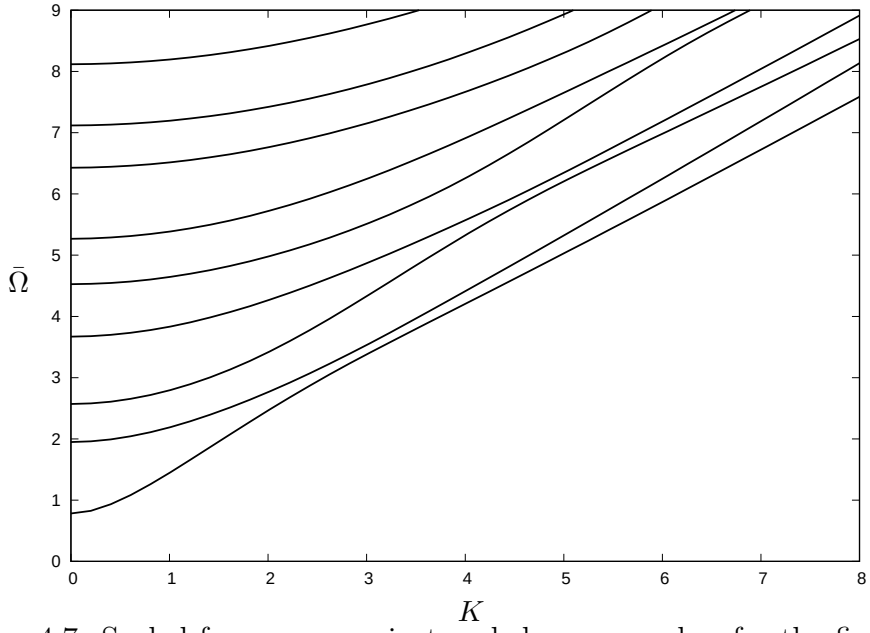

Figure 4.7: Scaled frequency against scaled wave number for the fixed-faces dispersion relation (4.19) for Varga material parameters in Table 4.1.

4.4 Long wave approximations

In this section we consider the long wave low frequency limit of the fundamental mode and long wave high frequency for both pre-stressed and linear isotropic elastic materials.

4.4.1 Long-wave low-frequency limit for free faces

It is well known that for this type of motion $\bar{v}$ is generally not very large as $K \to 0$. Thus, all the hyperbolic functions obtained in the dispersion relation (4.15) will be expanded by Taylor series, see (3.34) and (3.35) with $n = 1, 2, 3$.

$$\cosh q_n K = 1 + \frac{q_n^2 K^2}{2} + O(K^4), \quad \sinh q_n K = q_n K + O(K^3), \ n = 1, 2, 3. \tag{4.20}$$

We begin our derivation of long wave motions with an investigation of the dispersion relation of three layers with free faces for a pre-stressed case, thus we first will represent relation (4.15) in the form

$$\begin{aligned} &C^{(2)}_{2323} q_2 \left(C^{(1)}_{2323} q_1 \tanh(K q_1) + C^{(2)}_{2323} q_2 \tanh(K q_2) \right) + \\ &C^{(3)}_{2323} q_3 \left(C^{(1)}_{2323} q_1 \tanh(K q_1) \tanh(K q_2) + C^{(2)}_{2323} q_2 \right) \tanh(K q_3) = 0. \end{aligned} \tag{4.21}$$

Inserting expansion (4.20) into the dispersion relation (4.21) and making use of the solutions q_1, q_2 and q_3 (4.5), providing the following expansion

$$\beta_1 K^2 + \beta_2 + \beta_3 \bar{v}^2 K^2 + \beta_4 \bar{v}^2 + ... \approx 0. \tag{4.22}$$

where $\bar{v} = \dfrac{\bar{\Omega}}{K}$ in the above expansion with β_i coefficients in the following form

$$\begin{aligned}
\beta_1 &= \frac{C^{(1)}_{2323} C^{(2)}_{2323}}{C^{(2)}_{1313}} - \frac{1}{3}\left[\frac{C^{(1)}_{1313}}{C^{(1)}_{2323}} + \frac{C^{(2)}_{1313}}{C^{(2)}_{2323}} + \frac{C^{(3)}_{1313}}{C^{(3)}_{2323}}\right], \\
\beta_2 &= C^{(1)}_{1313} + C^{(2)}_{1313} + C^{(3)}_{1313}, \\
\beta_3 &= -\frac{1}{C^{(2)}_{2323}}\left(C^{(1)}_{1313} + C^{(2)}_{1313}\right) + \frac{2}{3}\left[\frac{C^{(1)}_{1313}}{C^{(1)}_{2323}} + \frac{C^{(2)}_{1313}}{C^{(2)}_{2323}} + \frac{C^{(3)}_{1313}}{C^{(3)}_{2323}}\right], \\
\beta_4 &= -3.
\end{aligned} \tag{4.23}$$

The squared scaled wave speed can be written as

$$\bar{v}^2 = \upsilon_0 + \upsilon_2 K^2 + O(K^4) + ... \tag{4.24}$$

The leading order term of the dispersion relation (4.21) as $K \to 0$ is readily established by using the solutions (4.5) together with the expansion (4.24)

and equating the like powers in (4.22)

$$\upsilon_0 = \frac{C^{(1)}_{1313} + C^{(2)}_{1313} + C^{(3)}_{1313}}{3}, \tag{4.25}$$

and the next order term in the expansion (4.24), gives

$$\upsilon_2 = -\frac{1}{9}\left[\left(\frac{1}{C^{(1)}_{2323}} - \frac{2}{C^{(2)}_{2323}} + \frac{1}{C^{(3)}_{2323}}\right)\upsilon_0 + 3\left(\frac{C^{(1)}_{1313} + C^{(3)}_{1313}}{C^{(2)}_{2323}}\right)\right.$$
$$\left. - 2\left(\frac{C^{(1)}_{1313}}{C^{(1)}_{2323}} + \frac{C^{(2)}_{1313}}{C^{(2)}_{2323}} + \frac{C^{(3)}_{1313}}{C^{(3)}_{2323}}\right) - 3\frac{C^{(1)}_{1313}C^{(3)}_{1313}}{C^{(2)}_{2323}}\right]. \tag{4.26}$$

The relations (4.25) and (4.26) may be now inserted into (4.24), establishing the scaled wave speed expansion associated to this case of boundary as

$$\bar{\upsilon}^2 = \upsilon_0 - \frac{1}{9}\left[\left(\frac{1}{C^{(1)}_{2323}} - \frac{2}{C^{(2)}_{2323}} + \frac{1}{C^{(3)}_{2323}}\right)\upsilon_0 - 2\left(\frac{C^{(1)}_{1313}}{C^{(1)}_{2323}} + \frac{C^{(2)}_{1313}}{C^{(2)}_{2323}} + \frac{C^{(3)}_{1313}}{C^{(3)}_{2323}}\right)\right.$$
$$\left. + 3\left(\frac{C^{(1)}_{1313} + C^{(3)}_{1313}}{C^{(2)}_{2323}}\right) - 3\frac{C^{(1)}_{1313}C^{(3)}_{1313}}{C^{(2)}_{2323}}\right] K^2 + O(K^4). \tag{4.27}$$

Accordingly, $\Omega_0 = 0$ as $K = 0$ and the corresponding scaled frequency may be written as

$$\bar{\Omega}^2 = \upsilon_0\, K^2 + \upsilon_2\, K^4 + ... \tag{4.28}$$

Figure 4.8 shows good agreement for the fundamental mode of numerical solution of (4.15) and asymptotic approximation (4.27). Figure 4.9 compares numerical solution obtained with the asymptotic expansion (4.28) taken to the leading order. The plot has been generated using the material parameters from Figure 4.3 and shows good agreement.

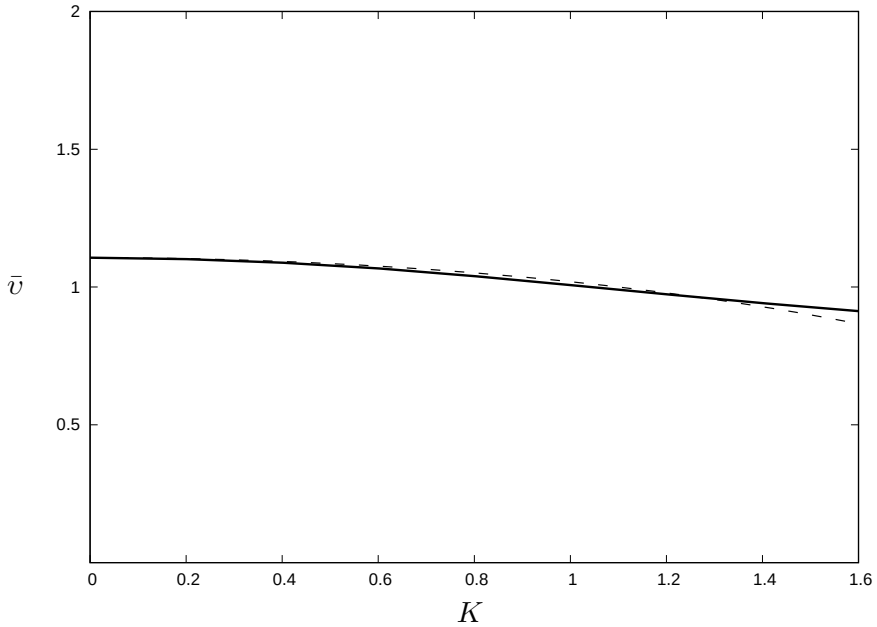

Figure 4.8: A comparison of fundamental mode from numerical solution of (4.15) and asymptotic expansion (4.27) for scaled wave speed against scaled wave number in Varga material with the free faces. The same material parameters from Figure 4.2 are used.

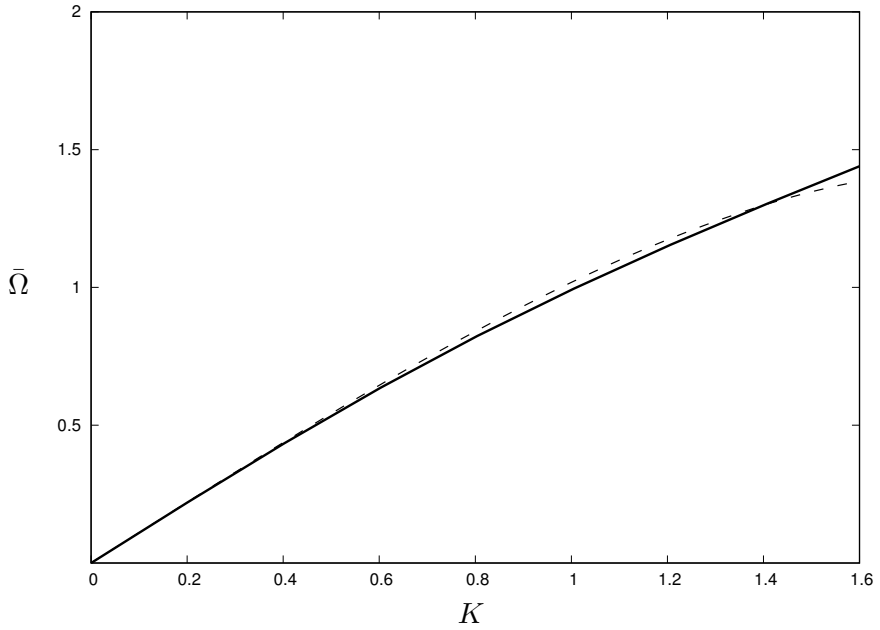

Figure 4.9: A comparison of fundamental mode from numerical solution of (4.15) and asymptotic expansion (4.28) for scaled wave speed against scaled wave number in Varga material with the free faces case. The same parameters from Figure 4.3 are used.

4.4.2 Long wave high-frequency limits

From the numerical results presented in this chapter, the so-called long wave high frequency motion, will be investigated in low wave number region. The cut-off frequencies of the harmonics for the three types of boundary value problems will be also obtained. We have previously mentioned that, in the long wave region $\bar{v}$ is not too small as $K \to 0$ and the solutions q_1, q_2 and q_3 are imaginary, then, it is convenient to put $q_n = i\widehat{q}_n$. Also, motivated by previously established results for the two layers problem, we will present the

squared scaled frequency as a function of powers of K^2 as

$$\bar{\Omega}^2 = \Omega_0 + \Omega_2 K^2 + O(K^4) + ... \tag{4.29}$$

Free-faces case

The long wave high frequency regime of the dispersion relation with free faces (4.15) will be examined. We start our derivation of long wave high-frequency motion by introducing the dispersion relation (4.15) in the following form

$$\left(C^{(1)}_{2323}\widehat{q}_1 \tan(K\widehat{q}_1)\tan(K\widehat{q}_2) - C^{2(2)}_{2323}\widehat{q}_2^2\right) C^{(3)}_{2323}\widehat{q}_3 \tan(K\widehat{q}_3) - C^{(2)}_{2323}\widehat{q}_2\left(C^{(1)}_{2323}\widehat{q}_1\tan(K\widehat{q}_1) + C^{(2)}_{2323}\widehat{q}_2\tan(K\widehat{q}_2)\right) = 0. \tag{4.30}$$

By expanding $\widehat{q}_n$ we may introduce the following expansion

$$K\widehat{q}_n = \frac{\bar{\Omega}}{C^{(n)}_{2323}}\left(1 - \frac{C^{(n)}_{1313}K^2}{2\bar{\Omega}^2} + ...\right).$$

Inserting then the above expansion into (4.30) and making use of (4.29), we obtain the leading order in the following expression

$$\sqrt{C^{(1)}_{2323}\,C^{(3)}_{2323}}F_1(\Omega_0)F_2(\Omega_0)F_3(\Omega_0) - C^{(2)}_{2323}F_2(\Omega_0) - \sqrt{C^{(1)}_{2323}\;C^{(2)}_{2323}}F_1(\Omega_0) - \sqrt{C^{(2)}_{2323}\,C^{(3)}_{2323}}F_3(\Omega_0) = 0, \tag{4.31}$$

where

$$F_n(\Omega_0) = \tan\left(\sqrt{\frac{\Omega_0}{C^{(n)}_{2323}}}\right),\ n = 1, 2, 3.$$

The next order frequency approximation Ω_2 is given by

$$\Omega_2 = \Lambda_1(\Omega_0)/\Lambda_2(\Omega_0), \tag{4.32}$$

where

$$\Lambda_1(\Omega_0) = \Big[\sqrt{\Omega_0}\left(\sqrt{C^{(2)}_{2323}}\ F_2(\Omega_0)(C^{(3)}_{1313} + C^{(1)}_{1313}) - \Omega_0 C^{(2)}_{2323}(F_1^2(\Omega_0)C^{(1)}_{1313}\right.$$
$$\left.+F_2^2(\Omega_0)C^{(2)}_{1313} + F_3^2(\Omega_0)C^{(3)}_{1313} + C^{(1)}_{1313} + C^{(2)}_{1313} + C^{(3)}_{1313}\right) - C^{(2)}_{1313}\sqrt{\Omega_0}$$
$$\left.F_2(\Omega_0)(C^{(2)}_{2323})^{3/2} + \sqrt{\Omega_0}\ \left(F_2^2(\Omega_0) + 1\right)\right)\Big]\ F_3(\Omega_0)\sqrt{C^{(3)}_{2323}} - (C^{(1)}_{1313} + C^{(2)}_{1313})$$
$$\sqrt{\Omega_0}C^{(2)}_{2323} + C^{(3)}_{1313}\sqrt{C^{(2)}_{2323}}F_2(\Omega_0)(F_3^2(\Omega_0) + 1))F_1(\Omega_0)\sqrt{C^{(1)}_{2323}} + \Big(-C^{(2)}_{2323}$$
$$\sqrt{\Omega_0}(C^{(3)}_{1313} + C^{(2)}_{1313}) + F_2(\Omega_0)C^{(1)}_{1313}(F_1^2(\Omega_0) + 1)\Omega_0\ \sqrt{C^{(2)}_{2323}}\Big)\ F_3(\Omega_0)\sqrt{C^{(3)}_{2323}},$$

and

$$\Lambda_2(\Omega_0) = -2F_2(\Omega_0)(C^{(2)}_{2323})^{3/2}\sqrt{\Omega_0} + \Big[\Big(2\sqrt{\Omega_0}\ \sqrt{C^{(2)}_{2323}}F_2(\Omega_0) + \Omega_0(1+$$
$$F_2^2(\Omega_0))\Big)\ F_3(\Omega_0)\ \sqrt{C^{(3)}_{2323}} - 2\sqrt{\Omega_0}C^{(2)}_{2323} + \Omega_0\sqrt{C^{(2)}_{2323}}F_2(\Omega_0)(1 + F_3^2(\Omega_0))\ \Big]$$
$$\times\ F_1(\Omega_0)\sqrt{C^{(1)}_{2323}} + \left(\sqrt{C^{(2)}_{2323}}F_2(\Omega_0)\Omega_0(F_1^2(\Omega_0) + 1) - 2\sqrt{\Omega_0}C^{(2)}_{2323}\right)\sqrt{C^{(3)}_{2323}}$$
$$\times\ F_3(\Omega_0) - \Omega_0 C^{(2)}_{2323}\left(F_1^2(\Omega_0) + F_2^2(\Omega_0) + F_3^2(\Omega_0) + 3\right).$$

Hence, we can conclude the following

$$\bar{\Omega}^2 = \Omega_0 + \frac{\Lambda_1(\Omega_0)}{\Lambda_2(\Omega_0)}\ \Omega_2 K^2 + O(K^4). \tag{4.33}$$

Also, as we mentioned previously that, the cut-off frequencies are not obtainable in explicit form. Thus, the first and the second order term in the scaled frequency form (4.33) may be obtained numerically.

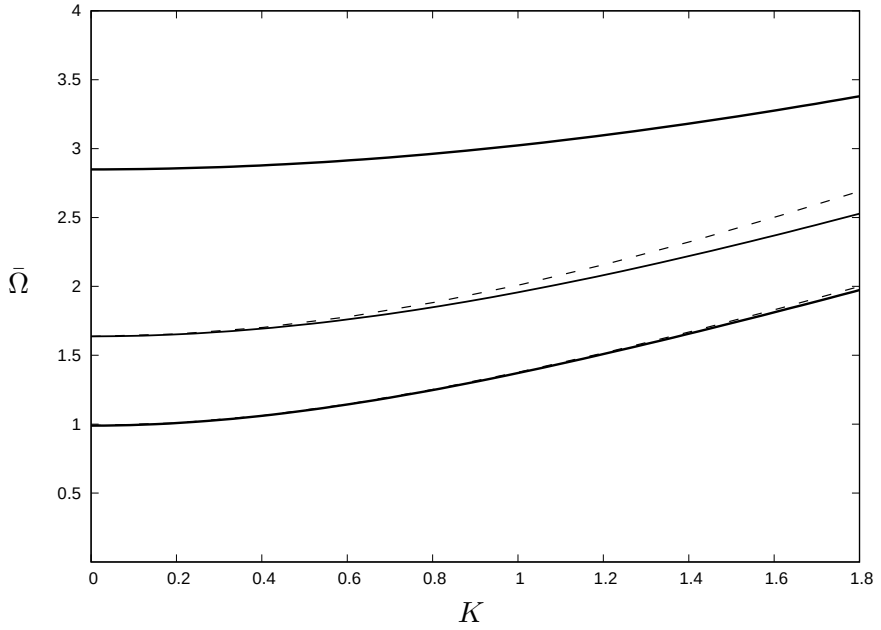

Figure 4.10: A comparison of numerical solution and asymptotic expansion for scaled frequency against scaled wave number for the free-faces dispersion relation (4.15) for Varga material parameters in Table 4.1. The same material parameters from Figure 4.3 are used.

In Figure 4.10 numerical analysis of dispersion curves with free faces (4.15) and asymptotic expansion (4.33) are presented for the first three harmonics. It is remarkable that this comparison showing excellent agreement

between numerical solution and asymptotic expansion and the cut-off frequency Ω_0 takes the values $\Omega_0 \approx 0.989$ at the first harmonic, $\Omega_0 \approx 1.6371$ at the second harmonic and $\Omega_0 \approx 2.848$ at the third harmonic.

Fixed-free faces case

The dispersion relation (4.17) may be rewritten as

$$\left(C^{(1)}_{2323}\widehat{q}_1 \tan(K\widehat{q}_1) + C^{(2)}_{2323}\widehat{q}_2 \tan(K\widehat{q}_2)\right) C^{(2)}_{2323}\widehat{q}_2 + \tan(K\widehat{q}_3)\left(\frac{C^{(1)}_{2323}\widehat{q}_1}{C^{(3)}_{2323}\widehat{q}_3}\tan(K\widehat{q}_1)\tan(K\widehat{q}_2) - 1\right) = 0. \quad (4.34)$$

A similar analysis to that just carried out in respect of the free-faces case can be performed for the fixed-free one, resulting in the leading order term of (4.34) in the following form

$$\sqrt{C^{(1)}_{2323}\, C^{(3)}_{2323}}F_1(\Omega_0)F_2(\Omega_0) + C^{(2)}_{2323}F_2(\Omega_0)F_3(\Omega_0) + \sqrt{C^{(1)}_{2323}\;\; C^{(2)}_{2323}}F_1(\Omega_0)F_3(\Omega_0) - \sqrt{C^{(2)}_{2323}\, C^{(3)}_{2323}} = 0, \quad (4.35)$$

and the next order term is in the form

$$\Omega_2 = \bar{\Lambda}_1(\Omega_0)/\bar{\Lambda}_2(\Omega_0), \quad (4.36)$$

with

$$\bar{\Lambda}_1(\Omega_0) = \Big(C^{(3)}_{1313}\ \Big(F_3^2(\Omega_0)+1\Big)\sqrt{\Omega_0} + \sqrt{C^{(3)}_{2323}}F_3(\Omega_0)\ \Big(C^{(2)}_{1313} - C^{(3)}_{1313}\Big)\Big)$$
$$F_2(\Omega_0)(C^{(2)}_{2323})^{3/2} + \sqrt{\Omega_0}\Big[F_1(\Omega_0)\Big(F_2^2(\Omega_0)C^{(2)}_{1313}\ C^{(3)}_{2323} + F_3^2(\Omega_0)C^{(2)}_{2323}\,C^{(3)}_{1313}$$
$$+ C^{(2)}_{1313}C^{(3)}_{2323} + C^{(2)}_{2323}\ C^{(3)}_{1313}\Big)\sqrt{C^{(1)}_{2323}} + F_3(\Omega_0)C^{(2)}_{2323}\sqrt{C^{(3)}_{2323}}\Big(F_1^2(\Omega_0)\ C^{(1)}_{1313}$$
$$+\ F_2^2(\Omega_0)C^{(2)}_{1313} + C^{(1)}_{1313} + C^{(2)}_{1313}\Big) + C^{(3)}_{2323}\sqrt{C^{(2)}_{2323}}F_2(\Omega_0)C^{(1)}_{1313}$$
$$\Big(F_1^2(\Omega_0)+1\Big)\Big] + F_1(\Omega_0)\Big(F_3(\Omega_0)\,C^{(2)}_{2323}\ \Big(C^{(1)}_{1313} - C^{(3)}_{1313}\Big)\sqrt{C^{(3)}_{2323}}$$
$$+ C^{(3)}_{2323}\sqrt{C^{(2)}_{2323}}F_2(\Omega_0)\Big(C^{(1)}_{1313} - C^{(2)}_{1313}\Big)\Big)\sqrt{C^{(1)}_{2323}},$$

$$\bar{\Lambda}_2(\Omega_0) = \Big(\sqrt{\Omega_0}\Big(F_3^2(\Omega_0)+1\Big) + \sqrt{C^{(3)}_{2323}}F_3(\Omega_0)\Big)\,F_2(\Omega_0)(C^{(2)}_{2323})^{3/2} +$$
$$\Big[F_1(\Omega_0)\Big(F_2^2(\Omega_0)\,C^{(3)}_{2323} + F_3^2(\Omega_0)C^{(2)}_{2323} + C^{(3)}_{2323} + C^{(2)}_{2323}\Big)\sqrt{C^{(1)}_{2323}} + C^{(2)}_{2323}$$
$$F_3(\Omega_0)\Big(F_1^2(\Omega_0) + F_2^2(\Omega_0) + 2\Big)\sqrt{C^{(3)}_{2323}} + C^{(3)}_{2323}\sqrt{C^{(2)}_{2323}}F_2(\Omega_0)\ \Big(F_1^2(\Omega_0)+1\Big)\Big]$$
$$\sqrt{\Omega_0} + F_1(\Omega_0)\Big(F_3(\Omega_0)\,C^{(2)}_{2323}\sqrt{C^{(3)}_{2323}} + C^{(3)}_{2323}\sqrt{C^{(2)}_{2323}}F_2(\Omega_0)\Big)\sqrt{C^{(1)}_{2323}}$$
$$- C^{(2)}_{2323}\,C3^{(3)}_{2323}.$$

Now, we can provide the scaled frequency for this case in the form

$$\bar{\Omega}^2 = \Omega_0 + \frac{\bar{\Lambda}_1(\Omega_0)}{\bar{\Lambda}_2(\Omega_0)}K^2 + O(K^4). \tag{4.37}$$

Figure 4.11 is presented to compare numerical and asymptotic solutions (4.37) with respect of Varga material parameter, for fixed-free faces problem. In this figure the first three harmonics with the three cut-off frequencies values at $0.446, 1.307$ and 2.287, respectively are presented, showing good agreement over the long wave region.

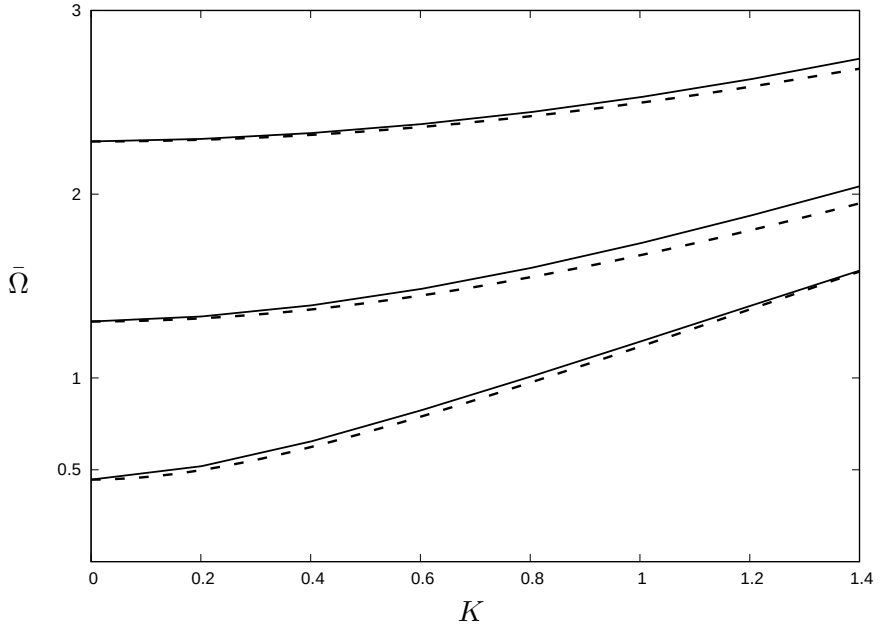

Figure 4.11: A comparison of numerical solution and asymptotic expansion (4.37) for scaled frequency against scaled wave number for the fixed-free faces dispersion relation (4.17) in the case of Varga material parameters in Table 4.1. The same material parameters from Figure 4.5 are used.

Fixed-faces case

For this case of boundaries we will first rewrite the dispersion relation (4.19) in the form

$$C^{(2)}_{2323}\widehat{q}_2\left(C^{(1)}_{2323}\widehat{q}_1 - C^{(2)}_{2323}\widehat{q}_2\tan(\widehat{q}_1)\tan(\widehat{q}_2)\right)\tan(\widehat{q}_3)+ \\ C^{(3)}_{2323}\widehat{q}_3\left(C^{(2)}_{2323}\widehat{q}_2\tan(\widehat{q}_1) + C^{(1)}_{2323}\widehat{q}_1\tan(\widehat{q}_2)\right) = 0. \tag{4.38}$$

Then, we follow previous procedures to provide the leading order and the next order of (4.38). The leading order term can be obtained numerically from

$$F_1(\Omega_0)F_2(\Omega_0)F_3(\Omega_0)C^{(2)}_{2323} - F_1(\Omega_0)\sqrt{C^{(2)}_{2323}C^{(3)}_{2323}}- \\ F_2(\Omega_0)\sqrt{C^{(1)}_{2323}C^{(3)}_{2323}} - F_3(\Omega_0)\sqrt{C^{(1)}_{2323}C^{(2)}_{2323}} = 0, \tag{4.39}$$

then the next order may be written as

$$\Omega_2 = \widetilde{\Lambda}_1(\Omega_0)/\widetilde{\Lambda}_2(\Omega_0), \tag{4.40}$$

with

$$\widetilde{\Lambda}_1(\Omega_0) = (F_2(\Omega_0)(F_1(\Omega_0)C^{(3)}_{1313}\left(F_3^2(\Omega_0)+1\right)\sqrt{C^{(1)}_{2323}} + (C^{(2)}_{2323})^{3/2}F_3(\Omega_0)$$
$$C^{(1)}_{1313}(F_1^2(\Omega_0)+1))\sqrt{C^{(3)}_{2323}} + F_1(\Omega_0)\sqrt{C^{(3)}_{2323}}F_3(\Omega_0)C^{(2)}_{2323}C^{(2)}_{1313}(F_2^2(\Omega_0)+1)$$
$$\sqrt{C^{(1)}_{2323}} - F_1^2(\Omega_0)C^{(2)}_{2323}C^{(3)}_{2323}C^{(1)}_{1313} - C^{(1)}_{2323}C^{(3)}_{2323}C^{(2)}_{1313}F_2^2(\Omega_0) - C^{(1)}_{2323}C^{(2)}_{2323}$$
$$C^{(3)}_{1313}F_3^2(\Omega_0) - (C^{(1)}_{2323}C^{(3)}_{1313} + C^{(3)}_{2323}C^{(1)}_{1313})C^{(2)}_{2323} - C^{(1)}_{2323}C^{(3)}_{2323}C^{(2)}_{1313})\Omega_0^{(5/2)} -$$
$$(F_1(\Omega_0)\sqrt{C^{(1)}_{2323}}\sqrt{C^{(3)}_{2323}}F_2(\Omega_0)F_3(\Omega_0)\left(C^{(1)}_{1313} - C^{(2)}_{1313} + C^{(3)}_{1313}\right)(C^{(2)}_{2323})^{3/2}$$
$$- F_1(\Omega_0)\sqrt{C^{(1)}_{2323}}C^{(2)}_{2323}C^{(3)}_{2323}C^{(1)}_{1313} - C^{(1)}_{2323}(C^{(3)}_{1313}\sqrt{C^{(3)}_{2323}}F_3(\Omega_0)C^{(2)}_{2323}$$
$$+ \sqrt{C^{(2)}_{2323}}F_2(\Omega_0)C^{(3)}_{2323}C^{(2)}_{1313}))\Omega_0^2,$$

$$\widetilde{\Lambda}_2(\Omega_0) = \Big(\left(F_1(\Omega_0)(F_3^2(\Omega_0)+1)\sqrt{C^{(1)}_{2323}} + \sqrt{C^{(3)}_{2323}}F_3(\Omega_0)(F_1^2(\Omega_0)+1)\right)$$
$$F_2(\Omega_0)(C^{(2)}_{2323})^{3/2} + F_1(\Omega_0)\sqrt{C^{(3)}_{2323}}F_3(\Omega_0)C^{(2)}_{2323}(F_2(\Omega_0)^2+1)\sqrt{C^{(1)}_{2323}} -$$
$$F_1^2(\Omega_0)C^{(2)}_{2323}C^{(3)}_{2323} - F_2^2(\Omega_0)C^{(1)}_{2323}C^{(3)}_{2323} - F_3^2(\Omega_0)C^{(1)}_{2323}C^{(2)}_{2323} + C^{(1)}_{2323}C^{(3)}_{2323}$$
$$- (C^{(1)}_{2323} + C^{(3)}_{2323})\,C^{(2)}_{2323}\Big)\,\Omega_0^{\frac{5}{2}} - \Omega_0^2\left(F_1(\Omega_0)(C^{(2)}_{2323})^{3/2}\,\sqrt{C^{(3)}_{2323}}F_2(\Omega_0)F_3(\Omega_0)\right.$$
$$\left. - C^{(2)}_{2323}C^{(3)}_{2323})\sqrt{C^{(1)}_{2323}} - C^{(1)}_{2323}\left(\sqrt{C^{(2)}_{2323}}F_2(\Omega_0)C^{(3)}_{2323} + \sqrt{C^{(3)}_{2323}}\,F_3(\Omega_0)C^{(2)}_{2323}\right)\right).$$

Hence, the scaled frequency for this case can be written in the following form

$$\bar{\Omega}^2 = \Omega_0 + \frac{\widetilde{\Lambda}_1(\Omega_0)}{\widetilde{\Lambda}_2(\Omega_0)}K^2 + O(K^4). \tag{4.41}$$

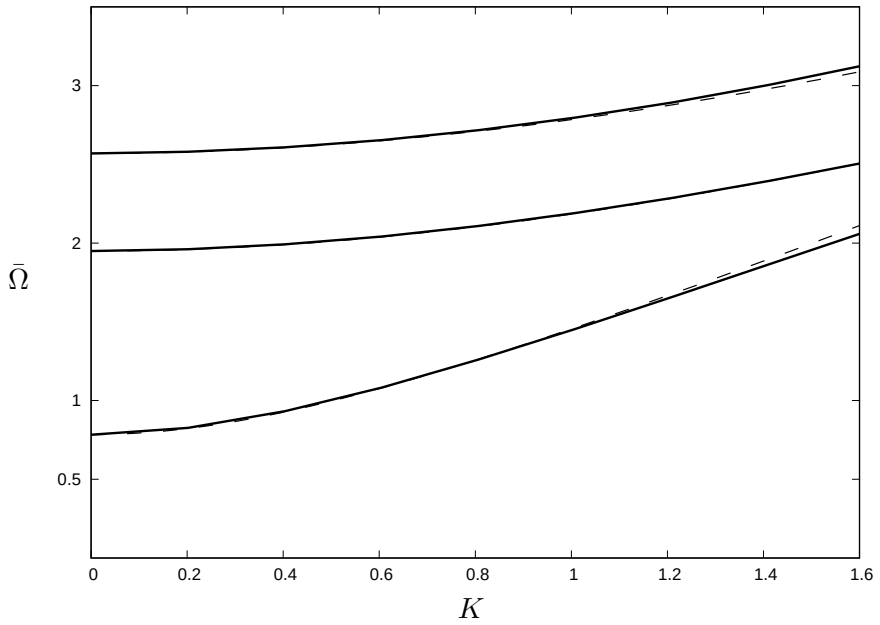

Figure 4.12: A comparison of numerical solution and asymptotic expansion (4.41) for scaled frequency against scaled wave number for the fixed-faces dispersion relation (4.19) in the case of the Varga material parameters in Table 4.1. The same material parameters from Figure 4.7 are used.

Figure 4.12 is presented to compare the asymptotic expansion (4.41) with the numerical solution (4.19) in case of Varga material, in the vicinity of cut-off frequencies for the first three harmonics, showing excellent agreement. The corresponding cut-off frequency Ω_0 takes the values, 0.783, 1.949 and 2.569 at the first, second and third harmonics, respectively.

Chapter 5

Long wave motion in a symmetric 3-layered laminate structure

In this chapter, the propagation of long wave anti-plane shear modes in a symmetrical 3-layered laminate (4-ply) will be investigated.

5.1 Governing equations

We consider a 3-layered sandwiched plate which is formed of a pre-stressed compressible elastic material. This laminate structure has identical outer layers of thickness h and an inner core of $2h$ thickness, which occupies the

region $-h < x_2 < h$, see Figure 5.1. Due to the symmetry about the mid-

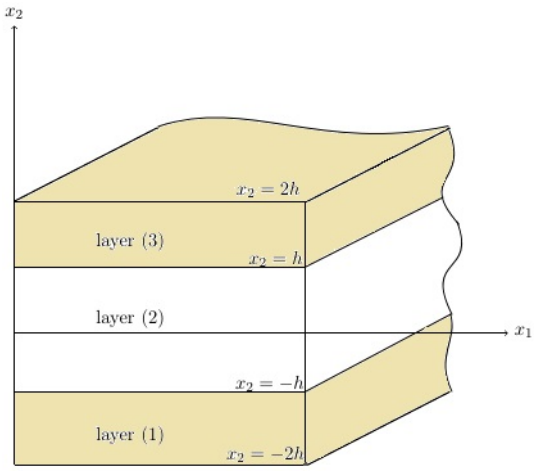

Figure 5.1: Three layered symmetric structure.

plane, the problem under consideration may be decomposed into symmetric (2-ply) and anti-symmetric (2-ply) solutions, allowing algebraic simplification. In Cartesian coordinates $x_i, i = 1, 2, 3$, we can write the equations of motion (3.1) in the form

$$C^{(l)}_{1313} u^{(l)}_{3,11} + C^{(l)}_{2323} u^{(l)}_{3,22} = \rho \ddot{u}^{(l)}_3, \;\; l = s, r, \tag{5.1}$$

where in what follows, the indices s and r correspond to outer layers and inner core, respectively. After inserting the travelling wave solution (3.2) into (5.1), we obtain the linearised equations of motion as provided in (3.3). From which we deduce that the two solutions (3.6) of (3.3), which are denoted

in this chapter by $q_l,\ l = r, s$, take the form

$$q_s = \frac{C^{(s)}_{1313} - \bar{v}^2}{C^{(s)}_{2323}}, \qquad q_r = \frac{C^{(r)}_{1313} - \bar{v}^2}{C^{(r)}_{2323}}. \tag{5.2}$$

We are now able to provide the displacements in terms of only two constants $A_i,\ B_i$ in the form

$$u_3^{(i)} = A_i \sinh(kq_l x_2) + B_i \cosh(kq_l x_2), \quad i = 1, 2. \tag{5.3}$$

After substitution of the above solutions into the surface traction components, we obtain the associated traction components, which are given by

$$\widehat{\tau}^{(i)} = C^{(l)}_{2323} q_l \left(A_i \cosh(kq_l x_2) + B_i \sinh(kq_l x_2) \right). \tag{5.4}$$

5.2 Derivation of the dispersion relations

5.2.1 Free-faces case

We shall now apply zero tractions on the upper and lower surface

$$C^{(s)}_{2323} q_s \left(A_3 \cosh(2kq_l h) + B_3 \sinh(2kq_s h) \right) = 0, \ \ x_2 = 2h, \tag{5.5}$$

$$C^{(s)}_{2323} q_s \left(A_1 \cosh(2kq_s h) - B_1 \sinh(2kq_s h)\right) = 0, \;\; x_2 = -2h, \tag{5.6}$$

with a set of two continuity conditions at each interface. Thus, the first set of the continuity conditions will be introduced at the interface $x_2 = h$ as $u_3^{(2)} = u_3^{(3)}$ and $\widehat{\tau}^{(2)} = \widehat{\tau}^{(3)}$, which may be expressed in the following forms

$$A_3 \sinh(kq_s h) + B_3 \cosh(kq_s h) - A_2 \sinh(kq_r h) - B_2 \cosh(kq_r h) = 0, \tag{5.7}$$

$$C^{(s)}_{2323} q_s (A_3 \cosh(kq_s h) - B_3 \sinh(kq_s h)) - C^{(r)}_{2323} q_r (A_2 \cosh(kq_r h) - B_2 \sinh(kq_r h) = 0. \tag{5.8}$$

Then, at the interface $x_2 = -h$, the next set of continuity conditions are given by $u_3^{(2)} = u_3^{(1)}$ and $\widehat{\tau}^{(2)} = \widehat{\tau}^{(1)}$, which can be provided as

$$-A_1 \sinh(kq_s h) + B_1 \cosh(kq_s h) + A_2 \sinh(kq_r h) - B_2 \cosh(kq_r h) = 0, \tag{5.9}$$

$$C^{(s)}_{2323} q_s (A_1 \cosh(kq_s h) + B_1 \sinh(kq_s h)) - C^{(r)}_{2323} q_r (A_2 \cosh(kq_r h) + B_2 \sinh(kq_r h)) = 0. \tag{5.10}$$

Due to the symmetry of the problem, this system may also be separated into two homogeneous linear systems of three equations in three unknowns. The condition that the system of six equations in six unknowns (5.5)-(5.10) admits non-trivial solutions provides the associated dispersion relation of the structure under consideration.

Symmetric case

If we start subtracting equation (5.5) from (5.6), we get

$$(A_3 - A_1)\cosh(2kq_sh) + (B_3 + B_1)\sinh(2kq_sh) = 0, \tag{5.11}$$

then subtracting equation (5.8) from (5.10)

$$(A_3 - A_1)C^{(s)}_{2323}q_s\cosh(2kq_sh) + (B_3 + B_1)C^{(s)}_{2323}q_s\sinh(kq_sh) - 2B_2C^{(r)}_{2323}q_r\sinh(kq_rh) = 0, \tag{5.12}$$

and adding equation (5.7) to (5.9)

$$(A_3 - A_1)\sinh(kq_sh) + (B_1 + B_3)\cosh(2kq_sh) - 2B_2\cosh(kq_rh) = 0. \tag{5.13}$$

The first (symmetric) system may be obtained from equations (5.11), (5.12) and (5.13). This system of three equations, which has a non-trivial solution,

may be represented in the following determinant of its coefficients is equal to zero

$$\begin{vmatrix} C^{(s)}_{2323} q_s \cosh(2kq_s h) & C^{(s)}_{2323} q_s \sinh(2kq_s h) & 0 \\ C^{(s)}_{2323} q_s \cosh(kq_s h) & C^{(s)}_{2323} q_s \sinh(kq_s h) & -2C^{(r)}_{2323} q_r \sinh(kq_r h) \\ \sinh(kq_s h) & \cosh(kq_s h) & -2\cosh(kq_r h) \end{vmatrix} = 0. \tag{5.14}$$

After making use of $\sinh(2kq_s h) = 2\sinh(kq_s h)\cosh(kq_s h)$, $\cosh(2kq_s h) = 2\cosh^2(kq_s h) - 1$ and a little algebraic manipulation, the symmetric dispersion relation with free faces can be written in the form

$$C^{(r)}_{2323} q_r \sinh(kq_r h)\cosh(kq_s h) + C^{(s)}_{2323} q_s \sinh(kq_s h)\cosh(kq_r h) = 0. \tag{5.15}$$

Anti-symmetric case

By adding the two tractions free conditions (5.5) to (5.6), we obtain

$$(A_3 + A_1)\cosh(2kq_s h) + (B_3 - B_1)\sinh(2kq_s h) = 0, \tag{5.16}$$

then, adding equation (5.8) to (5.10)

$$(A_3 + A_1)C^{(s)}_{2323}q_s \cosh(2kq_sh) + (B_3 - B_1)C^{(s)}_{2323}q_s \sinh(kq_sh) - 2A_2C^{(r)}_{2323}q_r \cosh(kq_rh) = 0, \quad (5.17)$$

and subtracting equation (5.7) from (5.9)

$$(A_3 + A_1)\sinh(kq_sh) + (B_1 - B_3)\cosh(2kq_sh) - 2A_2 \sinh(kq_rh) = 0. \quad (5.18)$$

We now arrive at the second (anti-symmetric) system 3×3, which has a non-trivial solution provided the determinant

$$\begin{vmatrix} C^{(s)}_{2323}q_s \cosh(2kq_sh) & C^{(s)}_{2323}q_s \sinh(2kq_sh) & 0 \\ C^{(s)}_{2323}q_s \cosh(kq_sh) & C^{(s)}_{2323}q_s \sinh(kq_sh) & -2C^{(r)}_{2323}q_r \cosh(kq_rh) \\ \sinh(kq_sh) & \cosh(kq_sh) & -2\sinh(kq_rh) \end{vmatrix} = 0. \quad (5.19)$$

Similar to the symmetric case, we may provide the anti-symmetric dispersion relation in the form

$$C^{(r)}_{2323}q_r \cosh(kq_rh)\cosh(kq_sh) + C^{(s)}_{2323}q_s \sinh(kq_rh)\sinh(kq_sh) = 0. \quad (5.20)$$

5.2.2 Fixed-faces case

To derive the dispersion relation in this case we will apply first the fixed boundary conditions, $u_3^{(1)} = 0$ and $u_3^{(3)} = 0$ on $x_2 = \pm 2h$

$$A_3 \sinh(2kq_s h) + B_3 \cosh(2kq_s h) = 0, \tag{5.21}$$

$$A_1 \sinh(2kq_s h) - B_1 \cosh(2kq_s h) = 0. \tag{5.22}$$

Then, we will make use of the continuity requirements at each perfectly bounded interfaces (5.7)-(5.10) to establish the homogeneous system of six equations in six unknowns which will be decomposed into the two following systems.

Symmetric case

By adding (5.10) to (5.21), (5.7) to (5.9) and subtracting (5.8) from (5.10), the non-trivial solution of the following determinant will provide the symmetric dispersion relation for fixed faces boundary conditions

$$\begin{vmatrix} 0 & \cosh(2kq_s h) & \sinh(2kq_s h) \\ -2C_{2323}^{(r)} q_r \cosh(kq_r h) & C_{2323}^{(s)} q_s \sinh(kq_s h) & C_{2323}^{(s)} q_s \sinh(kq_s h) \\ -2\sinh(kq_r h) & \sinh(kq_s h) & \cosh(kq_s h) \end{vmatrix} = 0, \tag{5.23}$$

which takes the form

$$C^{(r)}_{2323} q_r \sinh(kq_r h)\cosh(kq_s h) + C^{(s)}_{2323} q_s \sinh(kq_s h)\cosh(kq_r h) = 0. \quad (5.24)$$

Anti-symmetric case

In this case, the 3×3 determinant can be obtained by replacing the hyperbolic functions of the inner core $\sinh(kq_r h)$ by $\cosh(kq_r h)$ in the determinant (5.23)

$$\begin{vmatrix} 0 & \cosh(2kq_s h) & \sinh(2kq_s h) \\ -2C^{(r)}_{2323} q_r \sinh(kq_r h) & C^{(s)}_{2323} q_s \sinh(kq_s h) & C^{(s)}_{2323} q_s \sinh(kq_s h) \\ -2\cosh(kq_r h) & \sinh(kq_s h) & \cosh(kq_s h) \end{vmatrix} = 0. \quad (5.25)$$

The anti-symmetric dispersion relation for this case may be written as

$$C^{(s)}_{2323} q_s \cosh(kq_r h)\cosh(kq_s h) + C^{(r)}_{2323} q_r \sinh(kq_r h)\sinh(kq_s h) = 0. \quad (5.26)$$

5.2.3 Fixed-free case

Now we will consider the fixed-free faces problem. Therefore, zero displacement on the lower surface $x_2 = -2h$ and zero traction on the upper surface $x_2 = 2h$, will be imposed in conjunction with the four continuity conditions

(5.7)-(5.10) to establish a system of six equations in six unknowns

$$C^{(s)}_{2323}q_s(A_3\sinh(2kq_sh)+B_3\cosh(2kq_sh))=0, \tag{5.27}$$

$$A_1\sinh(2kq_sh)-B_1\cosh(2kq_sh)=0. \tag{5.28}$$

This system have a non-trivial solution provided the following determinants

$$\begin{vmatrix} C_s & -S_s & -\frac{2C^{(r)}_{2323}q_r}{C^{(s)}_{2323}q_s}C_r & 0 & C_s & S_s \\ C_s & S_s & 0 & \frac{2C^{(r)}_{2323}q_r}{C^{(s)}_{2323}q_s}C_r & 0 & 0 \\ S_s & -C_s & 0 & 2C_r & -S_s & -C_s \\ S_s & -C_s & -2S_r & 0 & S_s & C_s \\ -S_{2s} & C_{2s} & 0 & 0 & C^{(s)}_{2323}q_sC_{2s} & C^{(s)}_{2323}q_sC_{2s} \\ S_{2s} & -C_{2s} & 0 & 0 & C^{(s)}_{2323}q_sC_{2s} & C^{(s)}_{2323}q_sS_{2s} \end{vmatrix} = 0. \tag{5.29}$$

(5.29) provides the dispersion relation for fixed-free faces which may be represented in the explicit form

$$C^{(r)}_{2323}q_rC^{(s)}_{2323}q_sC_s^2C_r^2+2\left(C^{2(s)}_{2323}q_s^2+(q_r\,C^{(r)}_{2323})^2\right)C_rS_rC_sS_sC^{(r)}_{2323}q_r(q_s\,C^{(s)}_{2323})^2C_s^2- 2C^{(r)}_{2323}q_rq_s^2(C^{(s)}_{2323})^2\left(C_s^2+C_r^2\right)+C^{(r)}_{2323}q_rC^{(s)}_{2323}q_s=0, \tag{5.30}$$

where $C_{2s} = \cosh(2kq_sh)$, $S_{2s} = \sinh(2kq_sh)$ and $C_l = \cosh(kq_lh)$, $S_l = \sinh(kq_lh)$, $l = r, s$. In this case, we would mention that this system can not be separated into two systems of 3 equations in 3 unknowns because of the lack of symmetry about the mid-plane.

5.2.4 Reduction to linear isotropic case

We now consider linear isotropic material and derive the dispersion relations for the three types of boundary conditions. Also, we note here that $C^{(l)}_{1313} = C^{(l)}_{2323} = \mu_{(l)}$, thus, the two roots (5.2) may be written as

$$q_s = 1 - \frac{\bar{v}^2}{\mu_s}, \qquad q_r = 1 - \frac{\bar{v}^2}{\mu_r}. \tag{5.31}$$

For free faces symmetric dispersion relation (5.15) for the pre-stressed materials can be rewritten for linear isotropic materials as follows

$$\mu_r q_r \sinh(kq_rh)\cosh(kq_sh) + \mu_s q_s \sinh(kq_sh)\cosh(kq_rh) = 0, \tag{5.32}$$

while for anti-symmetric motion (5.20) reduces to

$$\mu_r q_r \cosh(kq_rh)\cosh(kq_sh) + \mu_s q_s \sinh(kq_rh)\sinh(kq_sh) = 0. \tag{5.33}$$

Equation (5.33) coincides with that for the anti-symmetric dispersion relation for the anti-plane problem in linear isotropic material, which has been looked by Prikazchikova et al. (2018).

For fixed faces, equations (5.24) and (5.26) will be reduced to

$$\mu_r q_r \sinh(kq_r h)\cosh(kq_s h) + \mu_s q_s \sinh(kq_s h)\cosh(kq_r h) = 0, \tag{5.34}$$

and

$$\mu_s q_s \cosh(kq_r h)\cosh(kq_s h) + \mu_r q_r \sinh(kq_r h)\sinh(kq_s h) = 0, \tag{5.35}$$

for symmetric and anti-symmetric cases, respectively.

In case of fixed-free boundary conditions equation (5.30) may be reduced to

$$\mu_r q_r \mu_s q_s C_s^2 C_r^2 + 2\left(\mu_r^2 q_s^2 + \mu_r^2 q_r^2\right) C_r S_r C_s S_s \mu_r q_r \mu_s^2 q_s^2 C_s^2 - 2\mu_r q_r \mu_s^2 q_s^2 \left(C_s^2 + C_r^2\right) + \mu_r q_r \mu_s q_s = 0. \tag{5.36}$$

5.3 Numerical results

We now restrict our concern to the behaviour of the antisymmetric dispersion relations associated to a pre-stressed 3-layered laminate structure. The

three layers chosen are the 4-ply considered as two unit cells. The numerical results for the symmetric case (upper cell) have been obtained in Chapter 3 and a similar numerical analysis, to that carried out in respect of the 2-ply structure, may perform next for the antisymmetric case (lower cell). These dispersion relations are then investigated numerically for pre-stressed dispersion relations in case of Mooney-Rivlin material. In this subsection, we show the numerical results chosen to reveal the character of the anti-symmetric dispersion relation for three types of boundaries considered. Two sets of material parameters are used in various configurations for the outer layers and inner core to generate the figures presented in this section, see Table 5.1.

Table 5.1: Mooney-Rivlin material (MRM) used in numerical results

Materials	$\mu_1^{(l)}$	$\mu_2^{(l)}$	$\lambda_1^{(l)}$	$\lambda_2^{(l)}$	$\lambda_3^{(l)}$	$C_{1313}^{(l)}$	$C_{2323}^{(l)}$
Inner core	1.2	0.3	1	1.1	1	1.42	1.65
Outer layers	1	1.1	2	2	10	0.64	0.54

The following set of six figures are presented using material parameters generated from the Mooney-Rivlin strain energy function. Moreover, the numerical results have been derived for anti-symmetric dispersion relation of both free and fixed boundary conditions. The dispersion curves for free-faces case are presented in Figure 5.2 for the material parameters presented in Table 5.1. It is clear that there is no fundamental mode in the long wave region, however its symmetric counterpart has a a finite wave speed

limit value . We also present Figure 5.3 showing scaled frequency $\bar{\Omega}$ against scaled wave number K. In this figure we can see that only non-zero cut-of frequencies values are possible for this boundary condition and the lowest value is $\Omega_0 \approx 0.84$.

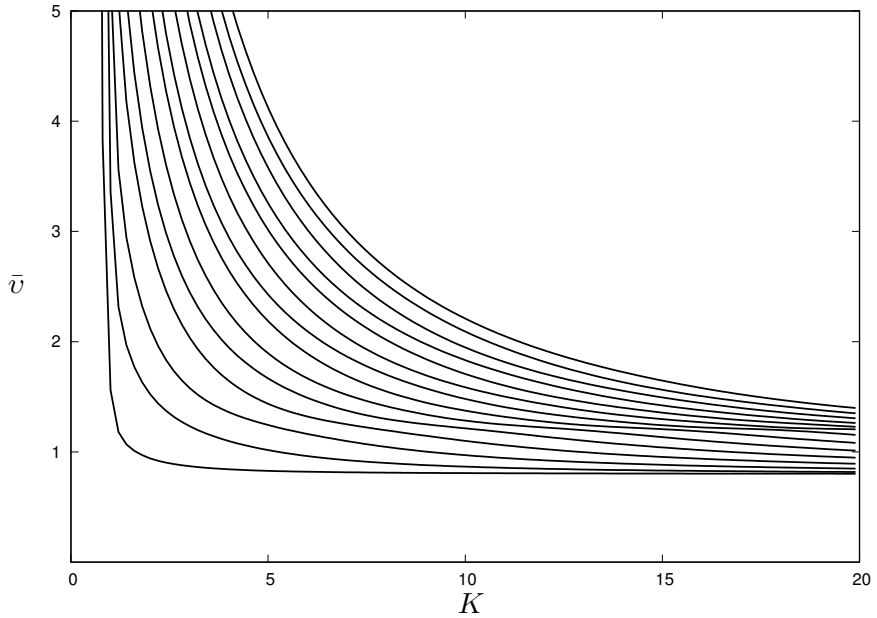

Figure 5.2: Scaled wave speed against scaled wave number for anti-symmetric Mooney-Rivlin dispersion relation (5.20) with free faces for the material parameters in Table 5.1.

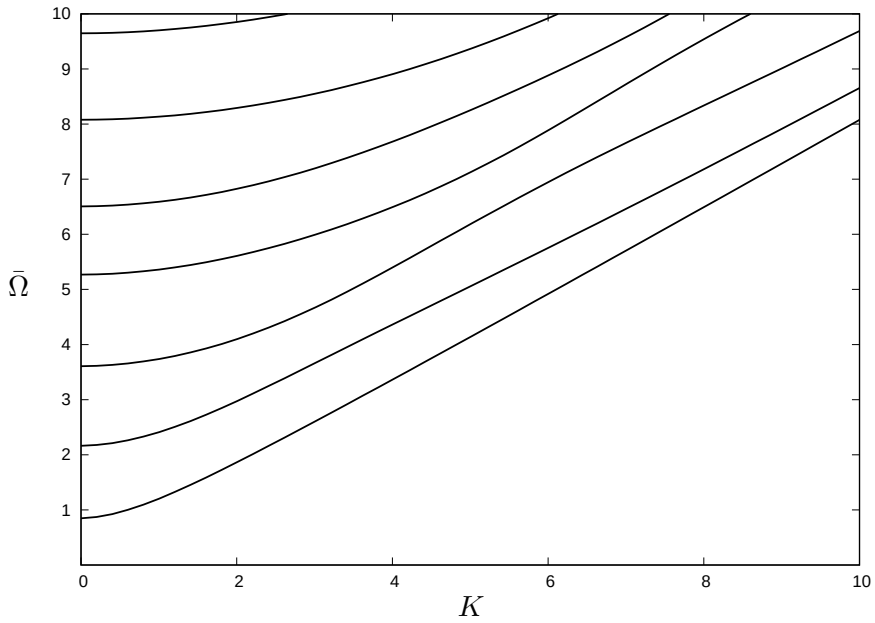

Figure 5.3: Scaled frequency against scaled wave number for anti-symmetric dispersion relation (5.20) with free faces in the case of Mooney-Rivlin material parameters in Table 5.1.

In Figure 5.4 a plot of scaled phase speed $\bar{v}$ against scaled wave number K is presented for the first seven branches in respect of the anti-symmetric dispersion relation associated with fixed faces. We first remark that the long wave limit of each harmonic is non-zero in anti-symmetric case. In Figure 5.5, corresponding plots of scaled frequency $\bar{\Omega}$ against scaled wave number are presented. We note from this figure that in the low wave number (long wave) region ($K \to 0$) the anti-symmetric limit of the fundamental mode is not-zero and the lowest cut-off frequency value is observed at $\Omega_0 \approx \sqrt{0.3767} \approx 0.608$. At the end of this subsection, fixed-free faces case has been investigated numerically. Thus, Figure 5.6 showed no dispersion curves have a finite wave

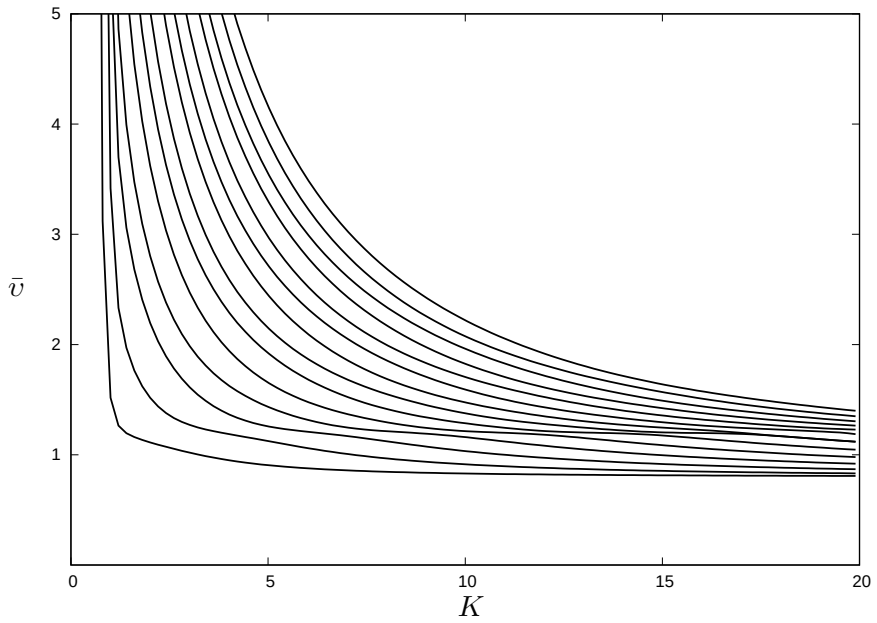

Figure 5.4: Scaled wave speed against scaled wave number for anti-symmetric Mooney-Rivlin dispersion relation (5.26) with fixed faces for the material parameters in Table 5.1.

speed and $\bar{v} \to \infty$ as $K \to 0$. Then, in Figure 5.7 it is observed that in the vicinity of the long wave all harmonics have non-zero limits. It is remarkable that the first harmonic in this case of boundaries has a lower cut-off frequency limit value than other cases.

5.4 Long wave limit approximations

In this section, asymptotic approximations of anti-symmetric dispersion relation will be carried out for the pre-stressed 3-layered sandwiched laminate. These approximations provide phase speed, and frequency, as an explicit

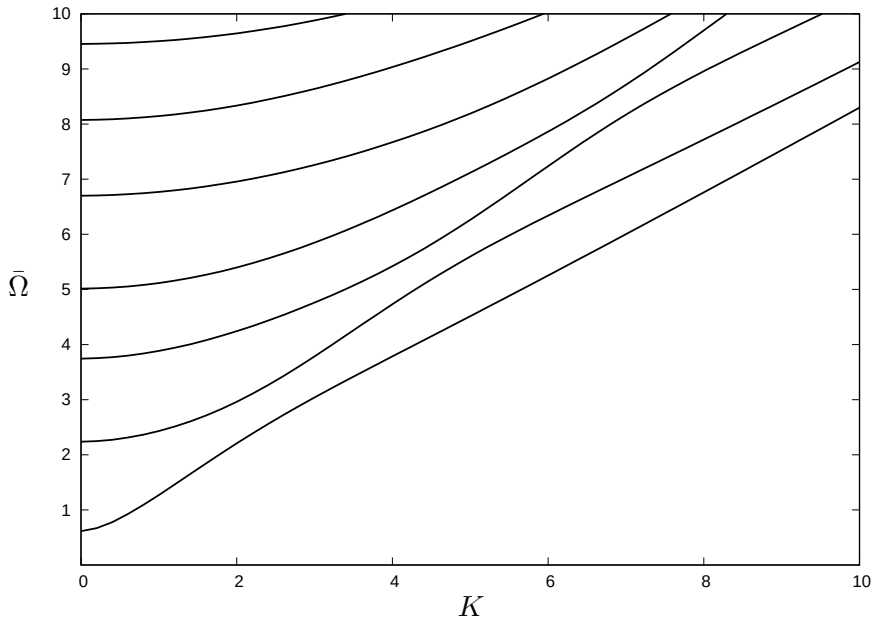

Figure 5.5: Scaled frequency against scaled wave number for anti-symmetric Mooney-Rivlin dispersion relation (5.26) with fixed faces for the material parameters in Table 5.1.

function of wave number for each mode. As previously mentioned in (chapters 3 and 4) for this type of motion $\bar{v}$ is generally very much larger than the associated body wave speeds in the long wave regime. The asymptotic analysis, however, is clearly form the numerical analysis that there are no fundamental modes in anti-symmetric motion. Thus, the long wave approximations will be limited to case of high frequency approximations for which the material parameters in each layer are of similar order.

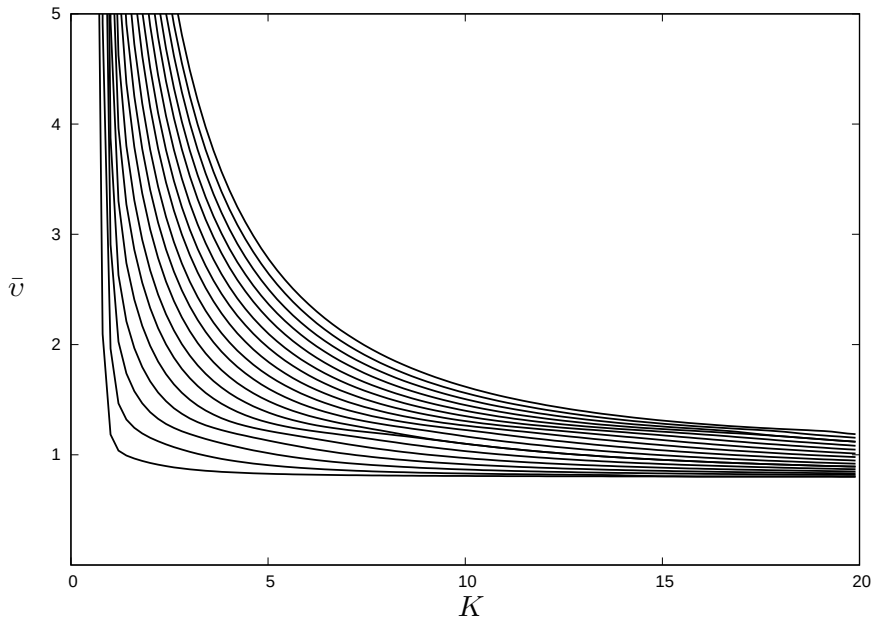

Figure 5.6: Scaled wave speed against scaled wave number for Mooney-Rivlin dispersion relation (5.30) with fixed-free faces for the material parameters in Table 5.1.

5.4.1 Pre-stressed elastic materials

Free-faces case

In this case, the scaled frequency will be introduced in the following form

$$\bar{\Omega}^2 = \Omega_0 + \Omega_2 K^2 + O(K^4),$$

and the anti-symmetric dispersion relation (5.20) will be written as

$$C^{(s)}_{2323} q_s \tan(K q_s) \tan(K q_r) - C^{(r)}_{2323} q_r = 0. \tag{5.37}$$

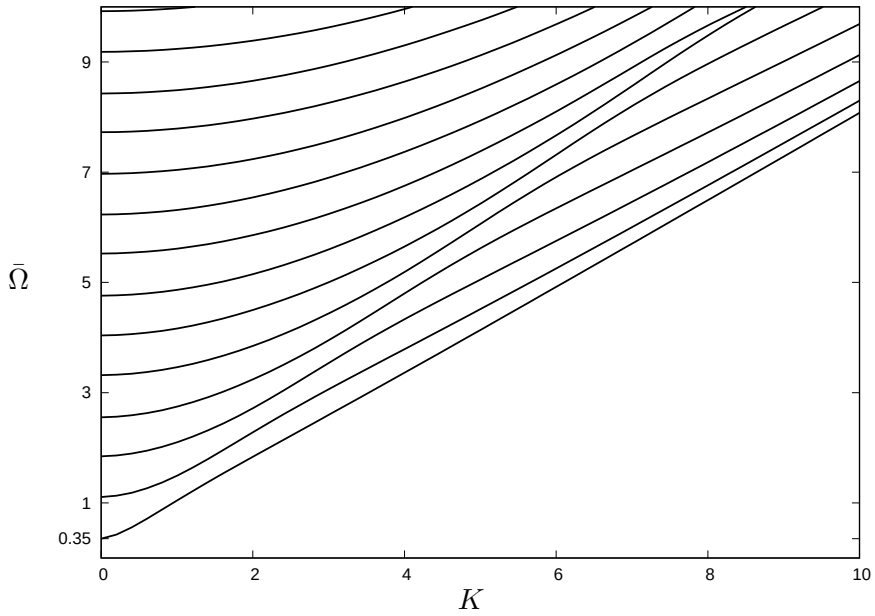

Figure 5.7: Scaled frequency against scaled wave number for dispersion relation (5.30) with fixed-free faces in the case of Mooney-Rivlin material parameters in Table 5.1.

By using expansions (3.48), the leading order term may be expressed explicitly by the following relation

$$\sqrt{C^{(s)}_{2323}}F_1(\Omega_0)F_2(\Omega_0) - \sqrt{C^{(r)}_{2323}} = 0, \tag{5.38}$$

where Ω_0 can be found by solving equation (5.38) numerically. The second term in this case can be introduced as

$$\Omega_2 = \bar{\Phi}_1(\Omega_0)/\bar{\Phi}_2(\Omega_0), \tag{5.39}$$

with

$$\bar{\Phi}_1(\Omega_0) = \sqrt{C^{(r)}_{2323}\, C^{(s)}_{2323}} F_1(\Omega_0) F_2(\Omega_0) C^{(s)}_{1313} - C^{(r)}_{1313} C^{(r)}_{2323}$$
$$+ \left(\sqrt{C^{(r)}_{2323}} F_1(\Omega_0) F_2^2(\Omega_0) C^{(s)}_{1313} + \sqrt{C^{(s)}_{2323}} F_1^2(\Omega_0) F_2(\Omega_0) C^{(r)}_{1313} \right.$$
$$\left. + \sqrt{C^{(r)}_{2323}} F_1(\Omega_0) C^{(s)}_{1313} + \sqrt{C^{(s)}_{2323}} F_2(\Omega_0) C^{(r)}_{1313} \right) \sqrt{\Omega_0},$$

and

$$\bar{\Phi}_2(\Omega_0) = -C^{(r)}_{2323} + \left(\sqrt{C^{(r)}_{2323}} F_1(\Omega_0) F_2^2(\Omega_0) + \sqrt{C^{(s)}_{2323}} F_1^2(\Omega_0) F_2(\Omega_0) \right.$$
$$\left. + \sqrt{C^{(r)}_{2323}} F_1(\Omega_0) C^{(s)}_{1313} + \sqrt{C^{(s)}_{2323}} F_2(\Omega_0) \right) \sqrt{\Omega_0}$$
$$+ \sqrt{C^{(r)}_{2323} C^{(s)}_{2323}} F_1(\Omega_0) F_2(\Omega_0).$$

We can now express $\bar{\Omega}^2$ in the following form

$$\bar{\Omega}^2 = \Omega_0 + \frac{\Phi_1(\Omega_0)}{\Phi_2(\Omega_0)} \; K^2 + O(K^4). \tag{5.40}$$

In Figure 5.8, $\bar{\Omega}$ is shown as a function of K and the asymptotic approximation (5.40) of dispersion relation has been shown to be in good agreement with the exact dispersion relation (5.20).

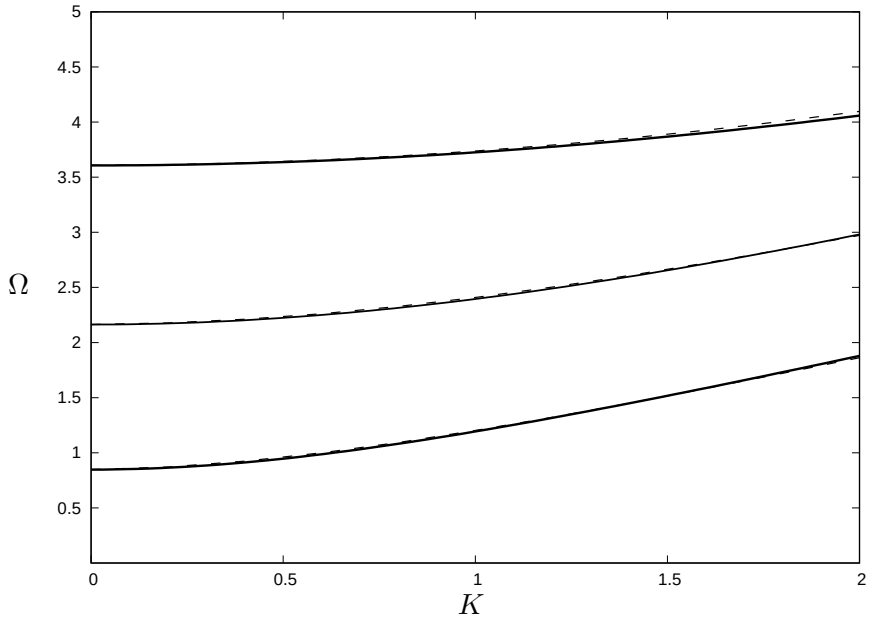

Figure 5.8: Comparison of numerical solution of (5.33) with asymptotic expansion (5.40) established for the anti-symmetric free faces case. The same material parameters from Figure 5.3 are used.

Fixed-faces case

For fixed faces case, we may consider dispersion relation (5.26) in the following form

$$C^{(r)}_{2323} q_r \tan(K q_r) \tan(K q_s) - C^{(s)}_{2323} q_s = 0. \tag{5.41}$$

The leading order term can be expressed explicitly from the numerical solution of the following relation

$$\sqrt{C^{(2)}_{2323}} F_1(\Omega_0) F_2(\Omega_0) - \sqrt{C^{(1)}_{2323}} = 0, \tag{5.42}$$

and the second term can be introduced as

$$\Omega_2 = \widetilde{\Phi}_1(\Omega_0)/\widetilde{\Phi}_2(\Omega_0), \tag{5.43}$$

with

$$\begin{aligned}\widetilde{\Phi}_1(\Omega_0) = \sqrt{C^{(r)}_{2323}\, C^{(s)}_{2323}}F_1(\Omega_0)F_2(\Omega_0)C^{(s)}_{1313} + \Big(\sqrt{C^{(s)}_{2323}}F_2(\Omega_0)C^{(r)}_{1313} \\ + \sqrt{C^{(s)}_{2323}}F_1^2(\Omega_0)\ F_2(\Omega_0)C^{(r)}_{1313} + \sqrt{C^{(r)}_{2323}}F_1(\Omega_0)C^{(s)}_{1313} \\ + \sqrt{C^{(r)}_{2323}}F_1(\Omega_0)F_2^2(\Omega_0)C^{(s)}_{1313}\Big)\sqrt{\Omega_0} - C^{(r)}_{1313}C^{(r)}_{2323},\end{aligned}$$

and

$$\begin{aligned}\widetilde{\Phi}_2(\Omega_0) = -C^{(r)}_{2323} + \Big(\sqrt{C^{(r)}_{2323}}F_1(\Omega_0)F_2^2(\Omega_0) + \sqrt{C^{(s)}_{2323}}F_1^2(\Omega_0)F_2(\Omega_0) \\ + \sqrt{C^{(r)}_{2323}}F_1(\Omega_0)C^{(s)}_{1313} + \sqrt{C^{(s)}_{2323}}F_2(\Omega_0)\Big)\sqrt{\Omega_0} \\ + \sqrt{C^{(r)}_{2323}\, C^{(s)}_{2323}}F_1(\Omega_0)F_2(\Omega_0).\end{aligned}$$

In this case, the scaled frequency by

$$\bar{\Omega}^2 = \Omega_0 + \frac{\widetilde{\Phi}_1(\Omega_0)}{\widetilde{\Phi}_2(\Omega_0)}\, K^2 + O(K^4). \tag{5.44}$$

The above relation is used with the exact dispersion relation (5.35) to provide excellent agreement in Figure 5.9. Also, the numerical solution and both the leading and second order approximations are presented in respect of the first

three harmonics associated with a Mooney-Rivlin material.

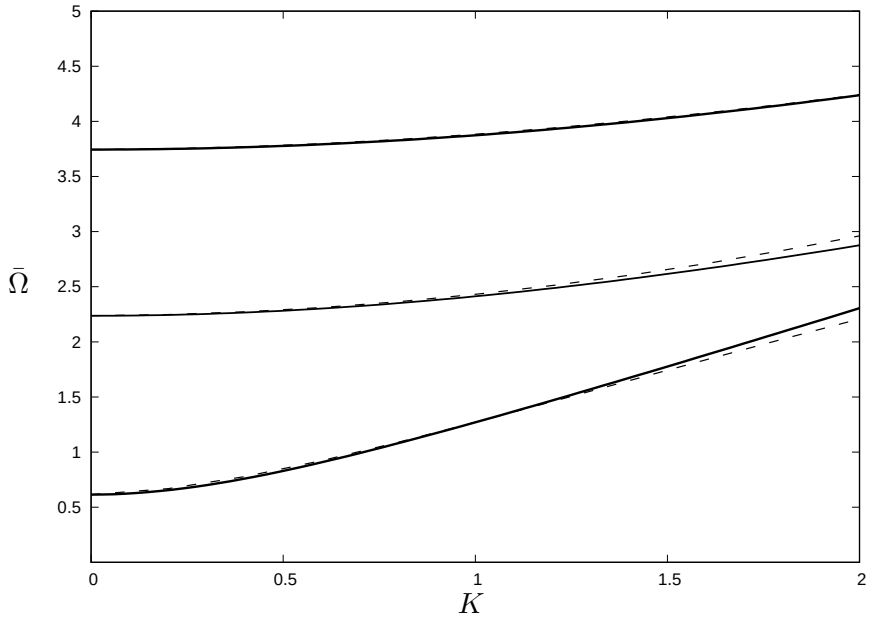

Figure 5.9: Comparison of numerical solution of (5.35) with asymptotic expansion (5.44) established for the anti-symmetric fixed faces case. The same material parameters from Figure 5.5 are used.

Fixed-free faces case

We begin our investigation of long wave high frequency in this case by expressing the dispersion relation (5.30) in the form

$$C_{2323}^{(r)}\, C_{2323}^{(s)}\, \widehat{q}_r\, \widehat{q}_s \left(4\, \cos^2\left(K\widehat{q}_s\right) \cos^2\left(K\widehat{q}_r\right) - 2\cos^2\left(K\widehat{q}_r\right) - 2\cos^2\left(K\widehat{q}_s\right) - 1\right)$$
$$+\, 2\, \cos\left(K\widehat{q}_s\right) \sin\left(K\widehat{q}_s\right) \cos\left(K\widehat{q}_r\right) \sin\left(K\widehat{q}_r\right) \left((C_{2323}^{(s)})^2 \widehat{q}_s^2 + (C_{2323}^{(r)})^2 \widehat{q}_r^2\right) = 0. \tag{5.45}$$

Then, providing the leading order term as

$$4\, C_{sp}^2 C_{rp}^2 \sqrt{C_{2323}^{(r)}} \sqrt{C_{2323}^{(s)}} - 2\, C_{sp}\, S_{sp}\, C_{rp}\, S_{rp}\, C_{2323}^{(r)} - 2\, C_{sp}\, S_{sp}\, C_{rp}\, S_{rp}\, C_{2323}^{(s)} -$$
$$2\, C_{sp}^2 \sqrt{C_{2323}^{(r)}} \sqrt{C_{2323}^{(s)}} - 2\, C_{sp}^2 \sqrt{C_{2323}^{(r)}} \sqrt{C_{2323}^{(s)}} + \sqrt{C_{2323}^{(r)}} \sqrt{C_{2323}^{(s)}} = 0, \tag{5.46}$$

where $C_{lp} = \cos\left(\sqrt{\dfrac{\Omega_0}{C_{2323}^{(l)}}}\right)$, $S_{lp} = \sin\left(\sqrt{\dfrac{\Omega_0}{C_{2323}^{(l)}}}\right)$, $l = r, s$. Then, the next order term can be written as

$$\Omega_2 = \Phi_1/\Phi_2, \tag{5.47}$$

with

$$\Phi_1 = \Big(4\sqrt{\Omega_0\, C^{(s)}_{2323}}C_{sp}\, S_{sp}\, C^{(r)}_{1313} + 2\Omega_0\, C^{(s)}_{1313}\,(C_{sp} - S_{sp})\,(C_{sp} + S_{sp})\Big)$$
$$\times\, C_{rp}\, S_{rp}\,(C^{(r)}_{2323})^{3/2} + C_{sp}\ (\ 2C^{(r)}_{1313}\,\Omega_0\,(C_{rp} - S_{rp})\,(C_{rp} + S_{rp}) +$$
$$4\, C_{rp}\,\sqrt{\Omega_0\, C^{(r)}_{2323}}S_{rp}\, C^{(s)}_{1313}\ )\, S_{sp}\,(C^{(s)}_{2323})^{3/2} - 4\,\Big({C_{rp}}^2 - 1/2\Big)\times$$
$$\Big(C^{(r)}_{1313} + C^{(s)}_{1313}\Big)\Big(C^2_{sp} - 1/2\Big)\, C^{(r)}_{2323}\, C^{(s)}_{2323}\,\sqrt{\Omega_0} + 2\,\Omega_0\,(\ \Big(4C^{(s)}_{2323}$$
$$\Big(C^{(r)}_{1313} + C^{(s)}_{1313}4\Big)\, C^2_{sp} - \ {S_{sp}}^2 C^{(s)}_{1313} - 2C^{(r)}_{1313}\ )\, C_{rp} S_{rp}\sqrt{C^{(r)}_{2323}} +$$
$$\Big(\Big(C^{(r)}_{1313} + 4\, C^{(s)}_{1313}\Big)\, C^2_{rp} - S^2_{rp} C^{(r)}_{1313} - 2\, C^{(s)}_{1313}\Big)\,\sqrt{C^{(s)}_{2323}} C_{sp}\, C^{(r)}_{2323} S_{sp}\ )\,,$$

$$\Phi_2 = 4\,\Big(\sqrt{C^{(s)}_{2323}}C_{sp}\, S_{sp}\sqrt{\Omega_0} + 1/2\, C^2_{sp}\Omega_0 - 1/2\, S^2_{sp}\Omega_0\Big)\,(C^{(r)}_{2323})^{3/2}$$
$$\times\, C_{rp}\, S_{rp} + 4\,\Big(\sqrt{C^{(r)}_{2323}}C_{rp}\, S_{rp}\,\sqrt{\Omega_0} + 1/2\, C^2_{rp}\Omega_0 - 1/2\, S^2_{rp}\Omega_0\Big)$$
$$\times\, C_{sp} S_{sp}\,\Big(C^{(s)}_{2323}\Big)^{3/2} + \ C^{(s)}_{2323} S_{rp}\,\Omega_0\, C_{rp}\ \Big(10\, C^2_{sp} - 2\, S^2_{sp} - 4\Big)$$
$$\times\,\sqrt{C^{(r)}_{2323}} + \ (C_{sp}\ S_{sp}\,\Omega_0\ \Big(10\, C^2_{rp} - 2\, S^2_{rp} - 4\Big)\,\sqrt{C^{(s)}_{2323}}$$
$$-8\, C^{(s)}_{2323}\,\Big(C^2_{rp} - 1/2\Big)\,\Big(C^2_{sp} - 1/2\Big)\,\sqrt{\Omega_0}\Big)\, C^{(r)}_{2323}.$$

Hence, the scaled frequency in this case can be written in the form

$$\bar{\Omega}^2 = \Omega_0 + \frac{\Phi_1(\Omega_0)}{\Phi_2(\Omega_0)}\, K^2 + O(K^4). \tag{5.48}$$

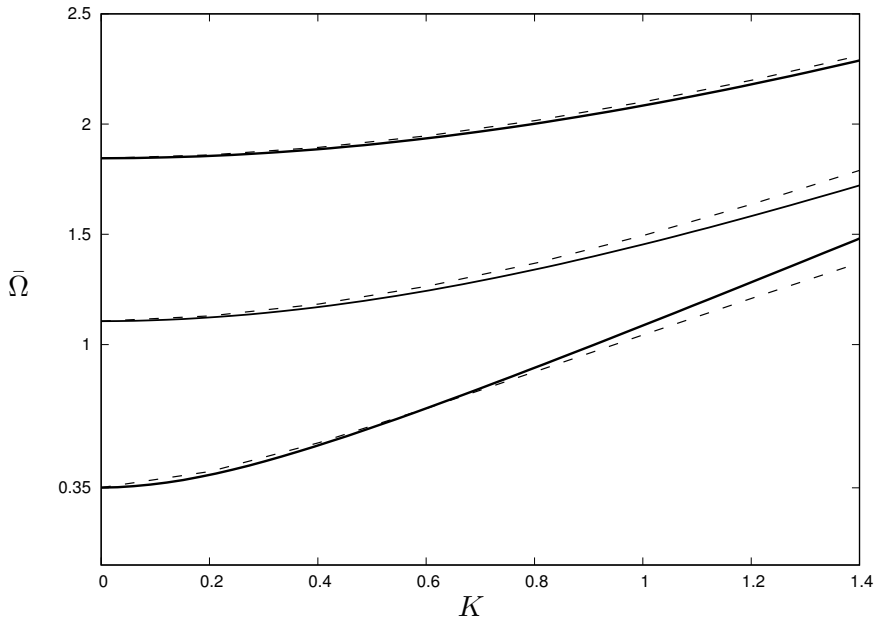

Figure 5.10: Comparison of numerical solution of (5.30) with asymptotic expansion (5.48) established for the anti-symmetric fixed free faces case. The same material parameters from Figure 5.7 are used.

Figure 5.10 provides excellent agreement between the numerical solution of (5.30) and asymptotic expansion (5.48).

We remark that case of antisymmetric of 4-ply with fixed-free faces might look similar to global low-frequency regimes, see Kaplunov et al. (2016). At the same time, there is a difference since the next cut-off frequency is still small, not of order unity.

Expanding the leading order in the low-frequency limit, we will get the

cut-off frequencies Ω_0

$$\sqrt{C^{(r)}_{2323}}\sqrt{C^{(s)}_{2323}}\Omega_0 + 4\left(\frac{1}{C^{(r)}_{2323}} - \frac{1}{C^{(s)}_{2323}}\right)\sqrt{C^{(r)}_{2323}}\sqrt{C^{(s)}_{2323}}\Omega_0^2 + O(\Omega_0)^3 \approx 0, \tag{5.49}$$

with

$$\Omega_0 = \frac{1}{4}\left(\frac{C^{(r)}_{2323}\, C^{(s)}_{2323}}{C^{(s)}_{2323} + C^{(r)}_{2323}}\right). \tag{5.50}$$

One of the possible physical interpretations of this small cut-off frequencies values as $\Omega_0 \ll 1$ is related to quasi-static behaviour of both inner and outer layers of the 4-ply laminate.

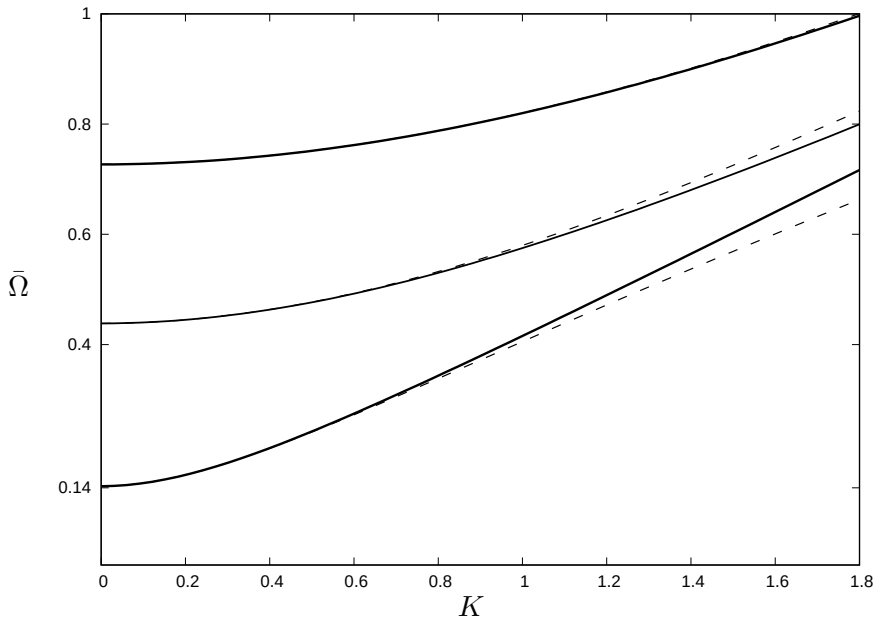

Figure 5.11: Comparison of numerical solution of (5.30) with asymptotic expansion (5.44) obtained for the anti-symmetric fixed-free faces case; $C^{(r)}_{2323} = C^{(r)}_{1313} = 0.2$, $C^{(s)}_{2323} = C^{(s)}_{1313} = 0.1$.

Figure 5.11 comparing numerical solution with asymptotic approximation in the case of fixed-free faces and showing good agreement. Three modes in this figure show low frequency limits. These limits corresponding to $\sqrt{0.204} \approx 0.14$ at the first harmonic curve, $\sqrt{0.192} \approx 0.438$ at the second curve and $\sqrt{0.5283} \approx 0.727$ at the third one.

5.4.2 Reduction to linear isotropic case

Free-faces case

To investigate the long wave limits in this case, we will first express the dispersion relation (5.33) as

$$\mu_s \widehat{q}_s \tan(Kq_r) \tan(Kq_s) - \mu_r \widehat{q}_r = 0. \tag{5.51}$$

Following similar procedures in the pre-stressed case, the leading order term may be written as

$$T_1(\Omega_0)T_2(\Omega_0)\sqrt{\mu_s} - \sqrt{\mu_r} = 0. \tag{5.52}$$

The next order term in the expansion (3.48) can be presented in the form

$$\Omega_2^2 = G_1/G_2, \tag{5.53}$$

with

$$G_1 = T_1(\Omega_0)T_1(\Omega_0)\mu_s^{3/2}\sqrt{\mu_r} + (T_1(\Omega_0)\mu_s(T_2^2(\Omega_0)+1)\sqrt{\mu_r} +$$
$$T_2(\Omega_0)\mu_r\sqrt{\mu_s}(T_1^2(\Omega_0)+1))\sqrt{\Omega_0} - \mu_r^2,$$

and

$$G_2 = T_1(\Omega_0)(T_2^2(\Omega_0)+1)\sqrt{\mu_r} + T_2(\Omega_0)\sqrt{\mu_s}(T_1^2(\Omega_0)+1))\sqrt{\Omega_0} +$$

$$T_1(\Omega_0)T_2(\Omega_0)\sqrt{\mu_r}\sqrt{\mu_s} - \mu_r.$$

Now, we can express the scaled frequency expansion (3.48) by substituting (5.52) and (5.53) as follows

$$\bar{\Omega}^2 = \Omega_0 + \frac{G_1}{G_2}\ K^2 + O(K^4). \tag{5.54}$$

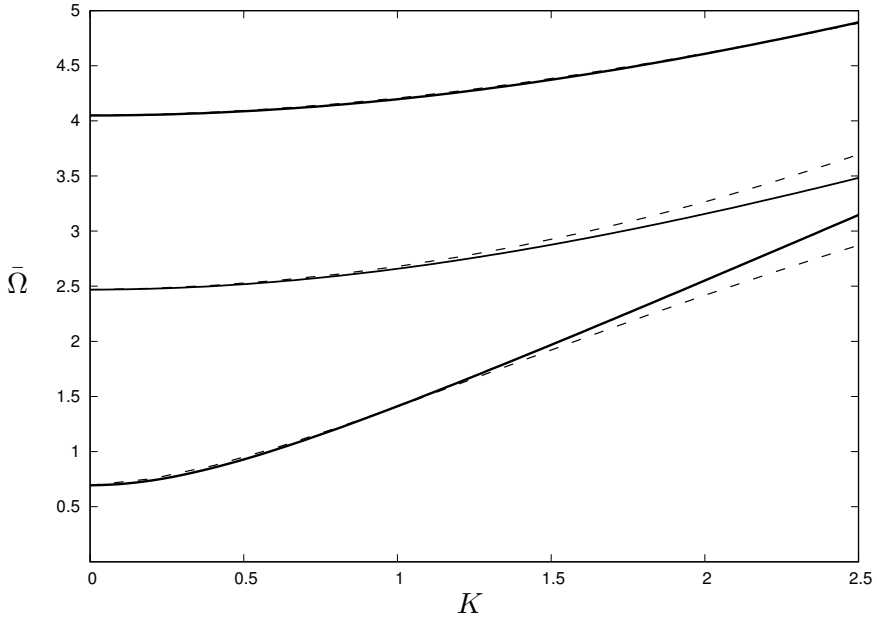

Figure 5.12: Comparison of numerical solution for anti-symmetric free-faces dispersion relation (5.33) and approximation (5.54) in the case of the linear isotropic material, corresponding to $\mu_s = 0.7$ and $\mu_r = 1.75$.

In Figure 5.12, a comparison of the asymptotic expansion (5.54) with numerical solution (5.33) is made for first three harmonics, showing excellent

agreement over the long wave region. It is worth to mention that in symmetric case with the same material parameters the lowest cut-off frequency limit reached $\Omega_0 = \sqrt{2.3645} \approx 1.53$ whereas in this case the lowest one is $\Omega_0 = \sqrt{0.35729} \approx 0.597$.

Fixed-faces case

Similarly to the previous case, we will express the dispersion relation (5.35) as

$$\mu_r \widehat{q}_r \tan(Kq_r) \tan(Kq_s) - \mu_s \widehat{q}_s = 0. \tag{5.55}$$

Then, the scaled frequency in this case will be introduced in the form

$$\bar{\Omega}^2 = \Omega_0 + \frac{\bar{G}_1}{\bar{G}_2} \ K^2 + O(K^4). \tag{5.56}$$

where The leading order term Ω_0 of the dispersion relation (5.55) can be obtained by solving the following relation numerically

$$T_1(\Omega_0) T_2(\Omega_0) \sqrt{\mu_r} + \sqrt{\mu_s} = 0. \tag{5.57}$$

Then, after a little algebraic manipulation an expression for the next approximation may be established,

$$\Omega_2 = \bar{G}_1/\bar{G}_2, \tag{5.58}$$

with

$$\bar{G}_1 = T_1^2(\Omega_0)T_2(\Omega_0)\mu_r\sqrt{\mu_s}\sqrt{\Omega_0} + T_1(\Omega_0)T_2^2(\Omega_0)\mu_s\sqrt{\Omega_0}\sqrt{\mu_r} +$$

$$T_1(\Omega_0)\mu_s\sqrt{\Omega_0}\sqrt{\mu_r} + T_1(\Omega_0)T_2(\Omega_0)\mu_r^{3/2}\sqrt{\mu_s} + T_2(\Omega_0)\mu_r\sqrt{\mu_s}\sqrt{\Omega_0} - \mu_s^2,$$

and

$$\bar{G}_2 = T_1^2(\Omega_0)T_2(\Omega_0)\sqrt{\mu_s}\sqrt{\Omega_0} + T_1(\Omega_0)T_2^2(\Omega_0)\sqrt{\Omega_0}\sqrt{\mu_r} +$$

$$T_1(\Omega_0)T_2(\Omega_0)\sqrt{\mu_r}\sqrt{\mu_s} + T_1(\Omega_0)\sqrt{\Omega_0}\sqrt{\mu_r} + T_2(\Omega_0)\sqrt{\mu_s}\sqrt{\Omega_0} - \mu_s.$$

Another comparison has been done in Figure 5.13 for fixed boundary value problem, which clearly shown good agreement for the first three branches. From this figure we noted that the lowest cut-off frequency limit in this case of anti-symmetric is $\Omega_0 = \sqrt{0.8319} \approx 0.912$, which is less than the value in its symmetric counterpart for the same material parameters at $\Omega_0 = \sqrt{2.8506} \approx 1.688$.

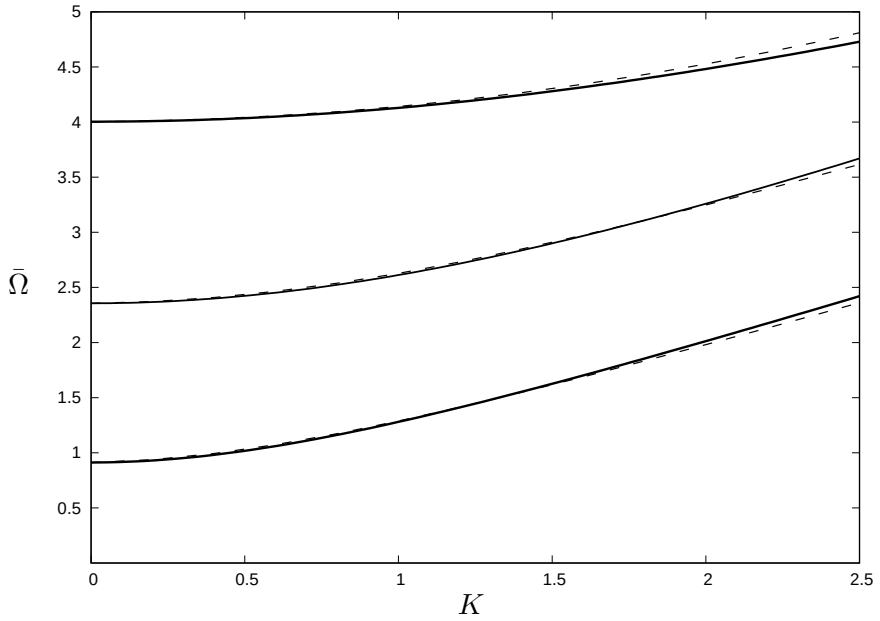

Figure 5.13: Comparison of numerical solution for anti-symmetric fixed-faces dispersion relation (5.35) and approximation (5.56) in the case of the linear isotropic material, corresponding to $\mu^{(s)} = 0.7$ and $\mu^{(r)} = 1.75$.

Fixed-free faces case

In this case we will express the dispersion relation (5.36) in the form

$$\mu_r\,\mu_s\,\widehat{q}_r\,\widehat{q}_s\left(4\,\cos^2\left(K\widehat{q}_2\right)\cos^2\left(K\widehat{q}_r\right)-2\cos^2\left(K\widehat{q}_s\right)-2\cos^2\left(K\widehat{q}_s\right)-1\right)$$

$$+\,2\,\cos\left(K\widehat{q}_s\right)\sin\left(K\widehat{q}_s\right)\cos\left(K\widehat{q}_r\right)\sin\left(K\widehat{q}_r\right)\left(\mu_r^2\widehat{q}_r^2+\mu_s^2\widehat{q}_s^2\right)=0. \qquad (5.59)$$

The leading order term can be obtained from (5.59)

$$\sqrt{\mu_r}\sqrt{\mu_s}\left(4\,C_{s_0}^2C_{r_0}^2-2\,C_{r_0}^2-2\,C_{s_0}^2+1\right)-2\,C_{s_0}C_{r_0}S_{s_0}S_{r_0}\left(\mu_r+\mu_s\right)=0, \qquad (5.60)$$

where $C_{l_0} = \cos\left(\sqrt{\frac{\Omega_0}{\mu_l}}\right), \quad S_{l_0} = \sin\left(\sqrt{\frac{\Omega_0}{\mu_l}}\right), \; l = r, s.$ Then, the next order term can be expressed as

$$\Omega_2 = \widetilde{G}_1/\widetilde{G}_2, \tag{5.61}$$

with

$$\widetilde{G}_1 = 3\,\Omega_0\,S_{r_0}\,C_{r_0}\,\mu_r\left(C_{s_0}^2 - \frac{1}{2}\right)\mu_r^{3/2} + 3\Omega_0\,S_{s_0}\left(C_{r_0}^2 - \frac{1}{2}\right)\mu_r C_{s_0}\,\mu_s^{3/2} +$$
$$C_{s_0}\,C_{r_0}\,S_{s_0}\,S_{r_0}\sqrt{\Omega_0}\left(\mu_r^{5/2}\sqrt{\mu_s} + \mu_s^{5/2}\sqrt{\mu_r}\right) - \mu_s\left(C_{r_0}^2 - \frac{1}{2}\right)\mu_r\left(C_{s_0}^2 - \frac{1}{2}\right)$$
$$(\mu_r + \mu_s)\sqrt{\Omega_0} + \Omega_0\left(C_{r_0}S_{r_0}\mu_s^2\left(C_{s_0}^2 - \frac{1}{2}\right)\sqrt{\mu_r} + \sqrt{\mu_s}C_{s_0}S_{s_0}\mu_r^2\left(C_{r_0}^2 - \frac{1}{2}\right)\right),$$

$$\widetilde{G}_2 = 3\,\Omega_0\,\left(C_{r_0}\,S_{r_0}\,\mu_s\left(C_{s_0}^2 - \frac{1}{2}\right)\sqrt{\mu_r} + \sqrt{\mu_s}C_{s_0}\,S_s\,\mu_r\left(C_{r_0}^2 - \frac{1}{2}\right)\right) +$$
$$\left(C_{s_0}\sqrt{\mu_s}\sqrt{\Omega_0}S_{s_0} + \Omega_0\left(C_{s_0}^2 - \frac{1}{2}\right)\right)S_{r_0}\,C_{r_0}\,\mu_r^{3/2} + S_{s_0}\left(C_{r_0}\sqrt{\mu_r\,\Omega_0}S_{r_0}\right.$$
$$\left. + \Omega_0\,\left(C_{r_0}^2 - \frac{1}{2}\right)\right)C_{s_0}\,\mu_s^{3/2} - 2\mu_s\left(C_{r_0}^2 - \frac{1}{2}\right)\mu_r\left(C_{s_0}^2 - \frac{1}{2}\right)\sqrt{\Omega_0}.$$

From the above knowledge, we can write the appropriate expansion for the scaled frequency in the form

$$\bar{\Omega}^2 = \Omega_0 + \frac{\widetilde{G}_1}{\widetilde{G}_2}\;K^2 + O(K^4). \tag{5.62}$$

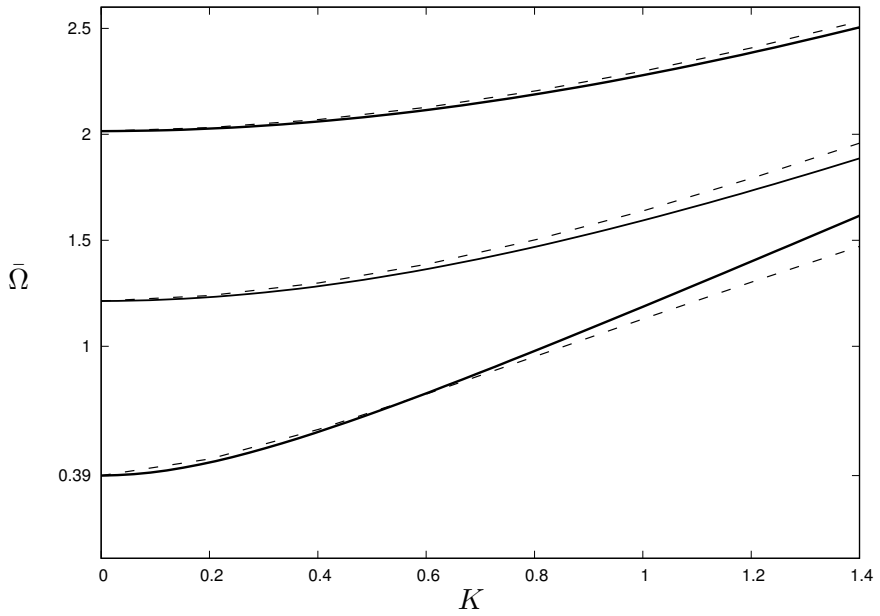

Figure 5.14: Comparison of numerical solution for anti-symmetric fixed free faces dispersion relation (5.36) and approximation (5.62) in the case of the linear isotropic material, corresponding to $\mu^{(s)} = 0.7$ and $\mu^{(r)} = 1.75$.

Chapter 6

Conclusion

Small-amplitude anti-plane wave motion in a pre-stressed compressible layered elastic structure subject to three different types of boundary conditions, namely free-face, fixed-free face and fixed-face, have been investigated in this thesis. The assumption of anti-plane motion allows significant simplification of generally complicated algebraic expressions expected in pre-stressed layered structures. First, the dispersion relation is derived and solved numerically. The derivations for layered structures rely on the propagator matrix technique. Predictably, the long-wave low-frequency behaviour is only possible for the free face boundary conditions, whereas for the other two types (fixed faces and fixed-free case) there is no fundamental mode. Then, explicit approximations for the phase velocity and frequency are obtained for two- and three-layered asymmetric laminates, as well as for a symmetric four-

ply layered structure, contributing to elucidating essential features of the dispersion phenomena. The efficiency of the derived long-wave asymptotic approximations is illustrated numerically, for several strain-energy functions, such as neo-Hookean, Mooney-Rivlin and Varga models. Both low- and high-frequency limits have been addressed. In particular, the expressions for the cut-off frequencies have been derived.

First, in Chapter 2 an introductory studies of dispersive wave phenomena in a single pre-stressed, elastic layer have been performed, along with a description of the propagator matrix technique. Then, in Chapter 3 a two-layered laminate is considered with perfect bonding on the interface. The dispersion relations have been derived for all three types of face boundary conditions. The numerical solutions of these relations are presented and compared with those for linearly isotropic elastic material, elucidating some specific features caused by the presence of a pre-stress. The long-wave approximations of the dispersion relations are constructed, including both low- and high-frequency domains. Explicit approximate dependencies of phase velocity and frequency on the wave number are obtained. In Chapter 4, the previously obtained results are generalised to a three-layered asymmetric laminate.

Finally, a particular type of a symmetric structure, namely, a four-ply laminate is studied. The presence of symmetry allows separate treatment of

symmetric and anti-symmetric motion for free-face or fixed-face boundary conditions. The analysis in fixed-free case remains relatively less straightforward, since the symmetry cannot be employed. It is demonstrated that in case of anti-symmetric motion of a symmetric structure subject to free-face boundary conditions, the solution matches results obtained in Prikazchikova et al. (2018). Other types of motion/boundary conditions are thoughtfully studied. It is demonstrated that in the long wave limit, depending on the pre-stress, at most one finite limiting phase speed may exist in the symmetric, free-face scenario, whereas, for all other examined boundary value problems such a mode does not exist.

Some possible further generalisations of the approach include, in particular, consideration of higher number of layers, including a more challenging case of n-layered structure, where propagator matrix technique will be especially useful, as well as taking into account effects of curvature, inhomogeneity, viscosity, etc. Moreover, the achieved results provide the basis for derivation of asymptotically consistent lower dimensional models for anti-plane motion of layered pre-stressed structures. Finally, we mention prospective development of multiparametric asymptotic analysis for strongly inhomogeneous high-contrast structures, bringing further the results in Prikazchikova et al. (2018).

Bibliography

[1] J. D. Achenbach. An asymptotic method to analyze the vibrations of an elastic layer. *Journal of Applied Mechanics*, 36(1):65–72, 1969.

[2] M. Ahmad, E. Nolde, and A. Pichugin. Explicit asymptotic modelling of transient love waves propagated along a thin coating. *Zeitschrift für Angewandte Mathematik und Physik*, 62(1):173–181, 2011.

[3] O. Aksentian and I. Vorovich. The state of stress in a thin plate. *Journal of Applied Mathematics and Mechanics*, 27(6):1621–1643, 1963.

[4] A. S. Alzaidi, J. Kaplunov, and L. Prikazchikova. Elastic bending wave on the edge of a semi-infinite plate reinforced by a strip plate. *Mathematics and Mechanics of Solids*, 24(10):3319–3330, 2019.

[5] I. Argatov and G. Mishuris. *Indentation testing of biological materials*, volume 91. Springer, 2018.

[6] M. Z. Aşık and S. Tezcan. A mathematical model for the behavior

of laminated glass beams. *Computers and Structures*, 83(21-22):1742–1753, 2005.

[7] M. Aßmus, K. Naumenko, and H. Altenbach. Mechanical behaviour of photovoltaic composite structures: influence of geometric dimensions and material properties on the eigenfrequencies of mechanical vibrations. *Composites Communications*, 6:59–62, 2017.

[8] T. Belyankova and V. Kalinchuk. On the problem of analyzing the dynamic properties of a layered half-space. *Acoustical Physics*, 60(5): 530–542, 2014.

[9] V. L. Berdichevsky. An asymptotic theory of sandwich plates. *International Journal of Engineering Science*, 48(3):383–404, 2010.

[10] D. Bigoni, M. Gei, and A. Movchan. Dynamics of a prestressed stiff layer on an elastic half space: filtering and band gap characteristics of periodic structural models derived from long-wave asymptotics. *Journal of the Mechanics and Physics of Solids*, 56(7):2494–2520, 2008.

[11] M. A. Biot. *Mechanics of incremental deformations: theory of elasticity and viscoelasticity of initially stressed solids and fluids, including thermodynamic foundations and applications to finite strain.* Wiley, 1965.

[12] P. J. Blatz and W. L. Ko. Application of finite elastic theory to the deformation of rubbery materials. *Transactions of the Society of Rheology*, 6(1):223–252, 1962.

[13] F. M. Borodich, B. A. Galanov, N. V. Perepelkin, and D. A. Prikazchikov. Adhesive contact problems for a thin elastic layer: Asymptotic analysis and the JKR theory. *Mathematics and Mechanics of Solids*, 24(5):1405–1424, 2019.

[14] P. Boulanger and M. Hayes. Finite-amplitude waves in deformed mooney-rivlin materials. *The Quarterly Journal of Mechanics and Applied Mathematics*, 45(4):575–593, 1992.

[15] E. Carrera and S. Brischetto. A survey with numerical assessment of classical and refined theories for the analysis of sandwich plates. *Applied Mechanics Reviews*, 62(1):010803, 2009.

[16] P. Chadwick. *Continuum mechanics: concise theory and problems*. Courier Corporation, 2012.

[17] P. Chadwick and D. Jarvis. Surface waves in a pre-stressed elastic body. *Proceedings of the Royal Society of London. A. Mathematical and Physical Sciences*, 366(1727):517–536, 1979.

[18] R. Chebakov, J. Kaplunov, and G. Rogerson. A non-local asymp-

totic theory for thin elastic plates. *Proceedings of the Royal Society A: Mathematical, Physical and Engineering Sciences*, 473(2203):20170249, 2017.

[19] I. M. Daniel, O. Ishai, I. M. Daniel, and I. Daniel. *Engineering mechanics of composite materials*, volume 3. Oxford University Press, New York, 1994.

[20] M. Dowaikh and R. Ogden. On surface waves and deformations in a pre-stressed incompressible elastic solid. *IMA Journal of Applied Mathematics*, 44(3):261–284, 1990.

[21] M. Dowaikh and R. Ogden. On surface waves and deformations in pre-stressed elastic media. *Stability and Applied Analysis of Continuous Media*, 1:27–44, 1991.

[22] M. Dowaikh and R. W. Ogden. Interfacial waves and deformations in pre-stressed elastic media. *Proceedings of the Royal Society of London. Series A: Mathematical and Physical Sciences*, 433(1888):313–328, 1991.

[23] B. Erbaş, E. Yusufoğlu, and J. Kaplunov. A plane contact problem for an elastic orthotropic strip. *Journal of Engineering Mathematics*, 70 (4):399–409, 2011.

[24] B. Erbaş, J. Kaplunov, D. A. Prikazchikov, and O. Şahin. The near-resonant regimes of a moving load in a three-dimensional problem for a coated elastic half-space. *Mathematics and Mechanics of Solids*, 22 (1):89–100, 2017.

[25] B. Erbaş, J. Kaplunov, A. Nobili, and G. Kılıç. Dispersion of elastic waves in a layer interacting with a winkler foundation. *The Journal of the Acoustical Society of America*, 144(5):2918–2925, 2018.

[26] B. Erbaş, J. Kaplunov, E. Nolde, and M. Palsü. Composite wave models for elastic plates. *Proceedings of the Royal Society A: Mathematical, Physical and Engineering Sciences*, 474(2214):20180103, 2018.

[27] B. Erbaş, J. Kaplunov, and M. Palsü. A composite hyperbolic equation for plate extension. *Mechanics Research Communications*, 99:64–67, 2019.

[28] J. Flavin. Surface waves in pre-stressed mooney material. *The Quarterly Journal of Mechanics and Applied Mathematics*, 16(4):441–449, 1963.

[29] K. Friedrichs and R. Dressler. A boundary-layer theory for elastic plates. *Communications on Pure and Applied Mathematics*, 14(1):1–33, 1961.

[30] Y. Fu and G. A. Rogerson. A nonlinear analysis of instability of a pre-stressed incompressible elastic plate. *Proceedings of the Royal Society of London. Series A: Mathematical and Physical Sciences*, 446(1927): 233–254, 1994.

[31] Y. Fu, J. Kaplunov, and D. Prikazchikov. Reduced model for the surface dynamics of a generally anisotropic elastic half-space. *Proceedings of the Royal Society A*, 476(2234):20190590, 2020.

[32] F. Gilbert and G. E. Backus. Propagator matrices in elastic wave and vibration problems. *Geophysics*, 31(2):326–332, 1966.

[33] A. Goldenveizer, J. Kaplunov, and E. Nolde. On Timoshenko-Reissner type theories of plates and shells. *International Journal of Solids and Structures*, 30(5):675–694, 1993.

[34] A. Goldenweiser. *Theory of Thin Elastic Shells*. Pergamon Press, NY, 1961.

[35] A. E. Green, R. Shield, and R. Rivlin. General theory of small elastic deformations superposed on finite elastic deformations. In *Collected Papers of RS Rivlin*, pages 589–616. Springer, 1997.

[36] N. A. Haskell. The dispersion of surface waves on multilayered media. *Bulletin of the seismological Society of America*, 43(1):17–34, 1953.

[37] R. Hauert. A review of modified DLC coatings for biological applications. *Diamond and Related Materials*, 12(3-7):583–589, 2003.

[38] M. Hayes and R. S. Rivlin. Surface waves in deformed elastic materials. *Archive for Rational Mechanics and Analysis*, 8(1):358–380, 1961.

[39] C. Horgan. Anti-plane shear deformations in linear and nonlinear solid mechanics. *SIAM review*, 37(1):53–81, 1995.

[40] C. Horgan and K. Miller. Antiplane shear deformations for homogeneous and inhomogeneous anisotropic linearly elastic solids. *Journal of Applied Mechanics*, 61(1):23–29, 1994.

[41] C. O. Horgan. The remarkable gent constitutive model for hyperelastic materials. *International Journal of Non-Linear Mechanics*, 68:9–16, 2015.

[42] C. O. Horgan and G. Saccomandi. Anti-plane shear deformations for non-gaussian isotropic, incompressible hyperelastic materials. *Proceedings of the Royal Society of London. Series A: Mathematical, Physical and Engineering Sciences*, 457(2012):1999–2017, 2001.

[43] I. V. Ivanov. Analysis, modelling, and optimization of laminated glasses as plane beam. *International Journal of Solids and Structures*, 43(22-23):6887–6907, 2006.

[44] Q. Jiang and M. F. Beatty. On compressible materials capable of sustaining axisymmetric shear deformations. part 1: Anti-plane shear of isotropic hyperelastic materials. *Journal of elasticity*, 39(1):75, 1995.

[45] Q. Jiang and J. K. Knowles. A class of compressible elastic materials capable of sustaining finite anti-plane shear. *Journal of Elasticity*, 25 (3):193–201, 1991.

[46] J. Kaplunov. Long-wave vibrations of a thinwalled body with fixed faces. *The Quarterly Journal of Mechanics and Applied Mathematics*, 48(3):311–327, 1995.

[47] J. Kaplunov and D. Markushevich. Plane vibrations and radiation of an elastic layer lying on a liquid half-space. *Wave Motion*, 17(3):199–211, 1993.

[48] J. Kaplunov and E. Nolde. Long-wave vibrations of a nearly incompressible isotropic plate with fixed faces. *The Quarterly Journal of Mechanics and Applied Mathematics*, 55(3):345–356, 2002.

[49] J. Kaplunov and D. A. Prikazchikov. Asymptotic theory for Rayleigh and Rayleigh-type waves. In *Advances in Applied Mechanics*, volume 50, pages 1–106. Elsevier, 2017.

[50] J. Kaplunov, L. Y. Kossovich, and G. Rogerson. Direct asymptotic

integration of the equations of transversely isotropic elasticity for a plate near cut-off frequencies. *Quarterly Journal of Mechanics and Applied Mathematics*, 53(2):323–341, 2000a.

[51] J. Kaplunov, E. Nolde, and G. Rogerson. A low-frequency model for dynamic motion in pre-stressed incompressible elastic structures. *Proceedings of the Royal Society of London. Series A: Mathematical, Physical and Engineering Sciences*, 456(2003):2589–2610, 2000b.

[52] J. Kaplunov, E. Nolde, and G. Rogerson. An asymptotically consistent model for long-wave high-frequency motion in a pre-stressed elastic plate. *Mathematics and Mechanics of Solids*, 7(6):581–606, 2002.

[53] J. Kaplunov, E. Nolde, and G. Rogerson. Short wave motion in a pre-stressed incompressible elastic plate. *IMA Journal of Applied Mathematics*, 67(4):383–399, 2002.

[54] J. Kaplunov, D. Prikazchikov, and G. Rogerson. Edge vibration of a pre-stressed semi-infinite strip with traction-free edge and mixed face boundary conditions. *Zeitschrift für Angewandte Mathematik und Physik ZAMP*, 55(4):701–719, 2004.

[55] J. Kaplunov, E. Nolde, and B. Shorr. A perturbation approach for eval-

uating natural frequencies of moderately thick elliptic plates. *Journal of Sound and Vibration*, 281(3-5):905–919, 2005.

[56] J. Kaplunov, G. Rogerson, and P. Tovstik. Localized vibration in elastic structures with slowly varying thickness. *The Quarterly Journal of Mechanics and Applied Mathematics*, 58(4):645–664, 2005.

[57] J. Kaplunov, E. Nolde, and G. A. Rogerson. An asymptotic analysis of initial-value problems for thin elastic plates. *Proceedings of the Royal Society A: Mathematical, Physical and Engineering Sciences*, 462 (2073):2541–2561, 2006.

[58] J. Kaplunov, D. Prikazchikov, and G. Rogerson. Edge bending wave on a thin elastic plate resting on a winkler foundation. *Proceedings of the Royal Society A: Mathematical, Physical and Engineering Sciences*, 472(2190):20160178, 2016.

[59] J. Kaplunov, D. Prikazchikov, and O. Sergushova. Multi-parametric analysis of the lowest natural frequencies of strongly inhomogeneous elastic rods. *Journal of Sound and Vibration*, 366:264–276, 2016.

[60] J. Kaplunov, D. Prikazchikov, and L. Prikazchikova. Dispersion of elastic waves in a strongly inhomogeneous three-layered plate. *International Journal of Solids and Structures*, 113:169–179, 2017.

[61] J. Kaplunov, D. Prikazchikov, and L. Prikazchikova. Dispersion of elastic waves in laminated glass. *Procedia Engineering*, 199:1489–1494, 2017.

[62] J. Kaplunov, D. Prikazchikov, and L. Sultanova. Justification and refinement of winkler–fuss hypothesis. *Zeitschrift für Angewandte Mathematik und Physik*, 69(3):80, 2018.

[63] J. Kaplunov, D. Prikazchikov, L. Prikazchikova, and O. Sergushova. The lowest vibration spectra of multi-component structures with contrast material properties. *Journal of Sound and Vibration*, 445:132–147, 2019.

[64] J. Kaplunov, D. Prikazchikov, and L. Sultanova. Elastic contact of a stiff thin layer and a half-space. *Zeitschrift für Angewandte Mathematik und Physik*, 70(1):22, 2019.

[65] J. Kaplunov, D. Prikazchikov, and L. Sultanova. Rayleigh-type waves on a coated elastic half-space with a clamped surface. *Philosophical Transactions of the Royal Society A*, 377(2156):20190111, 2019.

[66] J. D. Kaplunov, L. Y. Kossovitch, and E. Nolde. *Dynamics of thin walled elastic bodies*. Academic Press, 1998.

[67] P. Kayestha, A. C. Wijeyewickrema, and K. Kishimoto. Time-harmonic

wave propagation in a pre-stressed compressible elastic bi-material laminate. *European Journal of Mechanics-A/Solids*, 29(2):143–151, 2010.

[68] J. M. Kelly. Analysis of fiber-reinforced elastomeric isolators. *Journal of Seismology and Earthquake Engineering*, 2(1):19–34, 1999.

[69] L. Khajiyeva, D. Prikazchikov, and L. Prikazchikova. Hyperbolic-elliptic model for surface wave in a pre-stressed incompressible elastic half-space. *Mechanics Research Communications*, 92:49–53, 2018.

[70] J. K. Knowles. On finite anti-plane shear for imcompressible elastic materials. *The ANZIAM Journal*, 19(4):400–415, 1976.

[71] J. K. Knowles. A note on anti-plane shear for compressible materials in finite elastostatics. *The ANZIAM Journal*, 20(1):1–7, 1977.

[72] I. Kreja. A literature review on computational models for laminated composite and sandwich panels. *Open Engineering*, 1(1):59–80, 2011.

[73] A. Kudaibergenov, A. Nobili, and L. Prikazchikova. On low-frequency vibrations of a composite string with contrast properties for energy scavenging fabric devices. *Journal of Mechanics of Materials and Structures*, 11(3):231–243, 2016.

[74] H. Lamb. On the flexure of an elastic plate. *Proceedings of the London Mathematical Society*, 1(1):70–91, 1889.

[75] M. Lashhab, G. Rogerson, and L. Prikazchikova. Small amplitude waves in a pre-stressed compressible elastic layer with one fixed and one free face. *Zeitschrift für angewandte Mathematik und Physik*, 66 (5):2741–2757, 2015.

[76] M. Lashhab, G. Rogerson, and K. Sandiford. Dispersion phenomena in symmetric pre-stressed layered elastic structures. *International Journal of Solids and Structures*, 58:220–232, 2015.

[77] P. Lee and N. Chang. Harmonic waves in elastic sandwich plates. *Journal of Elasticity*, 9(1):51–69, 1979.

[78] M. Lutianov and G. A. Rogerson. Long wave motion in layered elastic media. *International Journal of Engineering Science*, 48(12):1856–1871, 2010.

[79] T. P. Martin, C. N. Layman, K. M. Moore, and G. J. Orris. Elastic shells with high-contrast material properties as acoustic metamaterial components. *Physical Review B*, 85(16):161103, 2012.

[80] R. Mindlin. Flexural vibrations of elastic sandwich plates. Technical report, Columbia University, New York, 1959.

[81] R. Mindlin. Waves and vibrations in isotropic, elastic plates. *Structure Mechanics*, pages 199–232, 1960.

[82] M. Mooney. A theory of large elastic deformation. *Journal of Applied Physics*, 11(9):582–592, 1940.

[83] A. Nobili and D. A. Prikazchikov. Explicit formulation for the Rayleigh wave field induced by surface stresses in an orthorhombic half-plane. *European Journal of Mechanics-A/Solids*, 70:86–94, 2018.

[84] E. Nolde. Qualitative analysis of initial-value problems for a thin elastic strip. *IMA Journal of Applied Mathematics*, 72(3):348–375, 2007.

[85] E. Nolde and G. Rogerson. Long wave asymptotic integration of the governing equations for a pre-stressed incompressible elastic layer with fixed faces. *Wave motion*, 36(3):287–304, 2002.

[86] E. Nolde, L. Prikazchikova, and G. Rogerson. Dispersion of small amplitude waves in a pre-stressed, compressible elastic plate. *Journal of Elasticity*, 75(1):1–29, 2004.

[87] E. Nolde, A. Pichugin, and J. Kaplunov. An asymptotic higher-order theory for rectangular beams. *Proceedings of the Royal Society A: Mathematical, Physical and Engineering Sciences*, 474(2214):20180001, 2018.

[88] A. K. Noor. Free vibrations of multilayered composite plates. *AIAA Journal*, 11(7):1038–1039, 1973.

[89] R. Ogden and D. Roxburgh. The effect of pre-stress on the vibration and stability of elastic plates. *International Journal of Engineering Science*, 31(12):1611–1639, 1993.

[90] R. W. Ogden. Large deformation isotropic elasticity–on the correlation of theory and experiment for incompressible rubberlike solids. *Proceedings of the Royal Society of London. A. Mathematical and Physical Sciences*, 326(1567):565–584, 1972.

[91] R. W. Ogden. *Non-linear elastic deformations*. Courier Corporation, 1997.

[92] H. Phan, Y. Cho, and J. D. Achenbach. Application of the reciprocity theorem to scattering of surface waves by a cavity. *International Journal of Solids and Structures*, 50(24):4080–4088, 2013.

[93] H. Phan, Y. Cho, Q. H. Le, C. V. Pham, H. T.-L. Nguyen, P. T. Nguyen, and T. Q. Bui. A closed-form solution to propagation of guided waves in a layered half-space under a time-harmonic load: An application of elastodynamic reciprocity. *Ultrasonics*, 96:40–47, 2019.

[94] A. V. Pichugin. *Asymptotic models for long wave motion in a pre-stressed incompressible elastic plate*. PhD thesis, University of Salford, 2001.

[95] A. V. Pichugin and G. A. Rogerson. A two-dimensional model for extensional motion of a pre-stressed incompressible elastic layer near cut-off frequencies. *IMA Journal of Applied Mathematics*, 66(4):357–385, 2001.

[96] A. V. Pichugin and G. A. Rogerson. An asymptotic membrane-like theory for long-wave motion in a pre-stressed elastic plate. *Proceedings of the Royal Society of London. Series A: Mathematical, Physical and Engineering Sciences*, 458(2022):1447–1468, 2002.

[97] A. V. Pichugin and G. A. Rogerson. Anti-symmetric motion of a pre-stressed incompressible elastic layer near shear resonance. *Journal of Engineering Mathematics*, 42(2):181–202, 2002.

[98] D. A. Polignone and C. O. Horgan. Axisymmetric finite anti-plane shear of compressible nonlinearly elastic circular tubes. *Quarterly of Applied Mathematics*, 50(2):323–341, 1992.

[99] D. A. Prikazchikov and G. A. Rogerson. On surface wave propagation in incompressible, transversely isotropic, pre-stressed elastic half-spaces. *International Journal of Engineering Science*, 42(10):967–986, 2004.

[100] L. Prikazchikova, I. Alejnikov, and G. Rogerson. Padé approximations

for low-frequency motion in a pre-stressed compressible elastic layer. *Mechanics Research Communications*, 33(5):699–704, 2006.

[101] L. Prikazchikova, Y. Ece Aydın, B. Erbaş, and J. Kaplunov. Asymptotic analysis of an anti-plane dynamic problem for a three-layered strongly inhomogeneous laminate. *Mathematics and Mechanics of Solids*, page 1081286518790804, 2018.

[102] M. S. Qatu. *Vibration of laminated shells and plates*. Elsevier, 2004.

[103] Y. Qin, X. Wang, and Z. L. Wang. Microfibre–nanowire hybrid structure for energy scavenging. *Nature*, 451(7180):809, 2008.

[104] M. Rao, K. Scherbatiuk, Y. Desai, and A. Shah. Natural vibrations of laminated and sandwich plates. *Journal of Engineering Mechanics*, 130(11):1268–1278, 2004.

[105] L. Rayleigh. On waves propagated along the plane surface of an elastic solid. *Proceedings of the London Mathematical Society*, 1(1):4–11, 1885.

[106] L. Rayleigh. On the free vibrations of an infinite plate of homogeneous isotropic elastic matter. *Proceedings of the London Mathematical Society*, 1(1):225–237, 1888.

[107] J. Reddy. *Mechanics of Laminated Composite Plates and Shells*. CRC Press, New York, 2004.

[108] E. L. Reiss and S. Locke. On the theory of plane stress. *Quarterly of Applied Mathematics*, 19(3):195–203, 1961.

[109] R. S. Rivlin and D. Saunders. Large elastic deformations of isotropic materials vii. experiments on the deformation of rubber. *Philosophical Transactions of the Royal Society of London. Series A, Mathematical and Physical Sciences*, 243(865):251–288, 1951.

[110] G. Rogerson. Some asymptotic expansions of the dispersion relation for an incompressible elastic plate. *International Journal of Solids and Structures*, 34(22):2785–2802, 1997.

[111] G. Rogerson and Y. Fu. An asymptotic analysis of the dispersion relation of a pre-stressed incompressible elastic plate. *Acta Mechanica*, 111(1-2):59–74, 1995.

[112] G. Rogerson and K. Sandiford. On small amplitude vibrations of pre-stressed laminates. *International Journal of Engineering Science*, 34 (8):853–872, 1996.

[113] G. Rogerson and K. Sandiford. Flexual waves in incompressible pre-stressed elastic composites. *The Quarterly Journal of Mechanics and Applied Mathematics*, 50(4):597–624, 1997.

[114] G. A. Rogerson and L. A. Prikazchikova. Generalisations of long wave

theories for pre-stressed compressible elastic plates. *International Journal of Non-Linear Mechanics*, 44(5):520–529, 2009.

[115] G. A. Rogerson and K. J. Sandiford. The effect of finite primary deformations on harmonic waves in layered elastic media. *International Journal of Solids and Structures*, 37(14):2059–2087, 2000.

[116] G. A. Rogerson and K. J. Sandiford. Some comments on the dispersion relation for periodically layered pre-stressed elastic media. *International Journal of Engineering Science*, 40(1):23–49, 2002.

[117] G. A. Rogerson, K. J. Sandiford, and L. A. Prikazchikova. Abnormal long wave dispersion phenomena in a slightly compressible elastic plate with non-classical boundary conditions. *International Journal of Non-Linear Mechanics*, 42(2):298–309, 2007.

[118] D. Roxburgh and R. Ogden. Stability and vibration of pre-stressed compressible elastic plates. *International Journal of Engineering Science*, 32(3):427–454, 1994.

[119] M. Y. Ryazantseva and F. K. Antonov. Harmonic running waves in sandwich plates. *International Journal of Engineering Science*, 59: 184–192, 2012.

[120] A. S. Sayyad and Y. M. Ghugal. Bending, buckling and free vibra-

tion of laminated composite and sandwich beams: A critical review of literature. *Composite Structures*, 171:486–504, 2017.

[121] S.-H. Schulze, M. Pander, K. Naumenko, and H. Altenbach. Analysis of laminated glass beams for photovoltaic applications. *International Journal of Solids and Structures*, 49(15-16):2027–2036, 2012.

[122] P. M. Sheridan, F. O. James, and T. S. Miller. Design of components. *Engineering with rubber*, pages 209–235, 1992.

[123] A. J. M. Spencer. *Continuum mechanics*. Courier Corporation, 2004.

[124] W. T. Thomson. Transmission of elastic waves through a stratified solid medium. *Journal of Applied Physics*, 21(2):89–93, 1950.

[125] R. Torr. Bridge bearings. *Close Liaison between Designer and Manufacturer essential. Highways and Public works*, 34:10–12, 1966.

[126] L. Treloar. Stress-strain data for vulcanised rubber under various types of deformation. *Transactions of the Faraday Society*, 40:59–70, 1944.

[127] L. R. G. Treloar. *The physics of rubber elasticity*. Oxford University Press, USA, 1975.

[128] Y. A. Ustinov. On the structure of the boundary layer in laminar slabs. *Doklady Akademii Nauk*, 229(2):325–328, 1976.

[129] O. H. Varga. Stress-strain behavior of elastic materials; selected problems of large deformations. *John Wiley and Sons*, 1966.

[130] K. Viverge, C. Boutin, and F. Sallet. Model of highly contrasted plates versus experiments on laminated glass. *International Journal of Solids and Structures*, 102:238–258, 2016.

[131] C. Wang, J. N. Reddy, and K. Lee. *Shear deformable beams and plates: Relationships with classical solutions*. Elsevier, 2000.

[132] A. Willson. Surface and plate waves in biaxially-stressed elastic media. *Pure and Applied Geophysics*, 102(1):182–192, 1973.

[133] A. Willson. The anomalous surface wave in uniaxially-stressed elastic material. *Pure and Applied Geophysics*, 112(4):665–674, 1974.